EFFECTS OF IRON AND OXIDATIVE STRESS IN SK-N-SH DOPAMINERGIC NEUROBLASTOMA CELLS: MODEL OF PARKINSON'S DISEASE

PATCHAREE KOONCUMCHOO

A THESIS SUBMITTED IN PARTIAL FULFILLMENT
OF THE REQUIREMENTS FOR
THE DEGREE OF DOCTOR OF PHILOSOPHY (NEUROSCIENCE)
FACULTY OF GRADUATE STUDIES
MAHIDOL UNIVERSITY
2005

ISBN 974-04-5642-1

EFFECTS OF IRON AND OXIDATIVE STRESS IN SK-N-SH DOPAMINERGIC NEUROBLASTOMA CELLS: MODEL OF PARKINSON'S DISEASE

…….
Mrs. Patcharee Kooncumchoo
Candidate

…….
Prof. Piyarat Govitrapong,
Ph.D.
Major-Advisor

…….
Assoc.Prof. Naiphinich Kotchabhakdi,
Ph.D.
Co-Advisor

……
Prof. Manuchair Ebadi,
Ph.D.
Co-Advisor

……
Assist.Prof. Banthit Chetsawang,
Ph.D.
Co-Advisor

.....
Assoc.Prof. Rassmidara Hoonsawat,
Ph.D.
Dean
Faculty of Graduate Studies

.....
Assoc.Prof. Naiphinich Kotchabhakdi,
Ph.D.
Chairman
Doctor of Philosophy (Neuroscience)
Institute of Science and Technology for
Research and Development

EFFECTS OF IRON AND OXIDATIVE STRESS IN SK-N-SH DOPAMINERGIC NEUROBLASTOMA CELLS: MODEL OF PARKINSON'S DISEASE

was submitted to the Faculty of Graduate Studies, Mahidol University
For the degree of Doctor of Philosophy (Neuroscience)
on
February 15, 2005

…….
Mrs. Patcharee Kooncumchoo
Candidate

……
Prof. Piyarat Govitrapong,
Ph.D.
Chair

……
Prof. Manuchair Ebadi,
Ph.D.
Member

…….
Assoc. Prof.Naiphinich Kotchabhakdi,
Ph.D.
Member

……
Prof. Anan Srikiatkhachorn,
M.D.
Member

……
Assist.Prof. Banthit Chetsawang,
Ph.D.
Member

……
Assoc.Prof. Rassmidara Hoonsawat,
Ph.D.
Dean
Faculty of Graduate Studies
Mahidol University

……
Prof. Kanok Pavasuthipaisit,
M.D., Ph.D.
Dean
Institute of Science and Technology for
Research and Development
Mahidol University

ACKNOWLEDGEMENT

The dissertation became successful with the extensive assistance support and guidance from my major advisor, Prof. Piyarat Govitrapong. Her advice has taught me in many ways, helps me grow up, and become responsible and mature. Moreover, she gave me a good opportunity to conduct my research and learn new experiences in USA.

I gratefully thank Prof. Manuchair Ebadi, from the Excellent Center in Neuroscience, School of Medicine and Health Science, University of North Dakota, USA, for his kindness which has given me a chance of learning in USA. His advice and suggestion provide further improvement for my knowledge as well as my life. He is a very impressive teacher who not only taught me for the studies but also on how to be a good and knowledgeable person.

I deeply thank my co-advisor, Assoc. Prof. Naiphinich Kotchabhakdi and Assist. Prof. Banthit Chetsawang. Their valuable advice and guidance in both in this research and my personal life help me get through troubles and become successful today.

I would like to thank Dr. Sushil Sharma and Dr. Shark Shavali for their assistance and guidance during my time in USA. Special thanks to Assoc. Prof. James Porter, for his valuable advice and guidance in the research techniques. I sincerely thank Lowry Wegner, Joann Johnson, Dani and Nichole in the Excellent Center in Neuroscience, School of Medicine and Health Science, University of North Dakota for their cheerfulness and kind support during my stay in USA. Thanks also go to all my friends, lecturers and staff in the Department of Pharmacology, Physiology and Therapeutics, School of Medicine and Health Science, University of North Dakota for their friendship and kindness.

I would like to thank The Ministry of Education of Thailand and Thammasat University for their financial support and gave me a chance to do research in University of North Dakota, USA.

Moreover, I am grateful to all the lecturers, staff, and friends from the Neuro-Behavioral Biology Center for their valuable advice and kind support.

Finally, I am grateful for the help and support from my family, their care, and love. The usefulness of this thesis, I dedicate to my father, my mother and all the teachers who have taught me since my childhood.

Patcharee Kooncumchoo

EFFECTS OF IRON AND OXIDATIVE STRESS IN SK-N-SH DOPAMINERGIC NEUROBLASTOMA CELLS: MODEL OF PARKINSON'S DISEASE

PATCHAREE KOONCUMCHOO 4336523 STNS/D

Ph.D.(NEUROSCIENCE)

THESIS ADVISORS: PIYARAT GOVITRAPONG, Ph.D., MUNUCHAIR EBADI, Ph.D., NAIPHINICH KOTCHABHAKDI, Ph.D., BANTHIT CHETSAWANG, Ph.D.

ABSTRACT

Parkinson's disease is one of the progressive neurodegenerative diseases, which is caused by an abnormal accumulation of iron in the affected brain areas. Parkinson's disease involves in the degeneration of dopaminergic neurons. Oxidative stress and transition metal, iron, have been linked to the Parkinson's disease pathogenesis. However, it is difficult to determine if oxidative stress is a cause or consequence of the degeneration process. By using SK-N-SH, a human dopaminergic neuroblastoma cell line, it was found that 100-250 μM $FeSO_4$ decreased cell viability, induced reactive oxygen species (ROS) production, and increased lipid peroxidation. These effects were reduced by 10 μM deferoxamine (DFO). Simultaneously, glutathione and metallothionein levels were increased in order to counteract the toxicity effects of $FeSO_4$. Furthermore, DFO, in the absence of $FeSO_4$, enhanced the levels of cellular adenosine triphosphate (ATP), but caused cell damage, chromatin condensation, and cell death. Morphological study revealed that $FeSO_4$ (50-100 μM) altered mitochondrial morphology, disrupted the nuclear membrane, and translocated α-synuclein from the perinuclear region into the disrupted nucleus. Moreover, $FeSO_4$ (100 μM) increased the transcription factor, NF-κB, levels and induced the activation of caspase-3 activity. Apoptotic protein studies showed a decrease in anti-apototic Bcl_2 protein levels, but not pro-apoptotic Bax protein levels.

The results of these studies suggest that excess $FeSO_4$ produces numerous reactive oxygen species that counteract with increased glutathione and metallothionein levels. These changes produce an oxidative stress environment, damaging the cells by disrupting mitochondrial functions, decreasing ATP, including lipid, protein, and DNA damage. DFO, an iron chelator, was able to reduce and attenuate iron-mediated oxidative stress. Unfortunately, in the absence of excess $FeSO_4$, DFO itself had deleterious effects on the cell morphology and hence integrity of dopaminergic neurons. Moreover, $FeSO_4$ caused cell death by increasing NF-κB levels, decreasing Bcl_2 levels, and increasing caspase-3 activity. These results indicate that oxidative stress induced by $FeSO_4$ lead to cell damage and cell death via the apoptotic pathway.

KEY WORDS: PARKINSON'S DISEASE / OXIDATIVE STRESS / IRON / DEFEROXAMINE / ANTIOXIDANT

121 P. ISBN 974-04-5642-1

ผลกระทบของเหล็กและ Oxidative stress ในเซลล์ประสาทโดปามีน SK-N-SH แบบจำลองของโรคพาร์กินสัน (EFFECTS OF IRON AND OXIDATIVE STRESS IN SK-N-SH DOPAMINERGIC NEUROBLASTOMA CELLS: MODEL OF PARKINSON'S DISEASE)

พัชรี คุณค้ำชู 4336523 STNS/D

ปร.ด. (ประสาทวิทยาศาสตร์)

คณะกรรมการควบคุมวิทยานิพนธ์ : ปิยะรัตน์ โกวิทตรพงศ์, Ph.D., MUNUCHAIR EBADI, Ph.D., นัยพินิจ คชภักดี, Ph.D., บัณฑิต เจตน์สว่าง, Ph.D.

บทคัดย่อ

ปริมาณของเหล็กอิสระที่มีมากผิดปกติ เป็นอาการบ่งชี้อย่างหนึ่งถึงความผิดปกติและอาจเป็นสาเหตุหนึ่งที่ทำให้เกิดความเสื่อมของเซลล์ประสาทภายในสมอง ความเสื่อมดังกล่าวนี้สามารถก่อให้เกิดความผิดปกติขึ้นได้มากมายรวมทั้งความผิดปกติที่เกิดขึ้นกับผู้ป่วยโรคพาร์กินสัน การเกิดภาวะ oxidative stress และปริมาณของเหล็กอิสระที่มีมากเกินไปอาจมีส่วนเกี่ยวข้องกับการเกิดโรคพาร์กินสัน แต่ก็ยังไม่มีผู้ทราบแน่ชัดว่าความเสื่อมดังกล่าวเกิดขึ้นก่อนหรือหลังภาวะ oxidative stress ในการศึกษาแบบจำลองของโรคพาร์กินสันด้วยเซลล์ประสาทโดปามีนของมนุษย์ชนิด SK-N-SH พบว่าปริมาณของเหล็กที่มีความเข้มข้นสูง (100-250 μM $FeSO_4$) สามารถก่อให้เกิดอนุมูลอิสระ ส่งผลให้เกิดความเสียหายต่อไขมันและทำให้เซลล์ตายมากขึ้น ความผิดปกติดังกล่าวนี้สามารถแก้ไขให้น้อยลงด้วยสาร DFO ซึ่งเป็นสารที่ทำหน้าที่กำจัดเหล็กอิสระ ในทางตรงกันข้ามคือในสภาวะที่ปราศจากเหล็กนั้น สาร DFO กลับก่อให้เกิดผลเสียมากกว่าผลดี โดยจะส่งผลทำให้เกิดการหดสั้นของโครมาติน ทำให้เกิดความผิดปกติในการทำงานและนำไปสู่การตายของเซลล์ได้เช่นกัน นอกจากนั้นเหล็กอิสระยังทำให้เกิดกระตุ้นการทำงานของ caspase-3 มากขึ้น ส่งผลให้มีการเพิ่มปริมาณการทำงานของ transcription factor (NF-κB) มากขึ้น ในขณะที่โปรตีนที่ทำหน้าที่ช่วยป้องกันอันตรายให้แก่เซลล์อย่างโปรตีน Bcl-2 กลับมีปริมาณลดลง แต่เหล็กไม่มีผลต่อการเปลี่ยนแปลงปริมาณของโปรตีน Bax ในขณะเดียวกันเหล็กยังกระตุ้นให้เกิดการเพิ่มขึ้นของสารต้านอนุมูลอิสระอย่าง glutathione และ metallothionein อีกด้วย จากการศึกษาลักษณะทางกายภาพของเซลล์แสดงให้เห็นว่าเหล็กที่มีความเข้มข้น 50-100 μM จะส่งผลกระทบต่อไมโตครอนเดีย ทำให้เกิดการฉีกขาดของผนังนิวเคลียสและมีการเคลื่อนย้าย α-synuclein จากบริเวณรอบๆนิวเคลียสเข้าไปยังภายในนิวเคลียสที่เกิดการฉีกขาด ทำให้เซลล์ตายเพิ่มมากขึ้น ผลจากการศึกษาในครั้งนี้ชี้ให้เห็นว่าปริมาณเหล็กอิสระที่มีมากเกินไปในเซลล์ สามารถก่อให้เกิดภาวะ oxidative stress และก่อให้เกิดความเสียหายแก่เซลล์ได้ แต่ความเสียหายดังกล่าวนี้สามารถป้องกันได้ด้วยสาร DFO แต่หากปราศจากเหล็กอิสระ สาร DFO กลับให้โทษและทำให้เซลล์ตายได้

121 หน้า. ISBN 978-04-5642-1

CONTENTS

CONTENTS (CONT.)

CONTENTS (CONT.)

LIST OF TABLES

LIST OF FIGURES

LIST OF FIGURES (CONT.)

LIST OF FIGURES (CONT.)

LIST OF ABBREVIATIONS

AIDS	=	Auto-immune deficiency syndrome
Ala	=	Alanine
ATP	=	Adenosine triphosphate
CSF	=	Cerebrospinal fluid
CNS	=	Central nervous system
CO_2	=	Carbon dioxide
Cu	=	Copper
DA	=	Dopamine
DCF	=	2′-7′-dichlorofluorescein diacetate
DFO	=	Defeoxamine, deferoxamine B mesylate
DMEM	=	Dulbecco's modified Eagle's medium
DMpl	=	Dorsomedial nucleus of thalamus
DMT1	=	Divalent metal transporter 1
DNA	=	Deoxyribonucleic acid
ECL	=	Enchanced chemiluminescence
EDTA	=	Ethylenediaminetetraacetic acid
FAD	=	Flavin adenine dinucleotide
Fe	=	Iron
Fe^{2+}	=	Iron (ferrous form)
Fe^{3+}	=	Iron (ferric form)
FMN	=	Flavin mononucleotide
GABA	=	Gamma (γ)-aminobutyric acid
GPe	=	Globus pallidus (external)
GPi	=	Globus pallidus (internal)
GPx	=	Glutathione peroxidase
GSH	=	Glutathione
GSSG	=	Oxidized glutathione

LIST OF ABBREVIATIONS (CONT.)

$H^{\bullet}$	=	Hydrogen atom
HL-60	=	Human myelocytic leukemia cell lines
HD	=	Huntington's disease
H_2O_2	=	Hydrogen peroxide
HO	=	Heme oxygenase
HOCl	=	Hydrochlorous acid
IL-1β	=	Interleukin-1β
IRP2	=	Iron regulatory protein-2
JC-1	=	5,5′,6,6′-tetrachloro-1,1′,3,3′-tetraethylbenzimidazol-carbocyanine iodide
MCB	=	Monochlorobimane
MDA	=	Malondialdehyde
MRI	=	Magnetic resonance imaging
mRNA	=	Messenger ribonucleic acid
MPTP	=	1-methyl-4-phenyl-1,2,3,6-tetrahydropyridine
MSA	=	Multiple system atrophy with strionigral degeneration
MT	=	Metallothionein
MTT	=	3-(4, 5-dimethylthiazol-2-yl)-2,5 diphenyltetrazoliumbromide
NaOH	=	Sodium hydroxide
NF-κB	=	Nuclear factor kappa B
NSC	=	Nonsignificant change
O_2	=	Diatomic oxygen molecule
$O_2^{\bullet-}$	=	Superoxide radicals
$^1O\Delta g$	=	Singlet oxygen
$^{\bullet}OH$	=	Hydroxyl radicals
6-OHDA	=	6-Hydroxydopamine
PBS	=	Phosphate-buffered saline
PD	=	Parkinson’s disease
PHGPx	=	Phospholipid hydroperoxide glutathione peroxidase

LIST OF ABBREVIATIONS (CONT.)

Pro	=	Proline
PSP	=	Progressive supranuclear palsy
PUFA	=	Polyunsaturated fatty acids
ROS	=	Reactive oxygen species
SN	=	Substantia nigra
SOD	=	Superoxide dismutase
TBA	=	2-Thiobarbituric acid
TCA	=	Trichloroacetic acid
HCl	=	Hydrochloric acid
TGFβ	=	Transforming growth factor β
TNF-α	=	Tumor necrosis factor-α
UV	=	Ultraviolet
Vamc	=	Ventral anterior nucleus of thalamus
VLm	=	Ventral lateral nucleus of thalamus (medial part)
Zn	=	Zinc

CHAPTER 1
INTRODUCTION

Parkinson's disease (PD) is the second most common neurodegenerative disorder after Alzheimer's disease, affecting approximately 0.5-1% among people aged between 65-69 years old, and rising to 1-3% among those of 80 years or older (Guttmacher and Collins, 2003). There is a worldwide increase in disease prevalence due to an increasing age of current human populations. A definitive neuropathological diagnosis of PD requires loss of dopaminergic neurons in the substantia nigra (SN) pars compacta, and related brainstem nuclei, and the presence of Lewy bodies in remaining nerve cells (Ebadi et al., 2001; Ebadi and Hiramatsu, 2000). The causes of PD remain unknown, and mechanisms responsible for dopaminergic cell loss are obscure. Nonetheless, several biochemical abnormalities in PD have been identified, including mitochondrial complex I deficiency, oxidative stress, and excess of iron (Campbell, et al., 2001).

Iron and multivalent transition metals such as copper and manganese are essential in most biological reactions and are cofactors of numerous enzymes, particularly those involved in mitochondrial respiration. Most importantly, iron, which serves as an essential component of numerous cellular enzymes, including cytochrome oxidase, a number of enzymes in the citric acid cycle, ribonucleotide reductase (the rate-limiting step for DNA synthesis) and NADPH reductase. With respect to neuronal activity, iron is involved in the action and synthesis of dopamine, serotonin, γ-aminobutyric acid (GABA), and possibly myelin formation. While being an essential nutrient, iron is also a potent toxin. As a consequence, an elegant system composed of tranferrin, tranferrin receptors, and ferritin has evolved to regulate the availability and timely delivery of iron to cells (Beard, et al., 1993)

However, abnormal tissue accumulation of redox-active transition metals can be cytotoxic because perturbations in metal homeostasis result in an array of cellular

disturbances characterized by increased free radical production. Oxidative stress, defined as the imbalance between biochemical processes, causes molecular cell damage leading to failure of biological functions and cell death.

Free iron, more likely than any other transition metals, has been implicated in redox transitions and consequential generation of oxygen free radicals. The potential of iron to cause an increase in oxidative events leading to cellular damage is controlled by a series of iron-binding proteins. Recent studies found that the level of iron is increased in senile plaques (Lovell, et al., 1998) and neurofibrillary tangles have been shown to induce hydrogen peroxide dependent oxidation (Sayre, et al., 2000). This indicates that metals may play a critical role in modulating oxidative stress events, which may eventually result in neurodegeneration.

Defeoxamine (DFO), an iron chelator, is a drug that we choose as a chelator of free iron in this study. DFO is a drug used in many treatments such as conditions of iron overload. As we know, treatment with L-dopa shows poor progression when used in a long term and it produces many adverse effects. It is likely that free iron chelator combined with preserved dopamine, a neurotransmitter, levels by L-dopa will protect dopaminergic neurons from damages.

In this study, we hypothesized that the imbalance in iron homeostasis and/or excess iron-induced toxicity may be a primary cause of the pathogenesis in PD. The chelating free iron may protect the cells, thus increase cell survive. If this hypothesis is correct, we may find a new solution to help people who suffer from this disease. By studying the role of iron-mediated neurotoxicity, it may possible to explain the cellular events. These insights may help us to find causation, pathogenesis and new treatment for PD. Moreover, the study of iron-mediated neurotoxicity will lead to the understanding of intracellular events occurring in patients, and to find new effective therapy for the disease.

CHAPTER 2
OBJECTIVES

The objectives of this study are as follows:

1. To study the mechanism of iron-mediated neurotoxicity in Parkinson's disease by using SK-N-SH dopaminergic cell lines as a model.
2. To study the effects of DFO of whether it can attenuate iron-mediated neurotoxicity in Parkinson's disease by using SK-N-SH dopaminergic cell lines as a model.
3. To investigate cellular defense mechanism that occurs during iron-mediated neurotoxicity.
4. To investigate the changes of transcription factor (NF-κB) during iron-mediated neurotoxicity.

CHAPTER 3
LITERATURE REVIEW

3.1 An overview of Parkinson's disease

Parkinson's disease was first described as "the shaking palsy" in 1817 by a British doctor James Parkinson. Because of Parkinson's early work in identifying symptoms, the disease came to bear his name. Parkinson's disease is one of a larger group of neurological conditions called motor system disorders. Historians have found evidence of the disease as far back as 5000 BC.

Parkinson's disease (PD) is the second most common neurodegenerative disorder after Alzheimer's disease, affecting approximately 0.5-1% among people ages between 65-69 years old, and rising to 1-3% of people at 80 years of age and older (Guttmacher and Collins, 2003). There is a worldwide increase in disease prevalence due to the increasing age of human populations. A definitive neuropathological diagnosis of PD requires loss of dopaminergic neurons in the substantia nigra (SN) pars compacta, and related brainstem nuclei, and the presence of Lewy bodies in remaining nerve cells (Ebadi et al., 2001; Ebadi and Hiramatsu, 2000).

In the normal brain, some nerve cells produce the chemical dopamine, which transmits signals within the brain to produce smooth movement of muscles. In Parkinson's patients, 80 percent or more of these dopamine-producing cells are damaged, dead, or otherwise degenerated. This causes the nerve cells to fire wildly, leaving patients unable to control their movements. Symptoms usually show up in one or more of four ways:

1. Resting tremor or trembling in hands, arms, legs, jaw, and face.
2. Muscular rigidity or stiffness of limbs and trunk.
3. Bradykinesia, or slowness of movement.
4. Postural instability or impaired balance and coordination.

Nationwide, as many as 1.5 million people in USA were suffering from Parkinson's, according to the Parkinson's Disease Foundation. A chronic and progressive disorder, Parkinson's strikes slightly more men than women and more whites than blacks in the United States. Parkinson's disease is found most often in-patients over 50 years old, but 10 percent of patients (Young-onset Parkinson's disease) are lower than 40 years old.

3.1.1 Anatomical structures of substantia nigra

The substantia nigra lies dorsal to the crus cerebri, ventral to the midbrain tegmentum and extends throughout the length of the mesencephalon. Descriptively, the substantia nigra commonly divided into two parts:

1. The compact part: a cell-rich region composed of large, pigmented cells.
2. The reticular part: a cell-poor region close to the crus cerebri.

Three types of nigral neurons have been described:

1. Large neurons distributed exclusively in the reticular part.
2. Medium and large neurons in the compact part.
3. Short-axon (Golgi type II) cells found in both the compact part and the reticular part.

Some ultrastructural studies do not support the division of the substantia nigra into two parts, though cells vary in size and regional distribution. Golgi studies reveal that dendrites of nigral neurons vary in size, branch once or twice and have specific orientations. There is considerable overlap of dendritic fields of most nigral neurons in the pars reticulata, which appears to represent the principal site of afferent synaptic articulations. Cells of the pars compacta contain high concentration of dopamine and appear to be a principle source of striatal (i.e., caudate nucleus and putamen) dopamine. The enzyme glutamate decarboxylase (GAD) utilized in the synthesis of gamma (γ)-aminobutyric acid (GABA) is found in high concentrations in the pars reticulata (Carpenter, 1978).

Figure 3.1 Transverse section of midbrain, upper is from Parkinson's disease patient and lower is from normal subject brain.

3.1.2 Pathways in the substantia nigra

Strionigral fibers are arising from the caudate nucleus and putamen constitutes the principal afferent system of the nigra. These fibers are topographically organized in that fibers from the caudate nucleus project to rostral parts of the nigral, while the putamen projects to all parts of the nigral. Strionigral fibers terminate mainly in the pars reticulata and are considered to convey GABA, an inhibitory neurotransmitter to the substantia nigra.

Corticonigral fibers are regarded as questionable in view of electron microscopic evidence. Efferent fibers of the substantia nigra project to the striatum and to certain thalamic nuclei. Ascending fibers from the nigral project rostrally into Forel's field H.

Nigrostriatal fibers are project dorsolaterally over the subthalamic nucleus and cross through the internal capsule. These fibers transverse parts of the globus pallidus en route to the caudate nucleus and putamen. There is a suggestion that nigrostriatal fibers are topographically organized in a manner reciprocal to that of strionigral fibers. Fibers in the caudal two-thirds of the nigral project to portions of the putamen, while rostral parts of the nigral appear related to the head of the caudate nucleus. Lateral parts of the caudal nigra project fibers to dorsal regions of the putamen, while medial regions are related to more ventral parts of the putamen.

Nigrostriatal fibers appear to arise mainly from the large cells of the pars compacta. The large cells of the pars compacta synthesize and transmit dopamine to axon terminals in the striatum where they are stored in varicosities. Strionigral and nigrostriatal fibers from a closed feedback loop. The afferent limbs of this loop (strionigral fibers) transmit GABA to the nigra, while the efferent limb of this loop conveys dopamine to the striatum. A neuron with acetylcholine as its transmitter may be interposed between nigrostriatal fibers and strionigral efferent neurons. Following lesions in the substantia nigra, dopamine in the nigrostriatal nerve terminals disappears.

Nigrothalamic fibers are arising primarily from cells of the pars recticularis, and project to:

1. The large-celled part of the ventral anterior nucleus (Vamc).
2. The medial part of the ventral lateral nucleus (VLm).
3. Parts of the dorsomedial nucleus (DMpl) (Carpenter, 1978).

3.1.3 Pathophysiology in Parkinson's disease

Many of these clinical features are also manifested by other basal ganglia disorders and often referred to as Parkinsonian syndromes (Table 3.1). Parkinsonian symptoms may occur with any disease that causes damage to nigrostiatal dopaminergic neurons or results in an imbalance diminishing the disinhibition in the indirect circuit.

Dopamine fibers in the substantia nigra pars compacta would normally increase the total disinhibition of the thalamus through both the excitatory D1 receptors in the direct circuit and the inhibitory D2 receptors in the indirect circuit. Thus, lesions of the pallidum, as well as those of the substantia nigra pars compacta, result in the appearance of Parkinson-like movement disorders (Table 3.2) (Dugan and Choi, 1999). The diagnosis is made clinically, although other disease with prominent symptoms and signs of Parkinsonism, such as post-encephalitic, drug-induced, and arteriosclerotic Parkinsonism, may be confused with Parkinson's disease until the diagnosis is confirmed at autopsy (Guttmacher and Collins, 2003).

Table 3.1 Striatal dopamine concentrations in Parkinson's disease and other neurodegenerative diseases **(**Dugan and Choi, 1999).

Disease	**% Normal Control Values**	
	Caudate nucleus	**Putamen**
Parkinson's disease	31	22
	10	4
	18	2
Postencephalitis Parkinsonism	6	6
	1.5	0.6
Parkinsonian syndromes		
Striatonigral degeneration	<0.4	<0.4
Steele-Richardson-Olszewski disease	20	27
Hallervorden-Spatz disease	1.4	0.9
Olivopontocerebellar atrophy	0.3	0.01
AIDS	43	-
Huntington's disease	86 (NSC)	99 (NSC)
Alzheimer's disease	61 (NSC)	50 (NSC)
Alzheimer's+ Lewy body pathology	16	5

(NSC: nonsignificant change)

Table 3.2 Classification of the various forms of Parkinsonism, based on differential etiology **(**Dugan and Choi, 1999).

Parkinson's disease	Idiopathic Parkinson's disease
Parkinsonian syndromes	Steele-Richardson-Olszewski disease Striatonigral degeneration Corticobasal degeneration Hallervorden-Spatz disease Wilson's disease Shy-drager syndrome
Symptomatic parkinsonism	Toxin-induced (e.g., MPTP, carbon monoxide, manganese) Drug-induced (e.g., reserpine, calcium antagonists, neuroleptics) Infectious (e.g., encephalitis lethargica, luetic) Vascular trauma Brain carcinomas

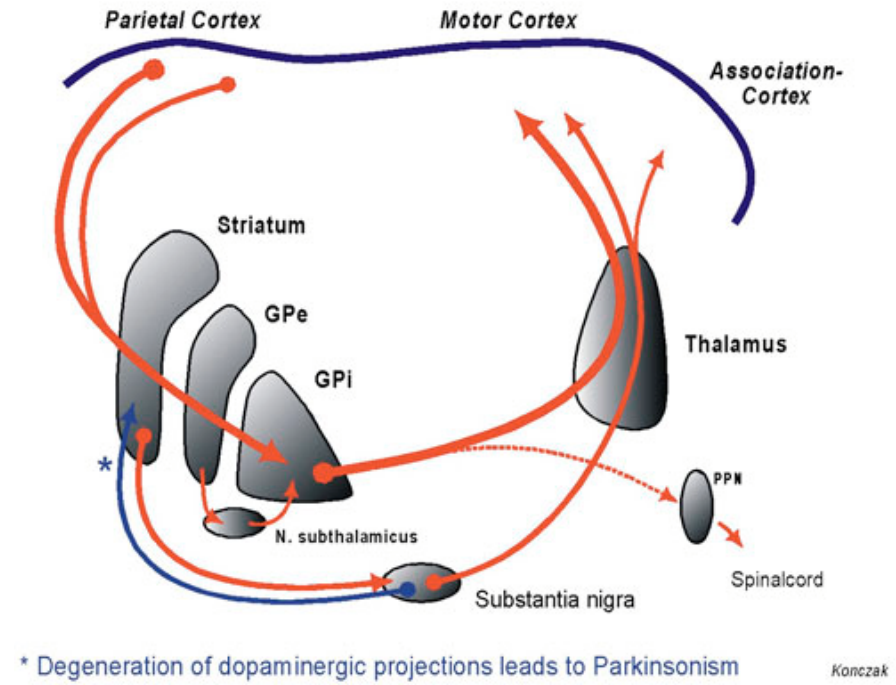

Figure 3.2 The schematic diagram of the efferent and afferent connections of the basal ganglia illustrates how the loss of dopamine producing cells in the substantia nigra affects the basal ganglia (striatum and GPe and GPi) and how this ultimately affects the activity of the motor cortex.

The diagram of the brain (Fig. 3.2) shows several structures related to Parkinson's disease. Basal ganglia affect normal movement and walking; substantia nigra is types of basal ganglia that produce the neurotransmitter dopamine, which sends messages that control muscles. The globus pallidus is part of a larger structure connected to the substantia nigra affecting movement, balance and walking. The thalamus serves as a relay station for brain impulses, and the cerebellum affects muscle coordination.

Though full-blown Parkinson's can be crippling or disabling, experts say early symptoms of the disease may be so subtle and gradual that patients sometimes ignore them or attribute them to the effects of aging. At first, patients may feel overly tired, "down in the dumps," or a little shaky. Their speech may become soft and they may become irritable for no reason. Movements may be stiff, unsteady, or unusually slow.

3.1.4 Genetic and Parkinson's disease

A genetic component in Parkinson's disease was long thought to be unlikely, because most patients had sporadic disease and initial studies of twins showed equally low rates of concordance in monozygotic and dizygotic twin. The view that genetic was involved in some forms of Parkinson's disease was strengthened, however, by the observation that monozygotic twins with an onset of disease before the age of 50 years do have a very high rate of concordance (much higher than that of dizygotic twins with early-onset disease).

However, the real advance occurred when a small number of families with early-onset, Lewy-body-positive autosomal dominant Parkinson's disease were identified. Investigation of these families of Mediterranean and German origin, led to the identification of two missense mutations (Ala 53Thr and Ala30Pro) in the gene encoding α-synuclein, a small presynaptic protein of unknown function (Polymeropoulos et al, 1997; Kruger et al, 1998).

The important of α-synuclein was greatly enhanced by the discovery that the Lewy bodies and Lewy neurites, found in Parkinson's disease, contain aggregates of α-synuclein (Spillantini et al, 1997). It is still unclear whether the aggregated of α-synuclein have a causative role or are simply marker for disease.

Lewy bodies not only found in the substantia nigra the locus ceruleus, and other brain stem and thalamic nuclei, but also in a more diffuse distribution, including the cortex in some patients as well as in dementia of the diffuse Lewy-body type (Louis and Fahn, 1996; Kosaka and Iseki, 1996). The aggregated of α-synuclein in glia is also a feature of multiple-systemic atrophy, leading to neurodengenerative disease that associated of α-synuclein called synucleinopathy (Guttmacher and Collins, 2003).

Autosomal recessive juvenile Parkinsonism is a rare case that shares many characteristics of Parkinsonism, including loss of nigrostiatal and locus ceruleus neurons and responsiveness to levodopa (L-dopa). It has a very early onset (before the age of 40 years), a slow in clinical course, and no Lewy bodies or Lewy neurites at autopsy (Matsumine et al, 1997).

Genetic mapping of the disease to chromosome 6q25-27 led to the identification of mutations for autosomal recessive juvenile Parkinsonism in a gene encoding Parkin

protein (Kitada et al, 1998). Parkin is expressed primarily in the nervous system and is one member of a family of E3 ubiquitin ligases, which attach short ubiquitin peptide chains to protein, a process called ubiquination. This was tagging them for degradation through the proteosomal degradation pathway (Guttmacher and Collins, 2003).

Autosomal recessive juvenile Parkinsonism is results from a loss of function of both copies of the Parkin gene, leading to autosomal recessive inheritance. In contrast, the missense mutations that alter α-synuclein will cause autosomal dominant inheritance. Recent evidence suggests that ubiquination by Parkin may be important in the normal turnover of α-synuclein (Shimura et al, 2001). The missense mutation in the gene coding a neuron-specific C-terminal ubiquitin hydrolase, is another gene that involved in ubiquitin metabolism (Leroy et al, 1998).

In addition to the α-synuclein, Parkin, and ubiquitin C-terminal hydrolase gene, at least five other loci have been proposed for autosomal dominant and autosomal recessive (Table 3.3).

Table 3.3 Single gene mutations in Parkinson's disease **(**Guttmacher and Collins, 2003).

Gene	Location	Mode of inheritance	Found
α-synuclein	4q21	Autosomal dominant	Greece, Italy, and Germany
Parkin	6q25-27	Autosomal recessive, may also be autosomal dominant	Ubiquitous
unknown	2p13	Autosomal dominant	Germany
unknown	4p15	Autosomal dominant	United states
ubiquitin C-terminal hydrolase	4p14	May be autosomal dominant	Germany
unknown	1p35	Autosomal recessive	Italy
DJ-1	1p36	Autosomal recessive	Netherlands
unknown	12p11.2-q13.1	Autosomal dominant	Japan

3.2 Oxidative stress and Parkinson's disease

Oxidative stress generally describes a condition in which cellular antioxidant defenses are inadequate to completely detoxify the free radicals being generated, due to excessive production of reactive oxygen species (ROS), loss of antioxidant defenses or, typically, both. This condition may occur locally, as antioxidant defenses may become overwhelmed at certain subcellular locations while remaining intact overall, and selectively with regard to radical species, as antioxidant defenses are radical-specific, for example, SOD for superoxide or glutathione for hydrogen peroxide (H_2O_2).

The brain has a number of characteristics, which make it especially susceptible to free radical-mediated injury. Brain lipids are highly enriched in polyunsaturated fatty acids (PUFA), and many regions of the brain, for example, the substantia nigra

and the striatum, have high concentrations of iron. Both of these factors increase the susceptibility of brain cell membranes to lipid peroxidation. Because the brain is critically dependent on aerobic metabolism, mitochondria respiratory activity is higher than in many other tissues, increasing the risk of free radical "leak" from mitochondria. Conversely, free radical damage to mitochondria in brain may be tolerated relatively poorly because of this dependent on aerobic metabolism.

A major consequence of oxidative stress is damage to cellular macromolecules. Addition of the free radical electron to fatty acid causes fragmentation of the lipid or alteration of its chemical structures. For example, the unconjugated *cis* double bounds in unsaturated fatty acids may be shifted to produce a conjugated *tran* double bound system. Peroxyl or hydroxyl groups may be added to the unsaturated fatty acid, or the fatty acid carbon chain may be cleaved during reaction with the free electron to generate a fatty aldehyde, both processes termed lipid peroxidation.

Fatty aldehydes such as 4-hydroxynonenal can then react with free thiol groups such as cysteines on proteins to produce thioesters, which may affect protein function and stability. Free-radical damage to proteins may cause cross-linking, carbonyl formation and protein denaturation. DNA bases may be modified by oxidation, resulting in single- and double-strand breaks or mispairing of purine and pyrimidine during DNA replication.

In addition, oxidative stress may trigger apoptosis. Exposure neurons to a free radical stress, either by application of H_2O_2, exposure to UV irradiation or depletion of antioxidant defenses, such as glutathione or superoxide dismutase (SOD), may trigger apoptosis. Free radicals not only serve as inducers of apoptotic cell death, they may also be a signal in the apoptotic cascade. Neurons deprived of growth factors demonstrate an early increase in oxygen free radical formation and can be rescued from growth factors deprivation-induced apoptosis by application of antioxidants. Thus, free radicals may serves as triggers, signals or effectors of neuronal apoptosis.

Persistent impairment of cellular energy metabolism may also play a role in triggering apoptotic cell death. Studies in cell culture and animal models by inhibited mitochondrial function by mitochondria toxins such as 3-nitropropionic acid or rotenones not only worsen excitotoxic injury but also trigger apoptotic neuronal cell death. Moreover, increased expression and enhanced concentrations of inflammatory

cytokines, such as interleukin-1β (IL-1β), tumor necrosis factor-α (TNF-α) and transforming growth factor β (TGFβ) are capable to trigger apoptosis in many cell types, including neurons (Dugan and Choi, 1999).

3.2.1 The effects of reactive oxygen species

Free radicals are molecules which posses an outer electron orbital with a solitary unpaired electron; these include the hydrogen atom ($H^{\bullet}$); the diatomic oxygen molecule (O_2), which posses two unpaired electrons with the same spin in two separate orbitals; $NO^{\bullet}$; superoxide ($O_2^{\bullet -}$); hydroxyl radicals ($^{\bullet}OH$); and transition metals, such as copper and iron.

While O_2 qualifies as a radical by having two unpaired electrons, its reactivity with nonradical compounds is limited because the unpaired electrons in O_2 have the same spin state. The two electrons in a covalent bound have opposite spins, so in order for O_2 to react with a nonradical, one of the electrons must undergo "spin inversion" so that both are anti-spin to the electrons on O_2, an extremely slow process. O_2 does react readily with radicals, accepting one electron at a time to form the very reactive superoxide radicals ($O_2^{\bullet}$), which has one unpaired electron.

Although some radical species may persist for prolonged periods, most are generally unstable and will attempt to donate their unpaired electron to a nearby molecule or to remove a second electron, usually in the form of a hydrogen atom, from a neighboring molecule to pair with their free electron. Free-radical reactions are intrinsic to a majority of the metabolic and synthetic reactions carried out by eukaryotic cells and are required for life.

ATP production by the mitochondrial electron chain, for example, uses a controlled set of oxygen radical reactions to couple the reaction of free-radical electrons with the movement of protons across the mitochondrial membrane. Cytochrome oxidase, complex IV of the mitochondrial electron transport chain, catalyzes transfer of these free electrons to molecular oxygen as the final acceptor with water as the end product.

The addition of oxygen to macromolecules, such as in the metabolism of arachidonic acid to the eicosanoids or the oxidation of small molecules by P450 enzymes, requires "activation" of molecular O_2 to permit transfer of atomic oxygen ($O^{\bullet}$) from O_2 to the biological compound. Most enzymes, which catalyze biological radical reactions, bind a metal ion (Fe, Cu, Co or the group VI element Se), which destabilizes the O_2 molecule. These reactions also involve cofactors such as flavin adenine dinucleotide (FAD) or flavin mononucleotide (FMN) to help stabilize the resulting oxygen atoms until the reaction is complete.

Although such reactions are generally very efficient, there is often some small amount of leak of ROS encompassing radicals such as $O_2^{\bullet-}$, its acid HO_2, hydroxyl radical ($^{\bullet}OH$) and $NO^{\bullet}$, as well as nonradicals such as hydrogen peroxide (H_2O_2), singlet oxygen ($^1O\Delta g$) and hydrochlorous acid (HOCl). While H_2O_2 is not a free radical, it can be rapidly decomposed via the Fenton reaction:

$$Fe^{2+} + H_2O_2 \longrightarrow Fe^{3+} + {}^{\bullet}OH + OH^-$$

In addition, superoxide, hydrogen peroxide and hydroxyl radical can be converted via the Haber-Weiss reaction:

$$Fe^{3+} + O_2^{\bullet-} \longleftrightarrow Fe^{2+} + O_2$$

$$Fe^{2+} + H_2O_2 \longrightarrow Fe^{3+} + {}^{\bullet}OH + OH^-$$

$$O_2^{\bullet-} + H_2O_2 \longrightarrow {}^{\bullet}OH + OH^- + O_2$$

Cuprous and cupric ions may substitute for ferrous and ferric ions in the Haber-Weiss reaction. Peroxynitrite can be formed from reaction of NO with superoxide via this reaction (Dugan and Choi, 1999):

$$NO^{\bullet} + O_2^{\bullet-} \longrightarrow ONOO^- \longrightarrow NO_2^{\bullet-} + {}^{\bullet}OH$$

3.2.2 Reactive oxygen species in Parkinson's disease

Although the etiology of PD is unknown, numerous theories, including damage of striatal neurons by endogenous and exogenous neurotoxins, have been proposed (Ebadi et al., 2001). The theory related to endogenous neurotoxin formation is based on the hypothesis that the loss of dopaminergic neurons in PD results in enhanced metabolism of dopamine (DA), enhancing the formation of H_2O_2, which in turn produced hydroxyl radicals ($OH^{\bullet}$) according to the following reactions:

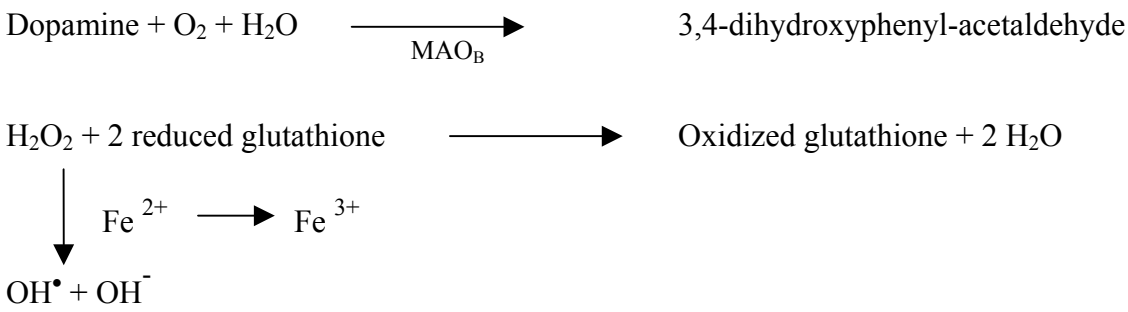

Another factor imposing increased oxidative stress is the accumulation of iron and progressive siderosis of SN. In addition, the level of ferritin, an iron-binding protein, is reduced in the SN and hence aggravating the iron-induced and hydroxyl radical-mediated lipid peroxidation. An increase in the activity of mitochondrial superoxide dismutase in the SN in PD may indicate a compensatory mechanism to nullify the augmented oxidative stress.

The contribution of genetic factors to the pathogenesis of PD is being increasing recognized. A point mutation that is sufficient to cause a rare autosomal dominant form of the disease has recently been identified in the α-synuclein gene on chromosome 4 in the much more sporadic, or 'idiopathic', form of PD, and a defect of complex I of the mitochondrial respiratory chain was confirmed at the biochemical level. Disease specificity of this defect has been demonstrated in SN (Ebadi et al., 2001).

Current concepts as to the cause of PD suggest an inherited predisposition to environmentally or endogenously produced toxic agents causing oxidative damage to

nigral cells for the following reasons: The level of reduced glutathione in SN is decreased. The depletion of reduced glutathione in the SN in PD could be the result of neuron loss. As a matter of fact, a positive correlation has been found to exist between the extent of neuronal loss and the depletion of glutathione. A decrease in the availability of reduced glutathione would impair the capacity of neurons to detoxify hydrogen peroxide (H_2O_2) and increase the risk of free radical formation and lipid peroxidation. Indeed, the SN contains increased malondialdehyde and hydroperoxides (Ebadi et al., 1996).

3.2.3 Mitochondria and energy production

Mitochondria are sausage-shaped organelles which feature a smooth outer membrane and an involutes inner membrane. The inner and outer membranes are fairly close together. The space between is referred to as the intermembrane space. The inner membrane contains the proteins and enzymes of the electron transport chain (Complexes I-V) which are responsible for oxidative phosphorylation (the generation of ATP from oxygen). The innermost space is called the matrix, which contains many enzymes of the citric acid cycle (and the mitochondrial DNA).

Figure 3.3 An electron microscopic picture of mitochondria.

The production of ATP is driven by the energy of oxidation. At its most simplistic level, hydrogen (a source of electrons) is combined with oxygen (which is electron-poor) to generate energy. In more detail, NADH electrons (donated to Complex I) are combined with atmospheric oxygen (provided to Complex IV) to pump protons (H+) from the mitochondrial matrix across the inner membrane into the inter-membrane space. The proton "pressure" is tapped by allowing the protons to flow back through Complex V to generate ATP.

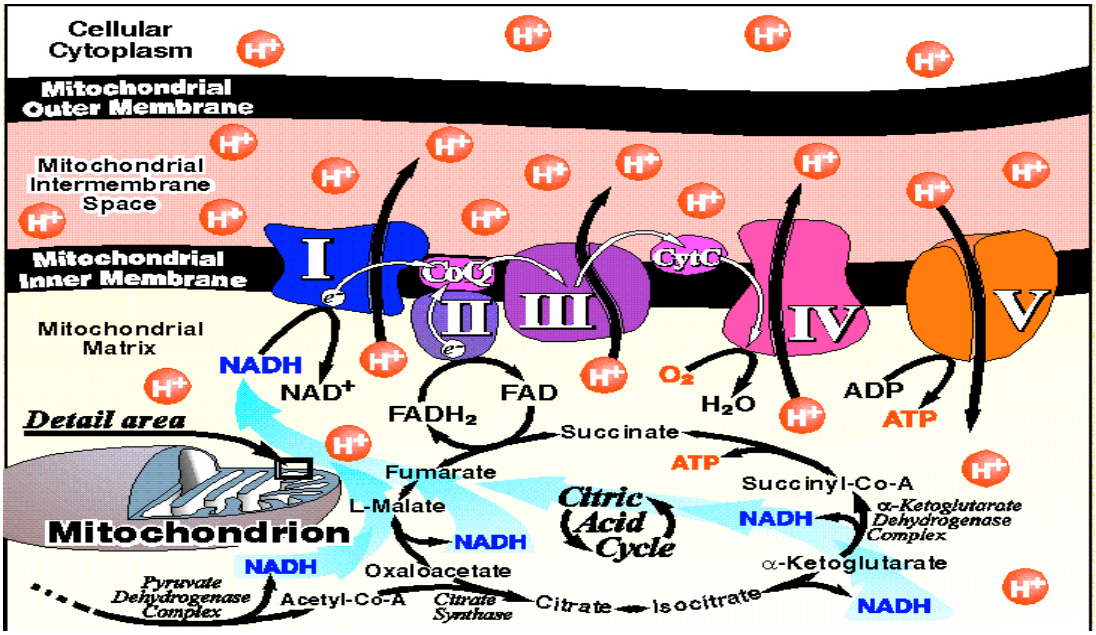

Figure 3.4 Schematic diagram represents the energy production in mitochondria.

In addition to the main electron transport path from Complex 1 to Complex III to Complex IV, there is a second path from Complex II to Complex III to Complex IV. The two paths converge at coenzyme Q, which serves as a mobile electron transfer agent linking Complexes I and II with Complex III. Complex 1 gets its electrons from NADH (reduced nicotinamide adenine dinucleotide), a niacin-derived nucleotide that is loosely associated with three dehydrogenase enzymes of the citric acid cycle that are distributed throughout the mitochondrial matrix.

Complex II gets its electrons from FADH2 (reduced flavin adenine dinucleotide), a riboflavin-derived nucleotide that is closely associated with succinate dehydrogenase, a flavoprotein enzyme that is localized on the inner surface of the inner mitochondrial membrane. Succinate dehydrogenase is the only enzyme of the citric acid cycle that is membrane bound. Each turn of the citric acid cycle generates three NADH and one FADH2. The three NADH feed Complex I and the one FADH2 feeds Complex II to keep the process of oxidative phosphorylation (oxygen-derived ATP production) at full flux. Each NADH molecule generates three ATP (one from Complex I, one from Complex III and one from Complex IV) and each FADH2 generates two ATP (one from Complex III and one from Complex IV) for a total of eleven ATP per revolution of the citric acid cycle. Since the citric acid cycle generates one ATP by itself, a total of a dozen ATP are produced per revolution.

3.2.4 Mitochondria and reactive oxygen species

Mitochondria were among the earliest sites of cellular ROS production to be identified. Studied on isolated mitochondria have suggested that as much as 3% of oxygen utilization by resting mitochondria may be lost as leak of ROS, although this estimate may be high.

Mitochondrial production of ROS can be enhanced by increased electron transport activity, as well as by disturbances in electron transfer down the transport chain. The lipid electron-transport molecule ubiquinone (Q_9, Q_{10}) is the major site of free radical leak from the mitochondria via the ubiquinone cycle.

Ubiquinone undergoes a two-electron reduction, first to a semiquinone and then to a diol, at mitochondria complex I (NADH dehydrogenase, NADH: ubiquinone oxidoreductase) or complex II (succinate dehydrogenase) and subsequently delivers the two-electrons to the iron-sulfur center of complex III (cytochrome bc_1 in mammalian mitochondria).

Inhibition of either complex I or complex III will impair the efficiency of electron transfer and may allow a free semiquinone to be produced. The semiquinone can then interact with O_2 to generate $O_2^{\bullet -}$. Elevated intracellular Ca^{2+}, exposure to fatty acids or other molecules which alter the physical properties of the mitochondrial

membrane and inhibition of mitochondrial respiratory components may enhance this leak of ROS from mitochondria.

Mitochondria appear to be an important and, perhaps, even dominant source of free radicals in brain tissues. Microdialysis studies show that mitochondria inhibitors such as rotenone eliminate ROS production. Elevated concentrations of intracellular Ca^{2+}, and Na^{+}, a consequence of energy failure and excitotoxic glutamate receptor stimulation can be expected to inhibit complex I as well as overproduction of superoxide anion. The resultant oxidative stress may leads to further inhibition of mitochondria respiratory components, promoting further free radical production in a vicious, feed-forward cycle (Dugan and Choi, 1999).

3.2.5 Brain antioxidant defense mechanisms

The high metabolic rate of brain cells implies a high baseline ROS production, and brain cells have high concentrations of both enzymatic and small molecule antioxidant defenses. SOD1 may represent as much as 1% of total protein in brain; it converts $O_2^{\bullet -}$ to H_2O_2, which is then further metabolized to water and oxygen by catalase and glutathione peroxidase.

The SOD1 gene is located on chromosome 21 and codes for a 16- to 18-kDa subunit, which binds one Cu^{2+} and one Zn^{2+}; the active enzyme is a homodimer. SOD2 is a homotetramer and the gene is on chromosome 6. An extracellular, glycosylated form, SOD3, has been shown in rodents to overlap in activity with SOD1. Several other enzymes unrelated to CuZn-SOD, for example, the atx1-HAH gene product, are also capable of acting as SODs.

Catalase and glutathione peroxidase provides two important cellular systems for eliminating H_2O_2. Catalase, a 56-kDa cytosolic hemeprotein homotetramer that can act without a cofactor, although it may bind NAD(P)H, functions as a peroxidase to convert H_2O_2 to water. It can be irreversibly inactivated by oxidation. Catalase is more abundant in astrocytes than in neurons and in white matter than in grey matter, but it can be induced in neurons by neurotrophins. There is a substantially less catalase activity in brain than in other tissues, such as liver.

The human genes have been identified for four members of glutathione peroxidase family of selenoproteins. Classical glutathione peroxidase (GPx1) is a complex of four 23-kDa subunits. Plasma GPx (GPx3), GPx2 and a fourth enzyme, phospholipid hydroperoxide glutathione peroxidase (PHGPx), are monomers with extensive homology to classical GPx1.

All four enzymes contain one selenium atom per subunit in the form of selenocysteine and use all glutathione (GSH) as a cofactor peroxidase to convert H_2O_2 to water. PHGPx is unique in its ability to detoxify not only H_2O_2 but fatty acid and cholesterol lipid hydroperoxides directly.

In addition, it has a cytosolic isoform and an isoform with mitochondrial targeting sequence. Both GPx1 and PHGPx proteins are present in the brain. The components of the glutathione peroxidase system, GPx, GSH, glutathione reductase and NAD(P)H, are present in the mitochondria as well as the cytoplasm. Several other proteins, including glutathione S-transferase, may contribute minor peroxidase activity.

Small-molecule antioxidants include glutathione, ascorbic acid (vitamin C), vitamin E and a number of dietary flavenoids. Because humans, in contrast to most other animals, are unable to synthesize vitamin C, this important antioxidant must be supplied entirely from dietary intake. Other proteins, such as thioredoxin and metallothionein, may also contribute to some extent to the cellular antioxidant pool (Dugan and Choi, 1999).

3.2.6 Glutathione and Parkinson's disease

The tripeptide glutathione (GSH; γ-L-glutamyl-L-cysteinlglycine) is the cellular thiol present in concentration up to 12 mM in mammalian cells. It has important functions as antioxidant, is a reaction partner for the detoxification of xenobiotica, is a cofactor in isomerization reactions, and is a storage and transport form of cysteine. In addition, glutathione is essential for cell proliferation and maintain the thiol redox potential in cells keeping sulfhydryl groups of proteins in the reduced form. Recent studies suggest that glutathione plays a role in the regulation of apoptosis.

The glutathione system (Fig. 3.5) is very important for the cellular defense mechanism. A high concentration of glutathione protects against a variety of different ROS. GSH reacts directly with radicals in non-enzymatic reactions and is also an electron donor in the reduction of peroxides catalyzed by glutathione peroxidase (GPx). It should be noted that the glutathione system is only part of the cellular defense mechanism. Other enzymes, such as SOD and catalase, as well as antioxidants, such as ascorbate and α-tocopherol, are also involved in ROS detoxification. These compounds, their metabolism of action as well as their interaction with the glutathione system have been review (Dringen, 2000).

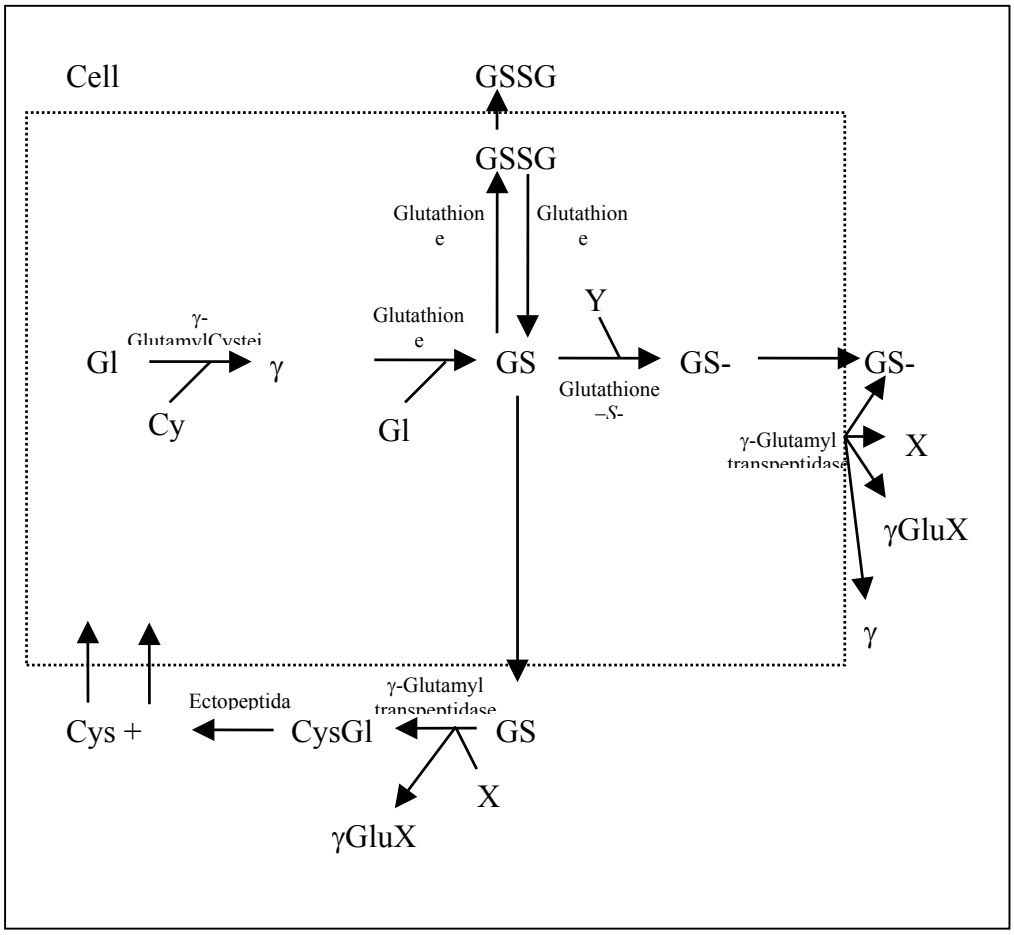

Figure 3.5 Schematic diagram presents glutathione metabolism within the cell membrane.

3.2.7 Metallothionein and Parkinson's disease

Metallothionein (MT) isoforms are low molecular weight (6000-7000) zinc-binding proteins containing 60-61 amino acid residues, 25-30% cysteine, no aromatic amino acids or disulfide bonds, and binging 5-7 g zinc/mole of protein. The mammalian MT family consists of 4 similar but distinct isoforms, designated as MT I-IV. MT I and MT II isoforms were first identified in rat brain. MT III containing 68 amino acids also known as a growth inhibitory factor and MT IV is expressed in stratified squamous epithelia. MT isoforms are found in glial cells as well as in neurons.

MT has been proposed to participate in transport, accumulation, and complementation of zinc in various brain regions, including the areas that have high concentration of zinc such as hippocampus. MT keeps the cellular concentration of free zinc very low, acting as a reservoir, releasing zinc in a process that is dynamically controlled by its interaction with both reduced (GSH) and oxidized glutathione (GSSG). Moreover, MT possesses 18-20 cystein residues; it is the most abundant and important thiol source in the brain. In those cells that can express MT genes, they are transcriptionally regulated by metals, glucocorticoid hormones, and cytokines.

6-Hydroxydopamine (6-OHDA), which generates free radicals and causes Parkinsonism in animal experiments, enhances the level of MT I mRNA in some brain areas such as hippocampus, arcuate nucleus, choroids plexus, and granular layer of cerebellum, but not in caudate and putamen. The results in these studies are interpreted to suggest that zinc or MT is altered in conditions where oxidative stress has taken place.

Moreover, it is proposed that areas of the brain, such as striatum containing high concentrations of iron but low levels of inducible MT, are particularly vulnerable to oxidative stress. Since both superoxide and hyhroxyl radicals are generated in excess in substantia nigra of Parkinson's disease patient and MT I and II isoforms are able to scavenge superoxide anions and hyhroxyl radicals, an augmentation of glutathione and MT levels may have potentially therapeutic benefits in attenuating oxidative

stress in neurodegenerative disease, including Parkinson's disease (Ebadi and Hiramatsu, 2000).

3.3 Distribution of Iron in the Brain

Iron is found throughout the brain, but the basal ganglia contained the highest levels (Hallgren and Sourander, 1958). However, both biochemical and histochemical studies indicate that white matter is a major site of iron concentration throughout the brain. Iron uptake into the brain is maximal during rapid brain growth, which coincides with the peak of myelinogenesis, although brain uptake of iron continues throughout life, with homogeneous uptake followed by redistribution to the basal ganglia. Magnetic resonance imaging (MRI) has recently been used to map iron distribution in the brains of children and adolescents. The highest concentrations are found in the globes pallidus, caudate nucleus, putamen, and SN, whereas the cortex and cerebellum contain substantially lower concentrations (Aoki, et al., 1989).

3.3.1 Iron Metabolism in the Central Nervous System

Iron (Fe) is essential for most organisms due to it participates in many critical metabolic processes including oxygen transport, electron transport, DNA synthesis, redox/non-redox reaction, and other cell functions (Lieu et al., 2001; Eisenstein, 2000). Cellular iron concentrations must be highly control by low iron solubility and the ability of iron to form toxic reactive oxygen species (free radicals) in most biological systems (Eisenstein, 2000).

One role of iron in the central nervous system (CNS) is for the biosynthesis of the neurotransmitters, dopamine (Rouault, 2001) and serotonin (D'Sa et al., 1996). It is important in the formation of myelin (Connor and Menzies, 1996), and also acts as an essential component of enzymes of oxidative metabolism, such as those catalyzed by the cytochromes and iron-sulfur enzymes.

In mammalian brains, iron accumulation increase with age by selective uptake in regions undergoing myelination (Connor et al., 1995). The accumulation of iron in humans occurs during adolescence in motor areas such as motor cortex and substantia

nigra (Connor et al., 1992; Aoki et al., 1989). Iron stores gradually increase until about age 40 and then remain steady (Bartzokis et al, 1997). Many of these iron-dependent events within the CNS are function of age, as is the case with myelination, or are regions specific, as is the case with dopamine synthesis in substantia nigra neurons (Connor et al., 2001).

In CNS, brain energy requirements are high, with particular demand for ATP as the principal energy source for stable cellular ionic gradients, synaptic transmission and axoplasmic transport (Connor et al., 2001). Thus, it is not surprising that Fe-related mitochondrial dysfunction has been associated with neurodegeneration (Beal, 1998). During CNS oxidative metabolism, free radicals are normally produced and metabolized, but an excess of free Fe results in rapid formation of toxic reactive oxygen species that may be one mechanism of CNS cell death in neurodegeneration (Connor et al., 2001).

3.3.2 Iron Uptake and Transport

In the brain iron uptake is limited by the blood-brain barrier and cerebrospinal fluid (CSF) barrier (Morris et al., 1992; Bradbury, 1997) maintained by tight junctions between microvascular endothelial cells and choroid plexus epithelium. Thus, CNS-related expression of transport proteins is required for iron uptake (Connor et al., 2001).

Iron uptake into the brain is mediated in part by transferrin receptor expression in the endothelial cells and choroid plexus cells (Moos, 1996) or lactoferrin receptor expression on neurons and microvessels (Kawamata et al., 1993; Leveugle et al., 1994). The Fe-transferrin complex or Fe-lactoferrin undergoes endocytosis, followed by release of Fe within the endothelial cell uptake (Connor et al., 2001).

Ceruloplasmin is a brain specific protein that involves in the movement of iron from cytosol to the extracellular spaces. It is expressed as a membrane anchored protein (Patel et al., 2000) and in situ hybridization reveals abundant of ceruloplasmin gene expression in specific populations of perivascular glial cells associated closely with dopaminergic melanized neurons in the substantia nigra (Klomp and Gitlin, 1996).

The subsequent transport of Fe into other areas of the brain is likely mediated by transferrin and non-transferrin-bound mechanism (Moos and Morgan, 2000). Serum transferrin is not found within the CNS unless there is a break down of the blood-brain barrier (Crowe and Morgan, 1992). Thus, the CNS must synthesis its own transferrin, a synthesis that is regulated by a nervous system-specific promoter (Rouault, 2001; Bowman et al., 1995). Cellular uptake may be stimulated by ceruloplasmin ferroxidase activity by means of a recently reported trivalent cation-specific transport mechanism (Attieh et al., 1999).

The divalent metal transporter 1 (DMT1, Nramp2) has been implicated in transport iron from endosomes and is localized in neurons and oligodendrocytes, which show a significantly decreased iron content in the Belgrade rat with a mutation in DMT1/Nramp2 (Burdo et al., 1999). Alternatively, Fe may be transport by glial cell processes, from astrocyte foot processes that surround the microvasculature, through the astrocyte cell extensions to remote areas (Qian et al., 2000)

Redistribution studies of cerebral iron show regional movement of iron that use axonal transport mechanisms to the area of axon projections (Dwork et al., 1990). Ferritin binding, presumably due to receptors, is distributed in iron-rich areas of the brain in contrast to the transferrin receptor that located primarily in the grey matter (Hulet et al., 1999). As a result, ferritin receptor binding has been postulated to play a role in iron uptake since its distribution were correlated with brain iron accumulation.

3.3.3 Iron Storage

Ferritin, a cytosolic protein, binds and stores intracellular iron in most cells within the CNS and prevents it from forming reactive oxygen species (Lieu et al., 2001). Ferritin synthesis occurs in the neuronal cell body and holoferritin is transported by axoplasmic flow within axons where it may be degraded by lysosomes (La Vaute et al., 2001; Donovan et al., 2000).

The expression of ferritin is induced by the presence of excess iron (Lieu et al., 2001). Intact human ceruloplasmin appears to be required for the incorporation and loading iron into ferritin (Van Eden and Aust, 2000).

Neuromelanin is another major iron storage mechanism in certain neuronal system such as the substantia nigra (Double et al., 2000). Intraneuronal membrane-bound Neuromelanin has a strong chelating ability for iron and may be another mechanism of intracellular iron sequestration (Zecca et al., 2001).

3.3.4 Intracellular Iron Utilization

Iron may be involve in many metabolic processes such as a cofactor for the enzymes, tyrosine hydroxylase and tryptophan hydroxylase, in the synthesis of dopamine and serotonin in neuron or incorporation into iron-sulfur cluster-containing proteins (Connor et al., 2001). This is also essential for the biosynthesis of CNS lipids and cholesterol, the important building blocks of myelin and as a co-factor for metabolic enzymes in oligodendroglia (Connor and Menzies, 1996).

Mitochondria is a particularly critical site of intracellular iron utilization since this organelles where iron is incorporated into protoporphyrin IX to form heme and where vital non-heme proteins, cytochromes *a, b*, and *c*, and cytochrome oxidase that are required for mitochondrial function (Connor et al., 2001).

Mitochondrial iron sequestration has been shown in dopamine-challenged astrocytes, providing a possible alternative pathogenetic mechanism for iron accumulation, mitochondrial damage and oxidative injury in neurodegenerative disease (Schipper et al., 1999).

Frataxin is another protein that involved in iron utilization. It has been shown localized to the mitochondrial membranes in several tissues, including the CNS (Campuzano et al., 1999). The crystal structure findings predict mechanisms of protein-protein and protein-iron interactions similar to ferritin suggest that frataxin may serve an iron storage function in mitochondria (Roy and Andrews, 2001).

3.3.5 Iron Recycling and Export

Most of iron in the brain and human body is extensively recycling and reused. Transferrin-bound Fe in the interstitial fluid could exit the CNS through the arachnoid villi that normally participate in the exit of CSF into the venous system.

Alternatively, vascular endothelial cells could export transferrin-bound iron back into the circulation (Rouault, 2001).

In addition, heme oxygenase (HO) is present in the brain in two forms (HO-1 and HO-2) that appear to have more functions than recycling alone (Maines, 2000). A high level of HO, especially in form of HO-2, was found in the substantia nigra (Calabrese et al., 2002). HO-1 appears to be involved in mitochondrial iron trapping via the mitochondrial transition pore which mediates the transfer of non-transferrin iron into mitochondria (Schipper et al., 1999).

Recent studies found cells from mice with a target deletion of the HO-1 gene demonstrated reduce iron efflux in HO-1-deficient fibroblasts (Ferris et al., 1999), suggesting a possible mechanism for intracellular iron accumulation and cell death.

3.3.6 Iron Homeostasis

Some fundamentals of CNS iron homeostasis remain unknown but animal models of iron metabolism dysregulation produced by target genetic deletions may uncover clues to these basic mechanisms. For example, iron regulatory protein-2 (IRP2) gene deletion in mice results in iron accumulation in distinctive brain regions and is associated with iron overload in degenerating neurons and in oligodendrocytes with ubiquitin positive inclusions. This lead to a neurodegenerative disease in IRP2-/- mice (La Vaute et al., 2001) suggesting possible contribution to the pathogenesis of comparable human neurological disease.

The function of haemochromatosis gene, *HFE*, in the brain is unclear but *HFE* protein has been localized to vascular endothelial cells in the cortex and cerebellum (Bastin et al., 1998). However, hereditary haemochromatosis, a disease typically associated with systemic iron overload, has not been associated with excessive brain iron levels or neurodegenerative disease. Recent studies found that high circulatory iron levels could cause brain iron accumulation (Moos et al., 2000), suggesting that there is exclusion of excess plasma iron from transfer into the brain.

3.3.7 Deferoxamine: An iron chelator agent

Deferoxamine (DFO; deferoxamine B mesylate) a bacterial siderophore and potent iron chelator used in conditions of iron overload (Torti et al., 1998). It is known to inhibit DNA synthesis and cell proliferation both in vivo and in vitro (Dezza et al., 1989; Cazzola et al., 1990). DFO is generally though to inhibit the iron-requiring enzyme ribonucleotide reductase, thereby alter the supply of deoxyribonucleotides and decreasing DNA synthesis (Hoffbrand et al., 1976).

Iron chelators have been shown to reduce iron overload-induced tissue damage in the cardiovascular system, protect against ischemia-induced brain injury (Wolfe et al., 1985; Krause et al., 1986), and protect dopaminergic neurons from the toxic effects of 6-hydroxydopamine (Ben-Shachar et al., 1991).

Growth inhibition by DFO was a disadvantage of it; this has been reported at different points of the cell cycle, as shown by accumulation at the G1 and apoptosis, in human myelocytic leukemia cell lines HL-60 and ML-1 (Fukuchi et al., 1994; Fukuchi et al., 1995).

3.4 Iron-mediated oxidative stress and Parkinson's disease

Free iron, more than other transition metal, has been implicated in redox transitions and consequential generation of oxygen free radicals (Campbell et al., 2001). Increased in total brain iron content is a feature of some neurodegenerative disease and an increased concentration has been found in specific brain regions. An abnormally high level of iron and oxidative stress has been demonstrated in a number of neurodegenerative diseases, including Parkinson's disease.

In Parkinson's disease, there is an increased in ferritin levels (Hirsch and Faucheux, 1998) and the iron deposits are found within degenerating neurons in the substantia nigra undergoing apoptosis and in Lewy bodies (Bartzokis et al., 1999). Because Fe is sequestered in substantia nigra and Lewy bodies (Castellani et al., 2000), increased iron transport into the substantia nigra and basal ganglia or redistribution of ferritin or Neuromelanin stores is suspected (Hirsch and Faucheux, 1998). Exactly how increased regional or cellular brain iron is involved in

pathophysiology of the disease is uncertain but there are several possible mechanisms. A pivotal role of iron in the pathogenesis of Parkinson's disease has been emphasized because of its capacity to enhance the production of oxygen radicals via Fenton reaction and accelerate neuronal degeneration. (Berg et al, 2001).

Total iron levels were decreased in the globus pallidus in PD. There were no consistent alterations of manganese levels in basal ganglia structures in any of the diseases studied. Copper levels were decreased in the SN in PD, and in the cerebellum in PSP, and were elevated in the putamen and possibly SN in HD. Zinc levels were only increased in PD, in SN and in caudate nucleus and lateral putamen.

Dexter et al., (1991) measured the levels of iron, copper, zinc and manganese by inductively coupled plasma spectroscopy in frozen postmortem brain tissue from patients with PD, progressive supranuclear palsy (PSP), multiple system atrophy with strionigral degeneration (MSA), and Huntington's disease (HD) compared with control subjects. Total iron levels were found to be elevated in the areas of basal ganglia showing pathological change in these disorders. In particular, total iron content was increased in SN in PD, PSP and MSA, but not in HD. Total iron levels in the striatum (putamen and/or caudate nucleus) was increased in PSP, MSA and HD but not in PD.

Levels of the iron binding protein ferritin were measured in the same patient groups using a radioimmunoassay technique. Increased iron levels in basal ganglia were generally associated with normal or elevated levels of ferritin immunoreactivity. The exception was PD where there was a generalized reduction in brain ferritin immunoreactivity, even in the SN.

Alternatively, the presence of high iron levels in Lewy bodies and senile plaques in Parkinson's disease suggests a possible relationship. Iron and oxidative stress might result in the damage and aggregation of proteins. In fact, in vitro iron has been shown to promote α-synuclein aggregation, reminiscent of Lewy bodies or amyloid (Hashimoto et al., 1999).

Hydroxyl radicals and other oxygen-free radicals are produced during normal brain metabolism (Hirsch and Faucheux, 1998). A significantly higher plasma levels of hydroxyl radicals was found in Parkinson's disease (Ihara et al., 1999), together with increased lipid peroxidation products in CSF and brain (Miyajima et al., 1998;

Yoshida et al., 2000), suggesting a role in neurodegeneration. Subsequently, the ubiquitin-proteosome system, essential for non-lysosomal catabolism, could fail to adequately clear damaged or aggregated proteins in CNS (McNaught et al., 2001).

It is noteworthy that iron associated with Neuromelanin significantly accumulates within the substantia nigra in Parkinson's disease (Bartzokis et al., 1999) and it has been suggested that this mechanism may play a role in the selective neurodegeneration seen in Parkinson's disease (Good et al., 1992).

HO immunoreactivity is greatly enhanced in Lewy bodies found in the substantia nigra of Parkinson's disease patients brain (Schipper, 2000). MPTP, a specific neuronal toxin found in the substantia nigra that cause parkinsonism, selectively induces HO expression in striatal astrocytes (Fernandez-Gonzalez et al., 2000), suggesting a possible role of HO in the pathogenesis of Parkinson's disease.

Lactoferrin is structural similar to transferrin and binds iron reversibly but the exact function of lactoferrin and lactoferrin receptor still remain unknown. Expression of lactoferrin receptor on neurons and microvessels has been found to be increased in mesencephalon of postmortem Parkinson brain tissue and suggest the possible link to iron overload in affected brain regions (Faucheux et al., 1995).

Although the etiology of PD and related neurodegenerative disorders is still unknown, recent evidence from human and experimental animal models suggests that a misregulation of iron metabolism, iron-induced oxidative stress and free radical formation are major pathogenic factors. These factors trigger a cascade of deleterious events leading to the ensuing biochemical disturbances of clinical relevance and neuronal death (Jellinger, 1999).

3.5 Transcription factors in the central nervous system

Transcription factors are categorized as *tran*-acting factors because they are regulatory agents, which are not part of the regulated gene. These *tran*-acting factors regulate gene transcription by binding directly or though an intermediate protein to the gene at a particular DNA sequence called a *cis*-regulatory region.

The *cis*-regulatory region is usually located in the 5'-flanking promoter region of the gene and is composed of a specific nucleotide sequence. There is also a class of

cis-regulatory elements called enhancers, which can be positioned anywhere in the gene and, consequently, are not restricted to the promoter region. Binding of the *tran*-acting factor to the *cis*-regulatory region alters the initiation of transcription, probably through a direct interaction of the *tran*-acting factor with the RNA-polymerase complex. This binding likely occurs to the secondary and tertiary structures of genomic DNA-protein complexes. Usually, transcription factors bind as dimers to the DNA, suggesting that there are dimerization sites on transcription factors, as well as DNA binding sites.

There are several types of transcription factors, which are grouped by virtue of sequence similarities in their protein interaction and/or DNA-binding domain. Similarities in protein-protein interaction sites suggest that monomers of different transcription factors can interact to form heterodimers. An individual heterodimer may bind to multiple *cis*-acting elements or, alternatively, interact with differing affinity for the same *cis*-acting element as compared with the homodimer. Indeed, these types of protein interactions do occur and provide a major source of regulatory complexity.

A particular *cis*-acting element may be present in multiple genes so that activation of a single transcription factor has potential for altering the expression of multiple target genes. Furthermore, an individual transcription factor may increase transcription of one gene while decreasing transcription of another gene. This difference is partly due to the positioning of the *cis*-acting element relative to the start of transcription, as well as to the identity of the protein partners in the heterodimer complex.

It is important to note that, with the increase in sequence information being generated by the Human Genome Project, *cis*-acting elements can be found in genes, suggesting potential gene regulatory mechanisms without any biological information. While *cis*-acting element sequence identification in a gene is indeed predictive and necessary, this is often not sufficient to fully characterize the transcriptional regulation of that gene. *cis*-Acting elements for a particular gene are commonly nonfunctional in all tissues and, even more often, silent in one tissue and active in another due to the differential distribution of transcription factors (Eberwine, 1999).

The response to severe oxidative stress may involve an additional effect in which redox-sensitive factors can be directly activated or inactivated through the oxidation of sulfhydryl residues. The DNA binding activity of transcription factors, such as AP-1, Sp-1, Egr-1, NF-κB, c-myb and p53, is also reduced or lost when critical cystein residues are oxidized or alkylated (Nose, 2000).

3.5.1 Nuclear factor kappa B and Apoptosis in Parkinson's disease

The nuclear factor kappa B (NF-κB) is composed of homo- and heterodimers of members of the Rel family of related transcription factors that are well characterized for controlling the expression of numerous immune and inflammatory response genes. Frequently, NF-κB is present as a heterodimer comprising a 50-kDa (p50) and a 60-kDa (p65) subunit that is sequestered in the cytoplasm by an inhibitory protein of the IκB family, with IκBα being the best characterized member of this family. NF-κB-inducing agents, such as cytokines, viruses, phorbol esters, and UV light, result in the phosphorylation and degradation of the IκB inhibitory protein allowing free NF-κB to enter nucleus, to bind to its cognate DNA sequences, and to induce target gene transcription (Heck et al, 1999).

Oxidative stress-induced neuronal cell death appears to be involved in certain neurodegenerative disease such as Alzheimer's and Parkinson's disease. Among NF-κB-inducing agents, reactive oxygen species (ROS) are widely used, and recent evidence strongly suggests that NF-κB may afford neuroprotection against oxidative insults in particular with respect to Alzheimer's disease. The situation is, however, much less clear in PD (Blum et al, 2001). Nuclear translocation of NF-κB is increased in dopaminergic neurons in PD post-mortem brains suggested that oxidative stress might be related to apoptotic death in PD through NF-κB-related signal transduction (Hunot et al, 1997).

At nontoxic concentrations, iron is known to promote macrophage functions, including antimicrobial effects and tumor necrotic factor (TNF)-mediated cytotoxicity. More specifically, recent evidence suggests the role of iron in promoting cytokine expression and NF-κB activation by hepatic macrophage (She et al, 2002).

Compounds that have antioxidant properties, such as DFO (Ferric iron chelator), PDTC (radical scavenger and metal chelator) and TEMPO (Ferric iron chelator and ROS scavenger), or lipid peroxidation (BHA) all inhibited NF-κB activation. These suggested that it may be due to iron-catalysed lipid peroxidation, rather than ROS generation, had a role to play in TNF-mediated NF-κB activation (Bowie and O'Neill, 2000).

3.6 Cell lines and Model for studying Parkinson's disease

Tissue culture was a technique devised as a method for studying the behavior of animal cells free of systemic variations that might arise in the animal both during normal and stress of an experiment. Tissue culture was used as a generic name for organ culture and cell culture.

The term organ culture implied to a three-dimensional culture of undisaggregated tissue retaining some or all of the histological features of the tissue in vivo. Whereas, cell culture was refer to a culture derived from dispersed cells taken from original tissue, primary cell culture, cell lines or cell strain by enzymatic, mechanical, or chemical disaggregation.

The demonstration that human tumors could give rise to continuous cell lines and show the finite life span of cells in culture, encourage interest in human tissue studied. The cultivation of human cells received a further stimulus when a number of different serum-free selective media were developed for specific cell types, such as epidermal keratinocytes, bronchial epithelium, and vascular epithelium.

The types of investigation that lend themselves particularly to tissue culture are:

1. Intracellular activity: the replication and transcription of deoxyribonucleic acid (DNA), protein synthesis, energy metabolism, and drug metabolism.
2. Intracellular flux: RNA, the translocation of hormone receptor complexes and signal transduction processes, and membrane trafficking.
3. Environmental interaction: nutrition, infection, cytotoxicity, carcinogenesis, drug action, and ligand receptor interactions.

4. Cell-cell interaction: morphogenesis, paracrine control, cell proliferation kinetics, metabolic cooperation, cell adhesion and motility, matrix interaction, organotypic models for medical prostheses and invasion.
5. Genetics, including genome analysis in normal and pathological conditions, genetic manipulation, transformation, and immortalization.
6. Cell products and secretion, biotechnology, bioreactor design, product harvesting, and down stream processing (Freshney, 2000).

3.6.1 Advantages of cell culture

The advantages of cell culture are:

1. Control of the environment: the physicochemical environment (pH, temperature, osmotic pressure, and O_2 and CO_2 tension) can be controlled very precisely, and the physiological conditions can kept constantly.
2. Characterization and homogeneity of sample: tissue sample are invariable heterogeneous. After one or two passages, culture cell lines assume a homogeneous (or at least uniform) constitution, as the cell are randomly mixed at each transfer and the selective pressure of the culture conditions tend to produce a homogeneous culture of the most vigorous cell type. Hence, at each subculture, replication samples are identical to each other, and the characteristics of the line may be perpetuated over several generations. This reduced the variation of statistic analysis.
3. Economy, Scale, and Mechanization: culture cells may be exposed directly to a reagent at low, and defined, concentration and with direct access to the cell. New developments in multi-well plates and robotics also have introduced significant economies in time and scale.
4. *In Vivo* Modeling: Perfusion techniques allow the diversity of specific experimental compounds to be regulated in concentration, duration of exposure, and metabolic rate. The development of histotypic and organotypic models also increases the accuracy of *in vivo* modeling (Freshney, 2000).

3.6.2 Limitations of cell culture

The limitations of cell culture are:

1. Expertise: due to culture techniques must be carried out under strict aseptic conditions, because animal cells grow slower than many of common contaminants, such as bacteria, molds, and yeasts. Furthermore, cells from multicellular animals do not normally exist in isolation and, consequently, are not able to sustain an independent existence without the provision of a complex environment stimulating blood plasma or interstitial fluid. Then, the operator needs more skills, awareness, and understanding in these limitations.
2. Dedifferentiation and Selection: dedifferentiation was the term that used for the condition that cells showed the loss of the phenotypic characteristics typical of the tissue from which the cells had been isolated. These may be due to the overgrowth of undifferentiated cells of the same or a different lineage. The development of serum-free selective media made the isolation of specific lineages quite possible; many of the differentiated properties of these cells may be restored.
3. Origin of cells: If differentiated properties are lost, it is difficult to relate the cultured cells to functional cells in the tissue from which they are derived. Stable markers are required for characterization of the cells; in addition, the culture may need to be modified so that these markers are expressed.
4. Instability: instability is a major problem with many continuous cell lines, resulting from their unstable aneuploid chromosomal constitution. Even with short-term cultures of untransformed cells, heterogeneity in growth rate and the capacity to differentiate within the population can produce variability for one passage to the next (Freshney, 2000).

3.6.3 Many Differences *IN VITRO*

The differences in cell behavior, between cells and their *in vivo* stem, are come from the dissociation of cells from three-dimentional genometry and their propagation on a two-dimentional substrate. Specific cell interactions characteristic of the

histology of the tissue are lost. As the cells spread out, become more mobile, and start to proliferate, so the growth fraction of the cell population increases. When a cell line forms, it may represent only one or two cell types, and many heterotypic cell-cell interactions are lost.

The culture environment also lacks the several systemic components involved in homeostasis regulation *in vivo*, mainly from the nervous and endocrine system. Without this control, cellular metabolism may be more constant *in vitro* than *in vivo*, but may not be truly representative of the tissue from which the cells were derived.

Energy metabolism *in vitro* occurs largely by glycolysis, and although the citric acid cycle is still functional, it plays a lesser role (Freshney, 2000).

3.6.4 Types of cell culture

Cell culture implies that the tissue, or outgrowth from the primary explants, is dispersed into a cell suspension which may then be cultures as an adherent monolayer on a solid substrate or as a suspension in the culture medium.

When cells are selected from a culture, the sub line is known as a cell strain. Cell lines or cell strains may be propagated as an adherent monolayer or in suspension. Normally, most cells will attach to the substrate (anchorage dependent) and showed in a monolayer form. Suspension cells, in contrast, can survive and proliferate without attachment (anchorage-independent); this ability is restricted to hematopoietic cells, transformed cell lines, and cells from malignant tumors. Cultured cell lines are more representative of precursor cell compartments *in vivo* than of fully differentiated cells, as, normally, most differentiated cells do not divided (Freshney, 2000).

3.6.5 Dopaminergic neuroblastoma cell lines

For studying in the dopaminergic system, cell lines that can produce tyrosine hydroxylase are gain more interest for investigator. SK-N-SH and SH-SY5Y, both are neuroblastoma cell line that come from brain at the metastatic site, and define as a bone marrow neuroblastoma.

SK-N-SH cell line is hyperdiploid human female (XX), with the modal chromosome number of 47. Normal chromosomes N9 and N22 are single. One copy of each of these chromosomes is structurally altered to form the two marker chromosomes 9q+ and 22q+. Chromosomes N7 is trisomic. Extra bands were found on one copy of chromosome N7, thereby forming a marker chromosome. These may have been translocated in part(s) to the q arms of chromosomes N9 and N22. Previously, SK-N-SH has been used as a target cell line in cell mediated cytotoxicity assays.

Whereas, SH-SY5Y is a thrice cloned (SK-N-SH -> SH-SY -> SH-SY5 -> SH-SY5Y) sub line of the neuroblastoma cell line SK-N-SH which was established in 1970 from a metastatic bone tumor. The advantage of SH-SY5Y cells is a reported saturation density greater than 1 X 10^6 cells/cm^2. The cells possess a unique marker comprised of a chromosome 1 with a complex insertion of an additional copy of a 1q segment into the long arm, resulting in trisomy of 1q.

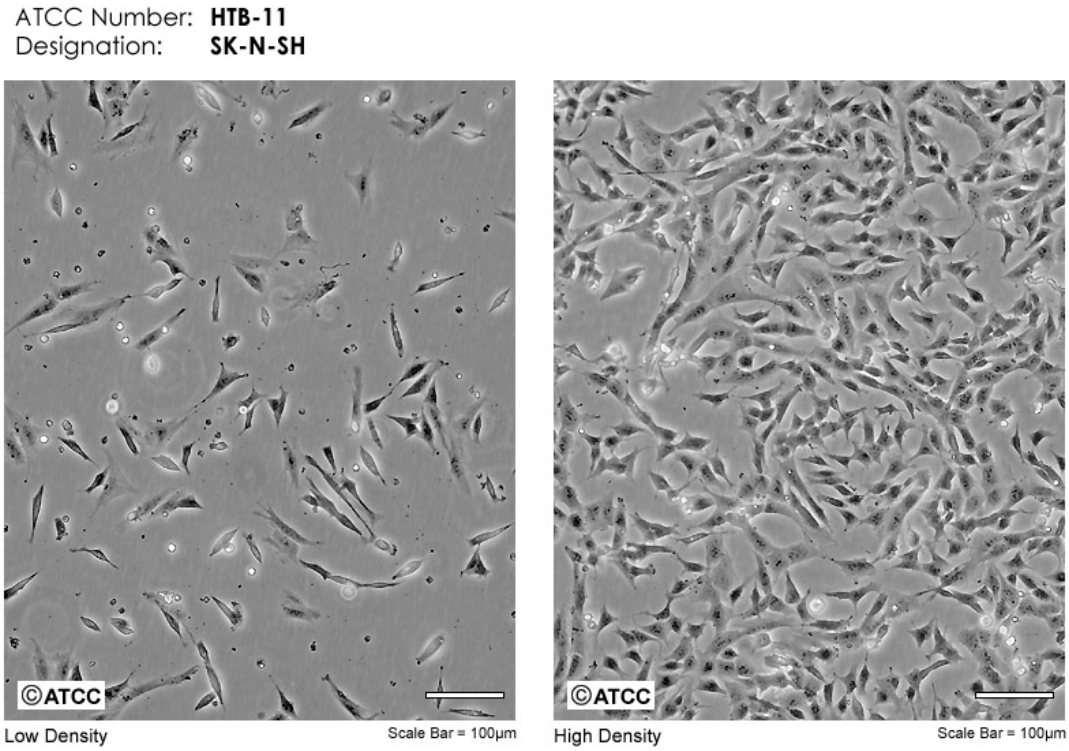

Figure 3.6 Microscopic pictures of low density and high density of SK-N-SH cell lines.

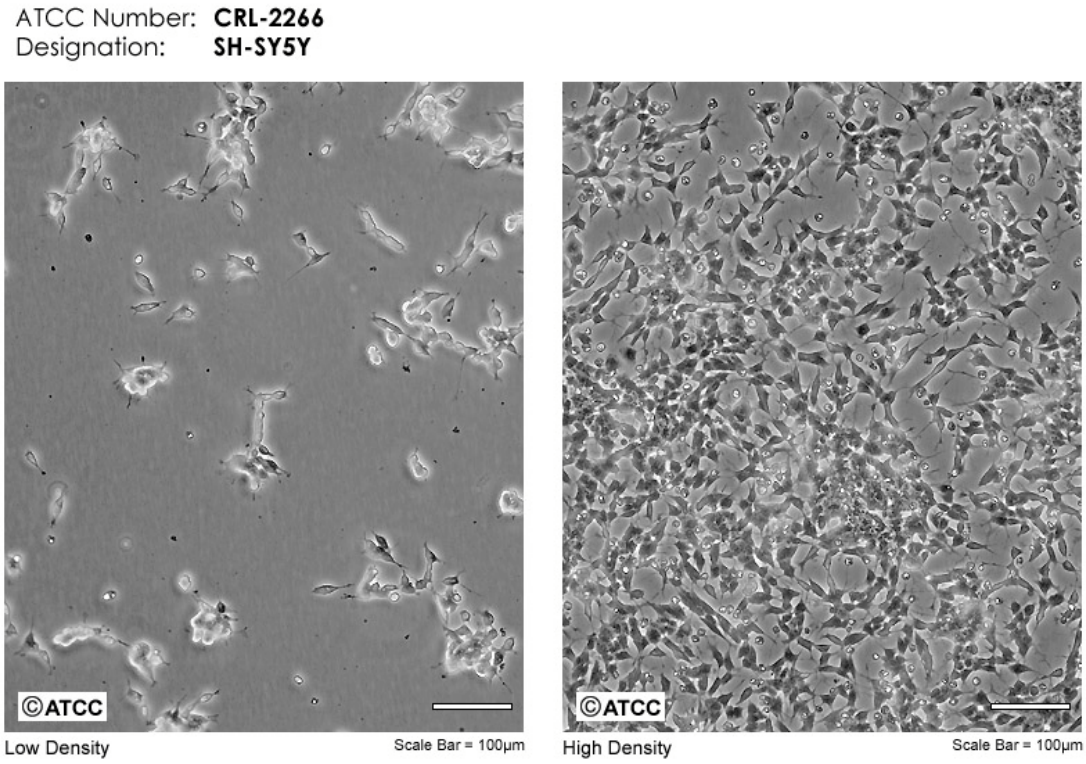

Figure 3.7 Microscopic pictures of low density and high density of SH-SY5Y cell lines.

CHAPTER 4
MATERIALS AND METHODS

4.1 Chemicals

All chemicals and supplies were purchased from Sigma (St. Loius, MO, USA), Fisher Scientific (Fair, NJ, USA), Gibco BRL (Rockville, MD, USA), Promega (Medison, WS, USA), Packard (Meriden, CT, USA), and BioRad (Hercules, CA, USA). Antibodies were purchased from Cell Signaling, Zymed and Santa Cruz., and ECL from Amersham Bioscience.

4.2 Cell Cultures

Materials

Disposable plastic ware

Filter paper 0.2 mm Milipore

Dulbecco's modified Eagle's medium (DMEM)

DMEM (high glucose) powder

3.7 g/L Sodium bicarbonate

10% fetal bovine serum

MEM-F-12 mixture medium

50% MEM

20% F-12

20% Hank Balance Salt Solutions

10% Fetal bovine serum

Antibiotic drugs (Pennicilin-steptomycin) 100 u/L

SK-N-SH cell lines

Apparatus

Laminar flow

CO_2 incubator

Water bath

Human neuroblastoma SK-N-SH cells were cultured in Dulbecco's modified Eagle's medium (Gibco BRL, Rockville, MD, USA) and were supplemented with 10% fetal bovine serum (Gibco BRL). The cells were incubated at 37°C in a humidified atmosphere containing 5% CO_2.

4.3 Assay of MTT Cell Viability

Materials

96-well plates plastic ware

3-(4, 5-dimethylthiazol-2-yl)-2, 5 diphenyltetrazoliumbromide (MTT)

Isoporpanol

0.04 N HCl

DFO

$FeSO_4$

Apparatus

Microtiter Plate Reader

One hundred microliter of cells was grown in 96-well plates for 1 day. The culture medium was replaced with a new medium, and then various concentrations of DFO (1-1,000 μM) (Sigma, St. Loius, MO, USA) or $FeSO_4$ (0-250 μM) (Fisher Scientific, Fair, NJ, USA) were added to the samples. The $FeSO_4$ was added either with or withoutn10 μM DFO. After 24 h, 10 μl of 5 mg/ml MTT (Sigma) was added in the medium and incubated at 37°C for 2 h. The culture medium was removed and replaced with 100 μl of isopropanol (Fisher Scientific) containing 0.04 N HCl in order to dissolve the dark blue formazan crystals that had formed. The solution was mixed thoroughly, and the absorbance was measured at 560 nm spectral wavelength using Microtiter Plate Reader equipped with SoftMax computer software.

4.4 Lipid Peroxidation Assay

Materials

12-well plates plastic ware

DFO

$FeSO_4$

0.1 M Phosphate-buffered saline (PBS)

0.25% Trypsin-EDTA

Trichloroacetic acid (TCA)

2-Thiobarbituric acid (TBA)

0.2 N hydrochloric acid (HCl)

Bradford Reagent

Apparatus

Spectrphotometer

Microtiter Plate Reader

Water bath

Levels of malondialdehyde (MDA), the product of lipid peroxidation, were measured and the lipid peroxidation assay was modified from that previously described (Buege and Aust, 1998). The cells were grown in 12-well plates for 2-3 days. The culture medium was replaced with a new medium, and then various concentrations of $FeSO_4$ (0-250 μM) were added to the samples. The $FeSO_4$ was added either with or withoutn10 μM DFO. After 24 h, the cells were trypsinized, harvested, washed once with phosphate-buffered saline (PBS; Gibco BRL) and resuspended in 250 μl of PBS. The cells were then sonicated, and 200 μl of the cell suspension was collected. One ml of 15% trichloroacetic acid-0.375% 2-thiobarbituric acid-0.2 N hydrochloric acid (TCA-TBA-HCl) reagent (Sigma) was added, and tubes were vortexes thoroughly. The solution was heated at 95°C for 20 min, cooled promptly, and centrifuged at 10,000 rpm for 10 min. The absorbance (optical density) was determined at 535 nm spectral length against a blank that contained all of the aforementioned reagents except for the sample. The protein

concentration was determined by a Bradford assay (BioRad, Hercules, CA, USA). All of the values were normalized for protein content.

4.5 Protein Carbonyl Assay

Materials

24-well plates plastic ware

DFO

$FeSO_4$

0.1 M Phosphate-buffered saline (PBS)

0.25% Trypsin-EDTA

Trichloroacetic acid (TCA)

10% streptomycin solution

2,4-dinitrophenylhydrazine

2 N HCl

Guanidinium hydrochloride

20 mM potassium phosphate

Ethanol-acetic acid mixture solution (1:1)

Bradford Reagent

Apparatus

Incubator

Spectrphotometer

Microtiter Plate Reader

Sonicator

The measurement of protein carbonyl content was modified from a previously described technique (Le Vine et al., 1991). The cells were grown in 24-well plates for 1-2 days. The culture medium was replaced with a new medium, and then various concentrations of $FeSO_4$ (0-250 μM) were added to the samples. The $FeSO_4$ was added either with or withoutn10 μM DFO. After 24 h, the cells were trypsinized, harvested, washed once with PBS and resuspended in 200 μl of PBS.

The cells were then sonicated, and 180 μl of the cell suspension was collected. The cell suspension was mixed with 20 μl of a 10% streptomycin solution (Sigma)

and incubated at room temperature for 10 min. After incubation, the samples were centrifuged for 10 min at 14,000 rpm. An aliquot of 150 μl supernatant was mixed with 150 μl of 20% TCA in order to precipitate the protein.

The samples were centrifuged for 10 min at 14,000 rpm, and the supernatant was discarded. Pellets were incubated with 500 μl of 10 mM 2,4-dinitrophenylhydrazine (Sigma) in 2 N HCl for 1 h at room temperature. 500 μl of 20% TCA were added and then centrifuged at 14,000 rpm for 3 min. The supernatant was discarded, and the pellets were washed with 500 μl of ethanol-acetic acid (1:1).

The pellets were incubated for 10 min at 37°C, and centrifuged for 3 min at 14,000 rpm. The supernatant was discarded, and this process was repeated three times. The final protein pellets were dissolved in 0.6 ml guanidine (Gibco BRL) solution (6 M guanidine in 20 mM potassium phosphate, pH 3.2), incubated at 37°C for 15 min, and centrifuged at 14,000 rpm for 3 min.

The absorbance of supernatant was determined at 405 nm spectral length against a blank that contained all of the aforementioned reagents except for the sample. The protein concentration was determined by a Bradford assay. All of the values were normalized for protein content.

4.6 Determination of Cellular ATP

Materials

24-well plates plastic ware

96-well plates plastic ware (black)

DFO

$FeSO_4$

0.1 M Phosphate-buffered saline (PBS)

0.25% Trypsin-EDTA

Trichloroacetic acid (TCA)

5 M NaOH

3% Triton X-100

ATP Lite™-M Kit

Bradford Reagent

Apparatus

Luminescent counter

Microtiter Plate Reader

Cells were grown in 24-well plates for 1-2 days. The culture medium was replaced with a new medium, and then various concentrations of $FeSO_4$ (0-250 μM) were added to the samples. The $FeSO_4$ was added either with or without 10 μM DFO.

After 24 h, the cells were lysed with 200 μl of lysis buffer (1:2 dilution of 5 M NaOH, 3% Triton X-100 in distilled water), and the level of ATP was determined using ATP Lite™-M Kit and by following a protocol which had been provided by the manufacturer (Packard, Meriden, CT, USA).

The samples were centrifuged for 5 min, washed once with PBS, and then re-suspended in 200 μl of PBS. The suspended cells were centrifuged for 10 min at 14,000 rpm, and the supernatant was used for an assay of the total ATP level. Two 25-μl samples of supernatant were added to a black 96-well plate.

In each well, 50 μl of ATP substrate (1:10 dilution of ATP substrate mixed in the substrate buffer) and 125 μl of distilled water were added. The plates were shaken, while being incubated in the dark for 5 min. The luminescent counter was used to determine the ATP values, which were normalized for protein determination.

4.7 DCF Fluorescence Determination

Materials

24-well plates plastic ware

96-well plates plastic ware

DFO

$FeSO_4$

0.1 M Phosphate-buffered saline (PBS)

0.25% Trypsin-EDTA

2′-7′-dichlorofluorescein diacetate (DCF)

Digitonin

Bradford Reagent

Apparatus

Incubator

Fluorometric plate reader

Microtiter Plate Reader

Cells were grown in 24-well plates for 1-2 days. The culture medium was replaced with a new medium, and then various concentrations of $FeSO_4$ (0-250 μM) were added to the samples. The $FeSO_4$ was added either with or without10 μM DFO. After 24 h, the cells were trypsinized, harvested, washed once with PBS, and resuspended in 220 μl of PBS.

A 200 μl of the cell suspension were incubated in 20 μM 2′-7′-dichlorofluorescein diacetate (DCF; Molecular Probes, Eugene, OR, USA) at 37°C for 30 min. The cells were centrifuged for 10 min at 14,000 rpm, and the pellets were resuspended in 50 μM digitonin (Sigma). After incubation at 37°C for 30 min, the solutions were centrifuged at 14,000 rpm for 10 min.

An aliquot of 100 μl of the supernatant was collected to measure the fluorescence at an excitation wavelength of 490 nm and an emission wavelength of 530 nm. All values were normalized for protein determination.

4.8 Apoptotic Morphological Analysis of Dopaminergic Neurons

Materials

6-well plates plastic ware

Glass cover slips

DFO

$FeSO_4$

0.1 M Phosphate-buffered saline (PBS)

Fluorescent dye mixture solutions (Acridine orange-Ethidium bromide-DAPI)

Microscopic glass slides

Mounting reagent

Bradford Reagent

Apparatus

Incubator

Digital fluorescence camera

Cells were grown on glass cover slips for 1 day, and then treated with various concentrations of $FeSO_4$ (0-250 μM) with or without10 μM DFO for 24 h. The cells were washed 3 times with PBS and incubated with 50 μl of 5 mM of fluorescent dye mixture solutions (acridine orange-ethidium bromide-DAPI; Promega, Medison, WS, USA) for 30 min.

The fluorescent dye mixture solutions were removed and washed 3 times with PBS prior to mounting onto microscopic glass slides. The microscopic glass slides were then dried in the dark area for 10 min prior to carrying out apoptotic cells morphology studies by using a digital fluorescence camera. The fluorescence images were analyzed by using ImagePro computer software (Leeds Instruments Co., Minneapolis, MN, USA).

4.9 Immunostaining Studies for α-Synuclein

Materials

6-well plates plastic ware

Glass cover slips

$FeSO_4$

0.1 M Phosphate-buffered saline (PBS)

α-Synuclein antibody

5,5′,6,6′-tetrachloro-1,1′,3,3′-tetraethylbenzimidazol-carbocyanine iodide (JC-1)

Sheep anti-mouse conjugated with FITC

Microscopic glass slides

Mounting reagent

Bradford Reagent

Apparatus

Incubator

Digital fluorescence camera

Cells were grown on glass cover slips for 1 day, and then treated with various concentrations of $FeSO_4$ (0-250 μM) for 24 h. Cells were washed once with PBS, then incubated with α-synuclein antibody (1: 400; Zymed, South San Francisco, CA, USA) in 5 μl of 5,5′,6,6′-tetrachloro-1,1′,3,3′-tetraethylbenzimidazol-carbocyanine iodide (JC-1, a mitochondrial membrane potential sensitive fluorescence probe; Molecular Probes), in 2 ml PBS.

Cells were incubated at 37°C for 45 min, washed once with PBS, and incubated in secondary antibody diluted (1:300; sheep anti-mouse conjugated with FITC; Sigma) for 30 min at room temperature. Then cells were washed with PBS once prior to mounting onto microscopic glass slides.

The microscopic glass slides were then dried in the dark area for 10 min prior to carrying out studies involving α-synuclein using a digital fluorescence camera. The fluorescence images were analyzed by using ImagePro computer software.

4.10 Determination of Metallothionein levels

Materials

6-well plates plastic ware

96-well plates plastic ware

$FeSO_4$

0.1 M Phosphate-buffered saline (PBS)

Metallothionein

Mouse anti-metallothionein antibodies

Bradford Reagent

Apparatus

Incubator

Microtiter Plate Reader

Cells were grown in 6-well plates for 2 days. The culture medium was replaced with serum-free medium and various concentrations of $FeSO_4$ were added to the samples. After 1 h, the cells were scraped, centrifuged and washed once with PBS, and re-suspended in 300 μl of PBS.

Metallothionein was determined by a highly sensitive competitive ELISA assay using mouse anti-metallothionein antibodies. Protein concentrations were determined using the Bio-Rad protein reagent (Bio-Rad). All values were normalized for protein determination.

4.11 Determination of Glutathione levels

Materials

6-well plates plastic ware

96-well plates plastic ware

$FeSO_4$

0.1 M Phosphate-buffered saline (PBS)

0.25% Trypsin-EDTA

monochlorobimane (MCB)

Mouse anti-metallothionein antibodies

Bradford Reagent

Apparatus

Incubator

Fluorometric plate reader

Microtiter Plate Reader

The levels of reduced glutathione (GSH) were measured using a fluorometric assay method and monochlorobimane (MCB). Cells were treated with 0-1 mM $FeSO_4$ for 24 h in 6-well plates. The medium was removed and cells were collected in 0.1M PBS, sonicated and centrifuged at 14,000 rpm for10 min.

The supernatant was used for GSH assay. 90 μl of supernatant was incubated with 10 μl of MCB for 37°C for 2 h. The fluorescence was measured in a fluorometric plate reader (Molecular Devices, Sunnyvale, CA) at 380/460 nm as excitation and emission wavelengths, respectively.

Protein concentrations were determined using the Bio-Rad protein reagent (Bio-Rad). All values were normalized for protein determination.

4.12 Caspase-3 activity

Materials

6-well plates plastic ware

96-well plates plastic ware

DFO

$FeSO_4$

0.1 M Phosphate-buffered saline (PBS)

20mM HEPES, pH 7.5

10% glycerol

Caspase-3 substrates (Ac-DEVD-AMC)

2 mM dithiothretol

Bradford Reagent

Apparatus

Incubator

Fluorometric plate reader

Microtiter Plate Reader

A Fluorometric assay of caspase-3 activity was performed as described previously [King et al, 2001] with minor modifications in 96-well plates, and all measurements were carried out in duplicate wells. Cells were treated with 100 μM $FeSO_4$ for 24 h in 6-well plates, either pretreatment 30 min with or without 10 μM DFO.

To each well, 200 μl of assay buffer (20mM HEPES, pH 7.5, 10% glycerol, 2 mM dithiothretol) was added. The peptide substrate for caspase-3 (Ac-DEVD-AMC) (Pharmingen) was added to each well to a final concentration (20 ng/μl). Two hundred microliter of Cell lysates were added to start the reaction and incubated at 37°C for 30 min.

Fluorescence was measured by a fluorescence plate reader (Packard, Meriden, CT) set at 360 nm excitation and 460 nm emission. Protein concentrations were

determined using the Bio-Rad protein reagent (Bio-Rad). All of the values were normalized/protein.

4.13 Western Blotting

Materials

25 cm^2 culture flask plastic ware

DFO

$FeSO_4$

0.1 M Phosphate-buffered saline (PBS)

RIPA lysis buffer

50 mM Tris-HCl; pH 7.4

150 mM NaCl

1 mM EDTA

0.1% Triton X-100

0.1 % SDS

1X Phosphatase inhibitor

1X Protease inhibitor

2X SDS/ Sample buffer/ Electrophoresis loading buffer

100 mM Tris

2% SDS

25 % Glycerol

0.01% Bromphenol blue

Adjust to pH 6.8

Add Beta Mercaptoethanol (2-ME) to 10%

SDS-polyacrylamide gel

- For Stacking gel

  30% Acrylamide mix (29.2% acrylamide, 0.8% bisacrylamide)

  1 M Tris-HCl; pH 6.8

  10% SDS

  10% Ammonium persulphate

  TEMED

  H_2O

- For Resolving gel

30% Acrylamide mix (29.2% acrylamide, 0.8% bisacrylamide)

1 M Tris-HCl; pH 8.8

10% SDS

10% Ammonium persulphate

TEMED

H_2O

Tank buffer (5X)

125 mM Tris

Glycine

SDS

Transfer buffer

25 mM Tris

192 mM Glycine

20% methanol

Nitrocellulose membrane

Poseau S

Rabbit anti-p65 antibody

Mouse anti-Bcl-2 antibody

Rabbit anti-Bax antibody

HRP conjugated goat anti-mouse IgG

HRP conjugated mouse anti-rabbit IgG

BSA

5% non-fat milk

Tris-Buffer Saline (TBS); pH 7.6

20mM Tris

NaCl

1 M HCl

0.1% Tween20

ECL detection kit

Bradford Reagent

Apparatus

Gel electrophoresis apparatus (Bio-Rad: Mini-protein II set)

Microtiter Plate Reader

Densitometer

Cells were grown in 25 cm^2 culture flask until 80-90% confluent. The culture medium was replaced with serum-free medium and 100 μM of $FeSO_4$ was added to the cells. The nuclear extracts were prepared by modified a mini-extraction protocol (Schreiber et al, 1989).

Cells were washed once with cold PBS and collected, centrifuged at 600 x g for 5 min. After discard supernatant, 300 μl RIPA lysis buffer were added and incubated at 4°C for 10 min. Samples were centrifuged at 14,000 rpm for 10 min. Supernatants (cytosolic part) were discard, pellets (nuclear part) were re-suspend again in 50 μl RIPA lysis buffer, sonicated 10 s before centrifuges at 14,000 rpm for 10 min. The supernatant were collected and stored at -20°C until assay. Protein concentrations were determined using the Bio-Rad protein reagent (Bio-Rad).

SDS-polyacrylamide gel electrophoresis

10% SDS-polyacrylamide gel were prepared as follow:

1. Set the gel sandwich, two glasses, two spacers and acrylic pressure plate.
2. Put the gel sandwich on the casting stand.
3. Prepare the resolving gel mixture solution.
4. Fill resolving gel mixture solution in the gel sandwich and leave a space 1 cm for overlay double-distilled water (DDW).
5. Allow the gel to polymerize at least 30 min.
6. After gel is formed, poured out DDW and dry it with filter paper.
7. Prepare the stacking gel mixture solution and fill it instead of DDW.
8. Place a comb in the gel sandwich.
9. Allow the gel to polymerize at least 15-30 min.
10. After the gel is casting, remove a comb.
11. Attach the gel sandwich to the inner cooling core.
12. Put the inner cooling core into tank.
13. Wash the wells with 1x tank buffer before add tank buffer to chamber completely and load sample.

14. Run the gel at 150 volts for 45-60 min.

Protein transfer to Nitrocellulose membranes

1. After the electrophoresis is finished, remove the stacking gel from the resolving gel.
2. Cut the right bottom corner and rinse gel in transfer buffer.
3. Soak the fiber pad and pre-cut filter paper in transfer buffer and in the negative sandwich side pack the fiber pad, filter paper, gel, nitrocellulose membrane, filter paper, filter pad in an order.
4. Close the cassette and put it into the holder.
5. Fill the chamber with transfer buffer completely and put the lid on.
6. Connect the power supply system.
7. Transfer protein at 100 volts for 1.5 h.
8. After transfer complete, remove the nitrocellulose membrane from the sandwich set.
9. Soak nitrocellulose membrane in Poseau S for 5 min.
10. Rinse the membrane in DDW 3 times.
11. Cut membrane as small as possible and cut at the right corner.
12. Wrap it with a thin saran wrap; keep in 4°C until immunostaining assay.

Sample preparation

Protein 20 μg for nuclear extracts was mixed with electrophoresis loading buffer (1:1), vortexed, boiled at 90-95°C for 3-5 min, and let it stand in room temperature until resolved on 10% SDS-polyacrylamide gel.

Immunostaining assay

1. Membrane was washed with TBS for 5 min.
2. Discard TBS and blocked membrane with 5% non-fat milk in TBS containing 0.1% Tween20 at 37 °C for 1 h.
3. Discard 5% non-fat milk in TBS containing 0.1% Tween20.
4. Then, washed 3 times with TBS containing 0.1% Tween20

5. Incubated membrane with an anti-p65 (1:1000 dilution in 5%BSA in TBS containing 0.1% Tween20; Cell Signaling) overnight at 4 °C.
6. Discard antibody.
7. Membrane were washed 3 times with TBS containing 0.1% Tween20
8. Incubated with mouse anti-rabbit conjugated with peroxidase (1:2000 dilution in 5%BSA in TBS containing 0.1% Tween20) for 1 h at 37 °C.
9. Discard antibody and visualized protein by the ECL detection kit.
10. Densitometer reading of the autoradiograph of the Western blot was performed using a GS-800 Calibrated Densitometer.

4.14 Statistical Analysis

One-way analysis of variance followed by the Dunnett's test and student's *t-test* were performed using the scientific statistic software SigmaStat version 2.03. The symbol * indicated that the values are significantly different from control at $p<0.05$. The symbol # and ## indicated that the values are significantly different from cells treated with $FeSO_4$ at $p<0.05$ and $p<0.001$, respectively.

CHAPTER 5
RESULTS

Effects of $FeSO_4$ and deferoxamine (DFO) on SK-N-SH cell lines

To study the effects of $FeSO_4$ and DFO on cell viability, a dopaminergic SK-N-SH cell lines were cultured in the presence of $FeSO_4$, DFO, or in combination between $FeSO_4$ and DFO. Cell viability was then assessed with MTT assay. SK-N-SH cells were treated with various concentrations of $FeSO_4$ (0, 1, 10, 100, 1000 μM) for 24 h. The results showed that cell survival decreased in a concentration-dependent manner (Fig. 5.1b).

DFO dose-response curve was studied by treating SK-N-SH cells with various concentrations of DFO (0, 1, 10, 100, 1000 μM) for 24 h. It was found that DFO at 1 and 10 μM did not influence cell survival. However, at higher doses (100 and 1000 μ M), DFO decreased cell survival (Fig. 5.1a).

Pre-treatment of SK-N-SH cells with 10 μM DFO for 30 min before treating with various concentrations of $FeSO_4$ (0, 1, 10, 100, 1000 μM) for 24 h showed that DFO increased survival of cells treated with $FeSO_4$. However, DFO decreased cell survival at low concentration of $FeSO_4$ (1 μM) (Fig. 5.1b).

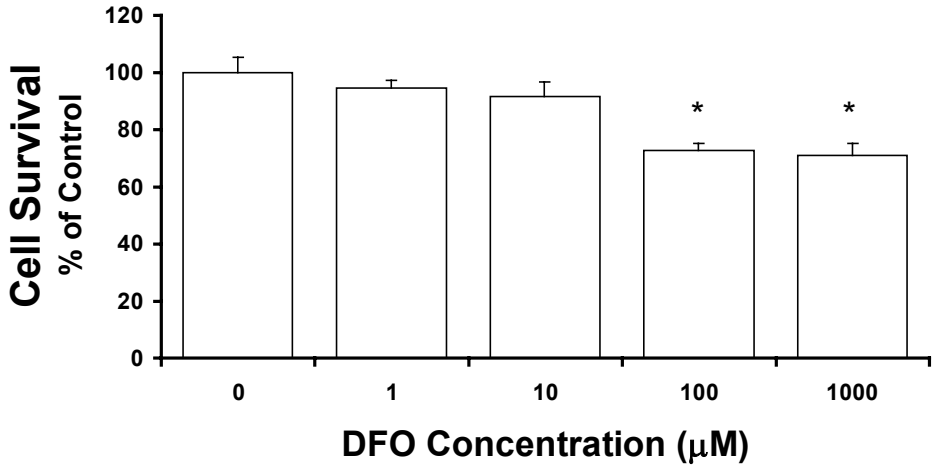

Figure 5.1a Cell viability in SK-N-SH cells treated with DFO. Cells were treated with 1-1000 μM DFO for 24 h and determination of cell viability was done by using the MTT assay. Results are expressed as percentage of controls and are means ± S.E.M. of 4 separated experiments (Sangchot et al., 2002). * $p<0.05$ compared to control

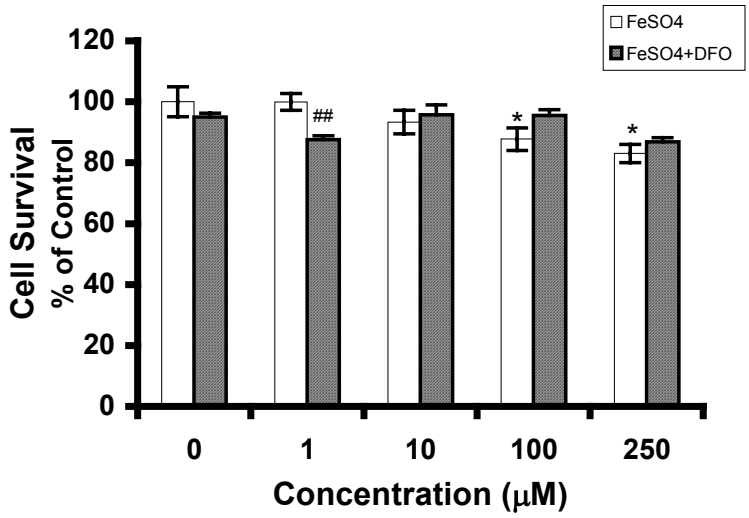

Figure 5.1b Cell viability in SK-N-SH cells treated with a combination of $FeSO_4$ and DFO. Cells were treated with $FeSO_4$ (0, 1, 10, 100, 250 μM) for 24 h with or without pretreated with 10 μM DFO for 30 min. Cell survival was assessed by using the MTT assay. Results are expressed as a percentage of control and are means ± S.E.M. of 4 separated experiments (Sangchot et al., 2002). * $p<0.05$ compared to control, ## $p<0.001$ compared to $FeSO_4$-treated group

Effect of $FeSO_4$ on lipid and protein damages

As described previously in the introduction, iron causes lipid peroxidation by generating hydroxyl radicals through Fenton reaction. Therefore, effects of $FeSO_4$ and DFO to induce lipid peroxidation were done in SK-N-SH cells. It was found that $FeSO_4$ slightly affected levels of lipid peroxidation and DFO (10 μM) decreased lipid peroxidation in $FeSO_4$-treated cells (Fig. 5.2a). When using DFO alone, lipid peroxidation was not influenced (Fig. 5.2b).

To study protein damage induced by oxidative stress, protein carbonylation was determined. It was found that $FeSO_4$ enhanced protein carbonylation in a concentration-dependent manner (Fig. 5.3a). Such effect could be prevented by DFO when 10 μM $FeSO_4$ was used. In contrast, at a low dose of $FeSO_4$ (1 μM), DFO enhanced protein carbonylation (Fig. 5.3a). Moreover, it was demonstrated that DFO, by itself, caused protein damage within the cells (Fig. 5.3b).

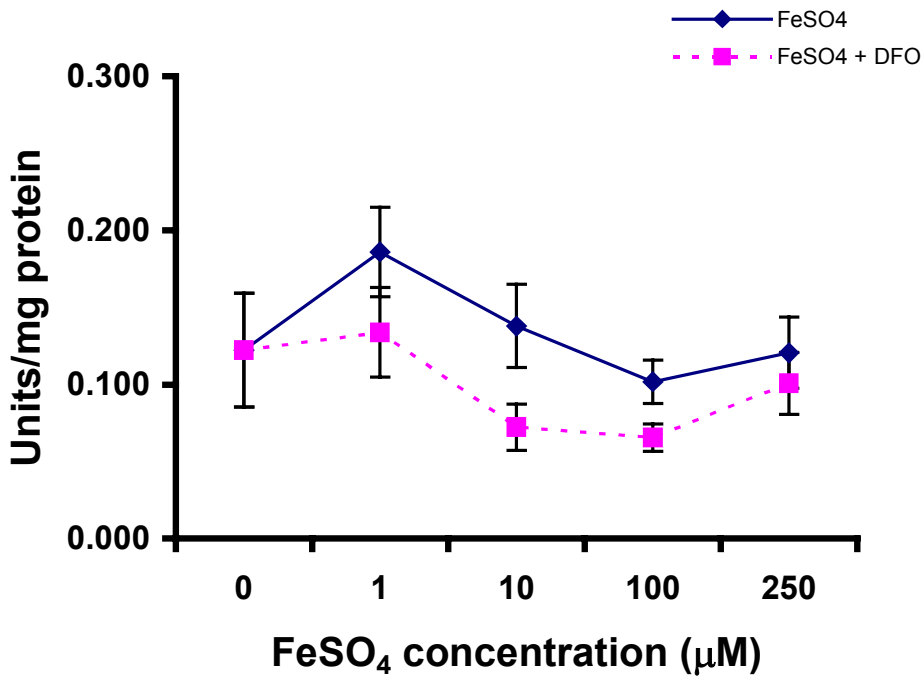

Figure 5.2a Lipid peroxidation in SK-N-SH cells treated with a combination of $FeSO_4$ and DFO. Cells were treated with $FeSO_4$ (0, 1, 10, 100, 250 μM) for 24 h with or without pretreated with 10 μM DFO for 30 min, then lipid peroxidation was measured. Results are expressed as means ± S.E.M. of 4 separated experiments (Sangchot et al., 2002).

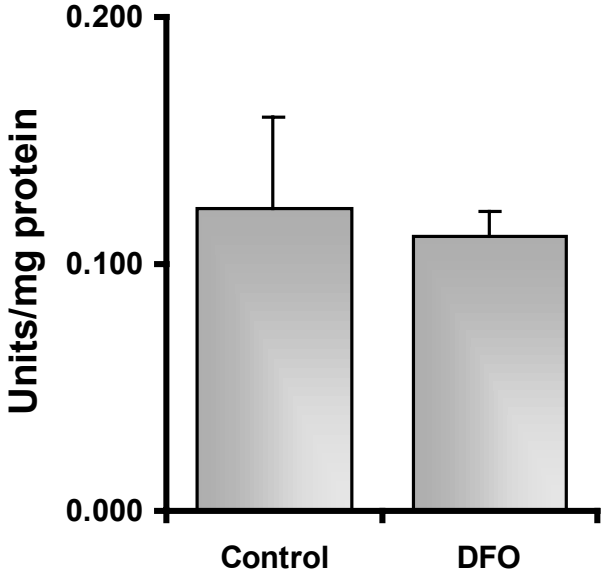

Figure 5.2b Lipid peroxidation in SK-N-SH cells treated with DFO. Cells were treated with 10 μM DFO for 24 h, and then lipid peroxidation was determined. Results are expressed as means ± S.E.M. of 4 separated experiments (Sangchot et al., 2002).

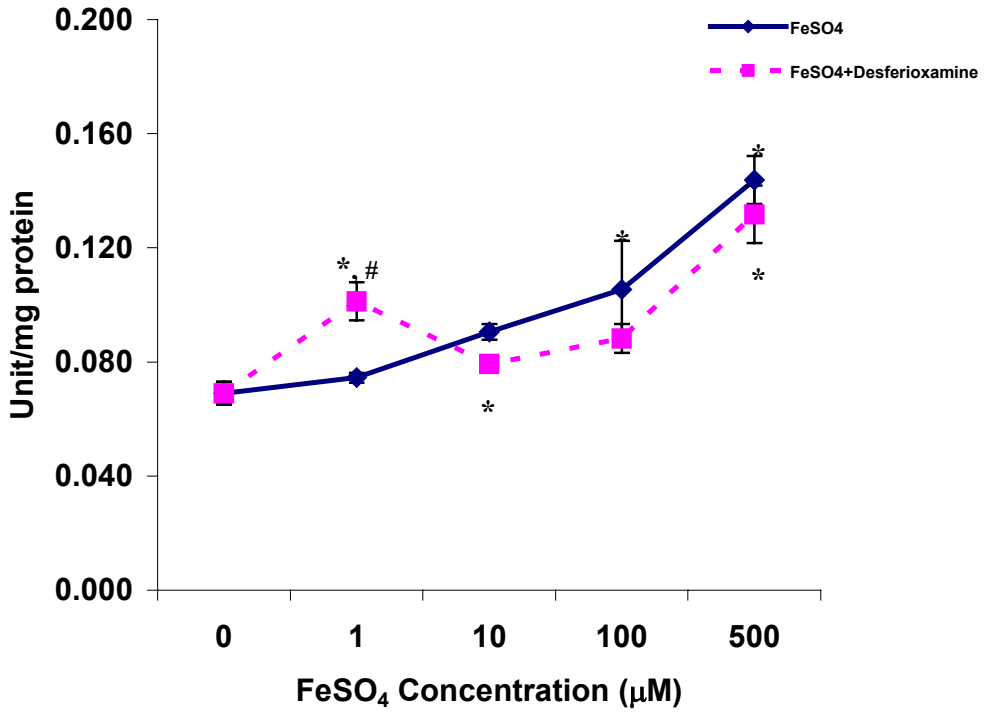

Figure 5.3a Protein carbonyl contents in SK-N-SH cells treated with a combination of $FeSO_4$ and DFO. Cells were treated with $FeSO_4$ (0, 1, 10, 100, 250 μM) for 24 h with or without pretreated with 10 μM DFO for 30 min, then level of protein carbonylation was measured. Results are expressed as means ± S.E.M. of 4 separated experiments (Sangchot et al., 2002). * $p<0.05$ compared to control, # $p<0.05$ compared to $FeSO_4$-treated group

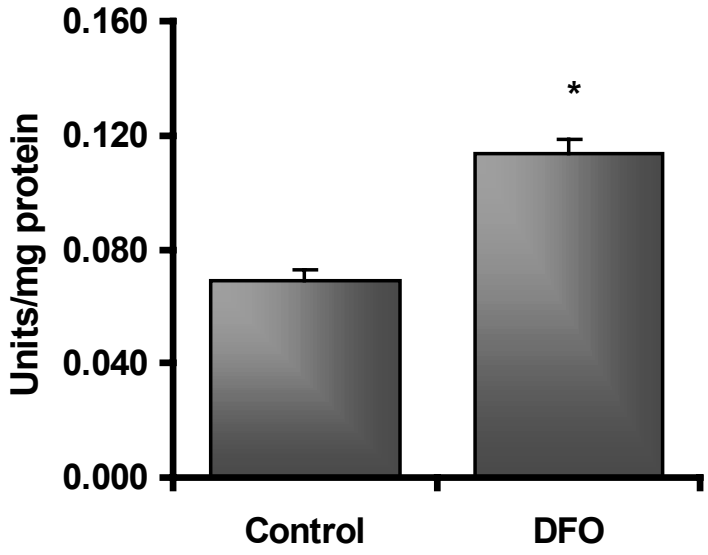

Figure 5.3b Protein carbonyl contents in SK-N-SH cells treated with DFO. Cells were treated with 10 μM DFO for 24 h, and then level of protein carbonylation was measured. Results are expressed as means ± S.E.M. of 4 separated experiments (Sangchot et al., 2002). * $p<0.05$ compared to control

Effect of $FeSO_4$ on ROS production and cellular ATP levels

Determination of ROS production by DCF fluorescence technique is an indirect technique to measure hydroperoxide production and lipid peroxidation. It was used in this research to demonstrate $FeSO_4$–induced free radical production in the dopaminergic neurons. Fe^{2+} caused a significant increase of ROS production within 1 h (Fig. 5.4a) in a dose-dependent manner (100-1000 μM). Peak values were observed at 500-1000 μM $FeSO_4$. In contrast, within 24 h there was no change in ROS production when compared to control, while DFO enhanced ROS production at all given doses of $FeSO_4$ (Fig. 5.4b).

However, DFO alone did not induce increases in DCF fluorescence, when compared to control (Fig. 5.4c). At low concentration of $FeSO_4$ (1 μM), DFO increased cellular ATP levels; while at higher concentrations (100 and 250 μM) did not produce any significant changes in the cellular ATP contents (Fig. 5.5a). It was observed that DFO alone increased cellular ATP contents in SK-N-SH cells as compared to control (Fig. 5.5b).

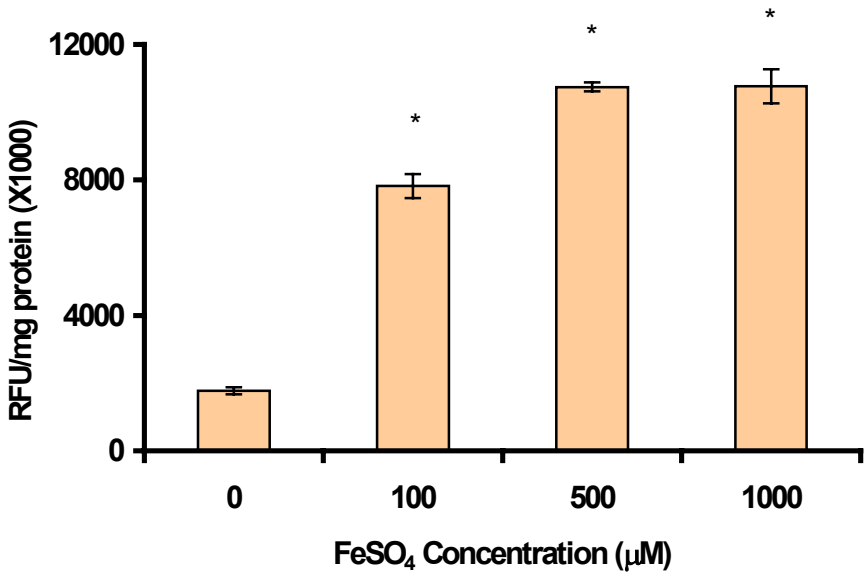

Figure 5.4a DCF fluorescence in SK-N-SH cells treated with $FeSO_4$ for 1 h. Cells were treated with $FeSO_4$ (0, 100, 500, 1000 μM) for 1 h, and then DCF fluorescence was measured. Results are expressed as means ± S.E.M. of 4 separated experiments. * $p<0.05$ compared to control

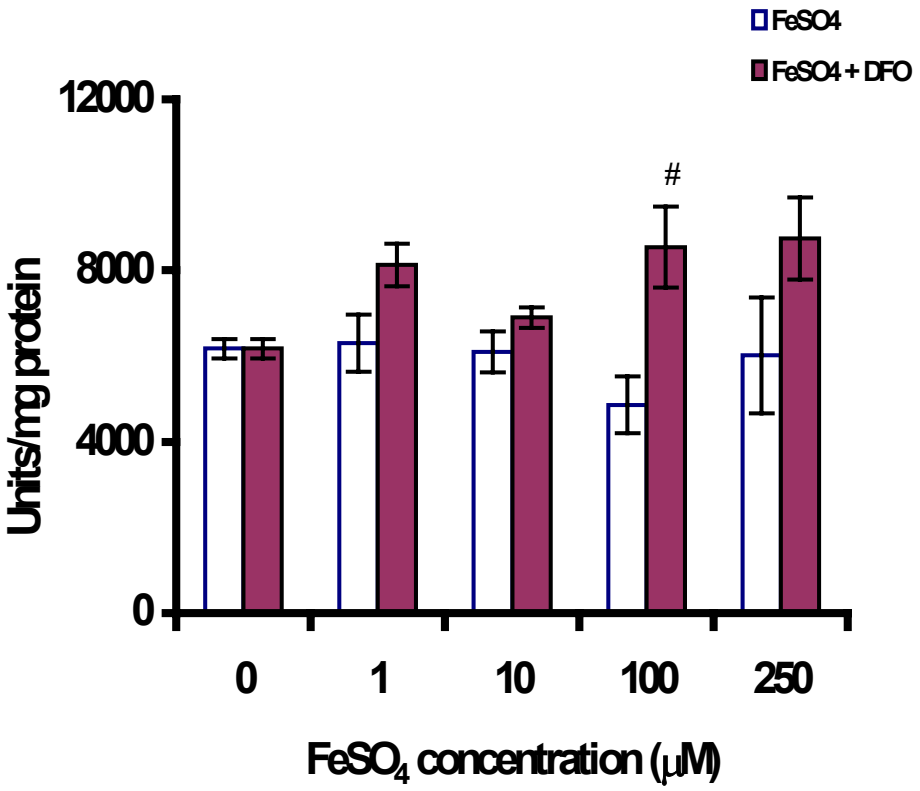

Figure 5.4b DCF fluorescence in SK-N-SH cells treated with a combination of $FeSO_4$ and DFO. Cells were treated with $FeSO_4$ (0, 1, 10, 100, 250 μM) for 24 h with or without pretreated with 10 μM DFO for 30 min, and then level of DCF fluorescence was measured. Results are expressed as means ± S.E.M. of 4 separated experiments (Sangchot et al., 2002). # $p<0.05$ compared to $FeSO_4$-treated group

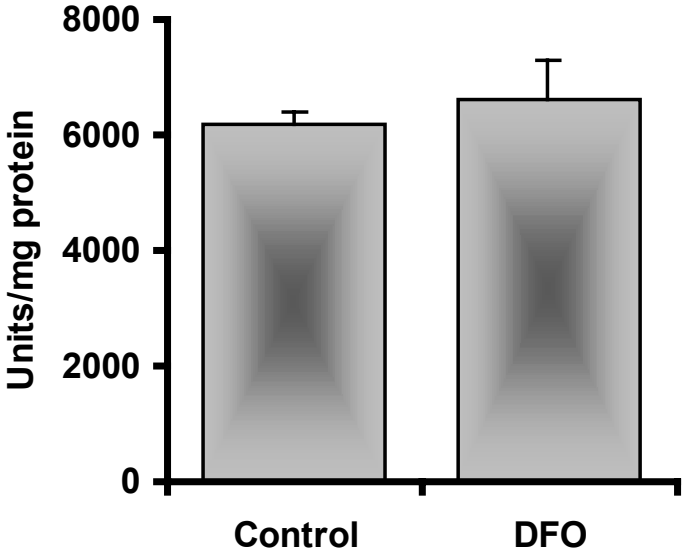

Figure 5.4c DCF fluorescence in SK-N-SH cells treated with DFO. Cells were treated with 10 μM DFO for 24 h, and then level of DCF fluorescence was measured. Results are expressed as means ± S.E.M. of 4 separated experiments (Sangchot et al., 2002).

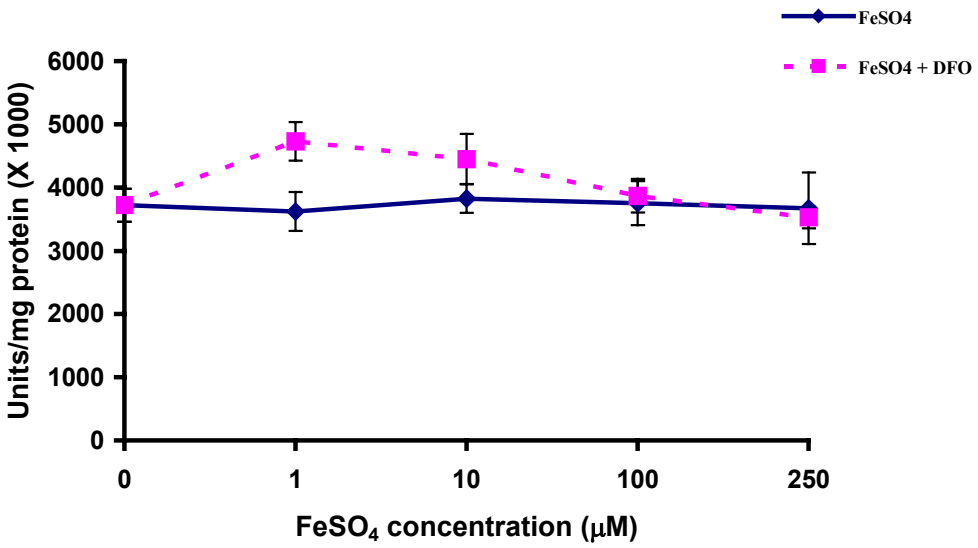

Figure 5.5a Cellular ATP levels in SK-N-SH cells treated with a combination of $FeSO_4$ and DFO. Cells were treated with $FeSO_4$ (0, 1, 10, 100, 250 μM) for 24 h with or without pretreated with 10 μM DFO for 30 min, and then cellular ATP levels were assessed. Results are expressed as means ± S.E.M. of 4 separated experiments (Sangchot et al., 2002).

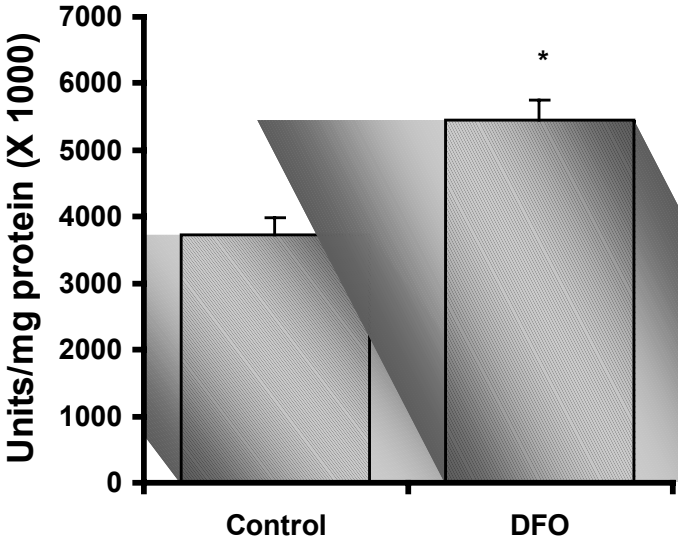

Figure 5.5b Cellular ATP levels in SK-N-SH cells treated with DFO. Cells were treated with 10 μM DFO for 24 h, and then cellular ATP levels were assessed. Results are expressed as means ± S.E.M. of 4 separated experiments (Sangchot et al., 2002). * $p<0.05$ compared to control

Effect of $FeSO_4$ on cell survival/death in morphological studies

The fluorescence imaging microscopic studies were conducted to correlate and confirm the altered neurochemical data observed when using MTT assay, lipid peroxidation, protein carbonylation, cellular ATP levels, and DCF fluorescence in the presence of $FeSO_4$ and/or DFO in SK-N-SH cells. Acridine orange in the left column was used to study living cells; ethidium bromide in the middle column was used to determine death cells; and DAPI in the right column was used to assess DNA (Fig. 5.6). Ten micromolar of $FeSO_4$ caused aggregation of SK-N-SH cells (Fig. 5.6, second panel) compared to control (Fig. 5.6, first panel). This aggregation was prevented by pretreatment with DFO (Fig. 5.6, third panel). At a high concentration, 100 μM $FeSO_4$ induced cell shrinkage, and DFO was able to prevent cell death but not the generation of apoptotic bodies (Fig. 5.6, fourth and fifth panels). In contrast, at 250 μM $FeSO_4$ caused high level of cell death and DFO was unable to prevent this effect (Fig. 5.6, sixth and seventh panels).

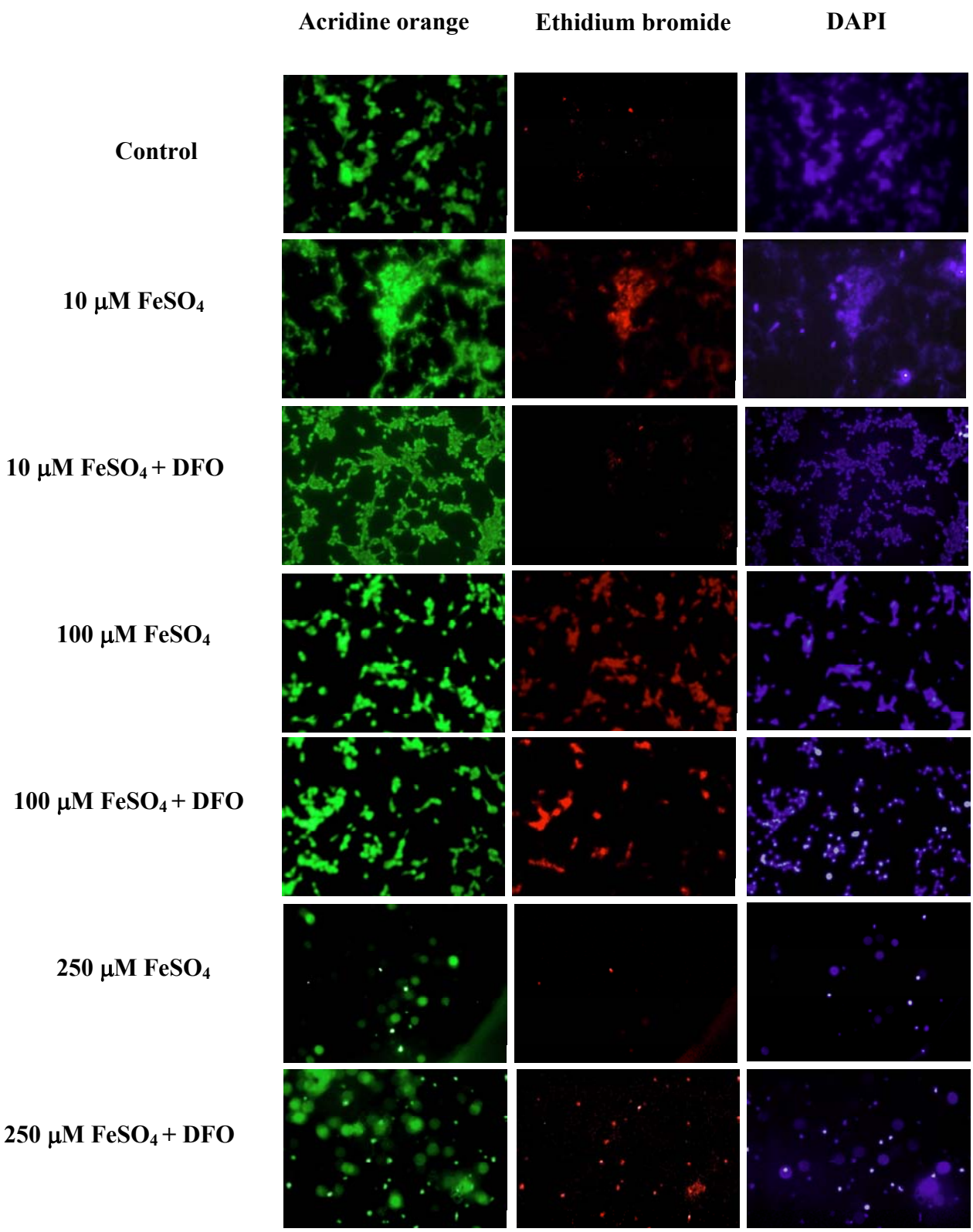
Acridine orange
Ethidium bromide
DAPI
Control
10 μM FeSO4
10 μM FeSO4 + DFO
100 μM FeSO4
100 μM FeSO4 + DFO
250 μM FeSO4
250 μM FeSO4 + DFO

Figure 5.6 Digital fluorescence imaging microscopic analysis of dopaminergic neurons (SK-N-SH) was shows a concentration-dependent increase in neuronal damage in response to $FeSO_4$ and the extent of neuroprotection with DFO pre-treatment. Three fluorochromes, Acridine orange (left column), ethidium bromide (middle column), and DAPI (right column) were used to illustrate cytoplasmic proteins, RNA, and fragmented DNA, respectively. Fluorescence images were captured employing SpotLite digital camera and analyzed by ImagePro computer software. Target accentuation and background inhibition computer software were employed to enhance the image quality (Sangchot et al., 2002).

Effect of $FeSO_4$ on mitochondria and α-synuclein

The effects of $FeSO_4$ on mitochondrial aggregation and translocation of α-synuclein are shown in Fig. 5.7-5.8. In Fig. 5.7, the left column represents mitochondria, using JC-1 as mitochondrial marker, the middle column shows α-synuclein immunoreactivity, and the right column depicts double labeling of α-synuclein and mitochondria in SK-N-SH cells.

When compared to control (Fig. 5.7, first panel), 100 nM of $FeSO_4$ caused mitochondrial clumping and α-synuclein aggregation near the perinuclear regions (Fig. 5.7, second panel); and these deleterious effects were increased when 1 and 10 μ M of $FeSO_4$ were used (Fig. 5.7, third and fourth panels).

At high concentration of $FeSO_4$ (50 and 100 μM), nuclear membrane became disrupted and mitochondria became visible in the damaged nucleus. Similarly, α-synuclein immunoreactivity was seen in the disrupted nucleus (Fig. 5.7, fifth and sixth panels).

The right column (Fig. 5.7) illustrates double labeling of α-synuclein and JC-1 fluorescence demonstrating fluorescence accentuation. Fig. 5.8 shows double labeling of α-synuclein and mitochondria in SK-N-SH cells examined in a high magnification (100 X).

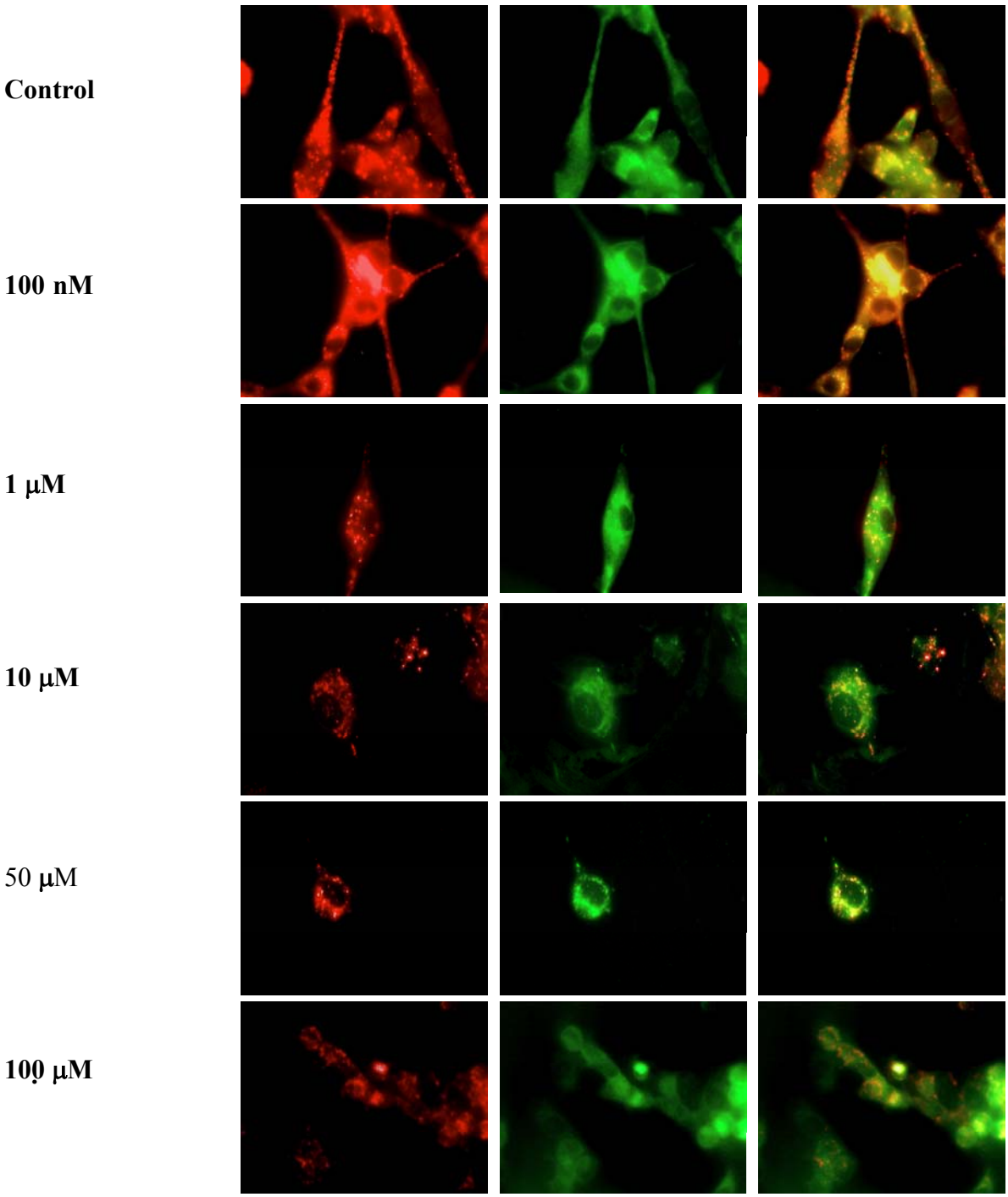
Control
100 nM
1 μM
10 μM
50 μM
100 μM

Figure 5.7 α-synuclein and JC-1 fluorescence observed with digital fluorescence imaging microscopic analysis of dopaminergic neurons (SK-N-SH). Concentration-dependent increases in mitochondrial and α-synuclein aggregation in response to $FeSO_4$ are shown. Two markers, JC-1 was used as a marker for mitochondria (left column), and α-synuclein antibody was used as a marker for α-synuclein immunoreactivity (middle column); then and double labeling of mitochondria and α-synuclein was shown in the right column. Fluorescence images were captured employing SpotLite digital camera and analyzed by ImagePro computer software. Target accentuation and background inhibition computer software was employed to enhance image quality (Sangchot et al., 2002).

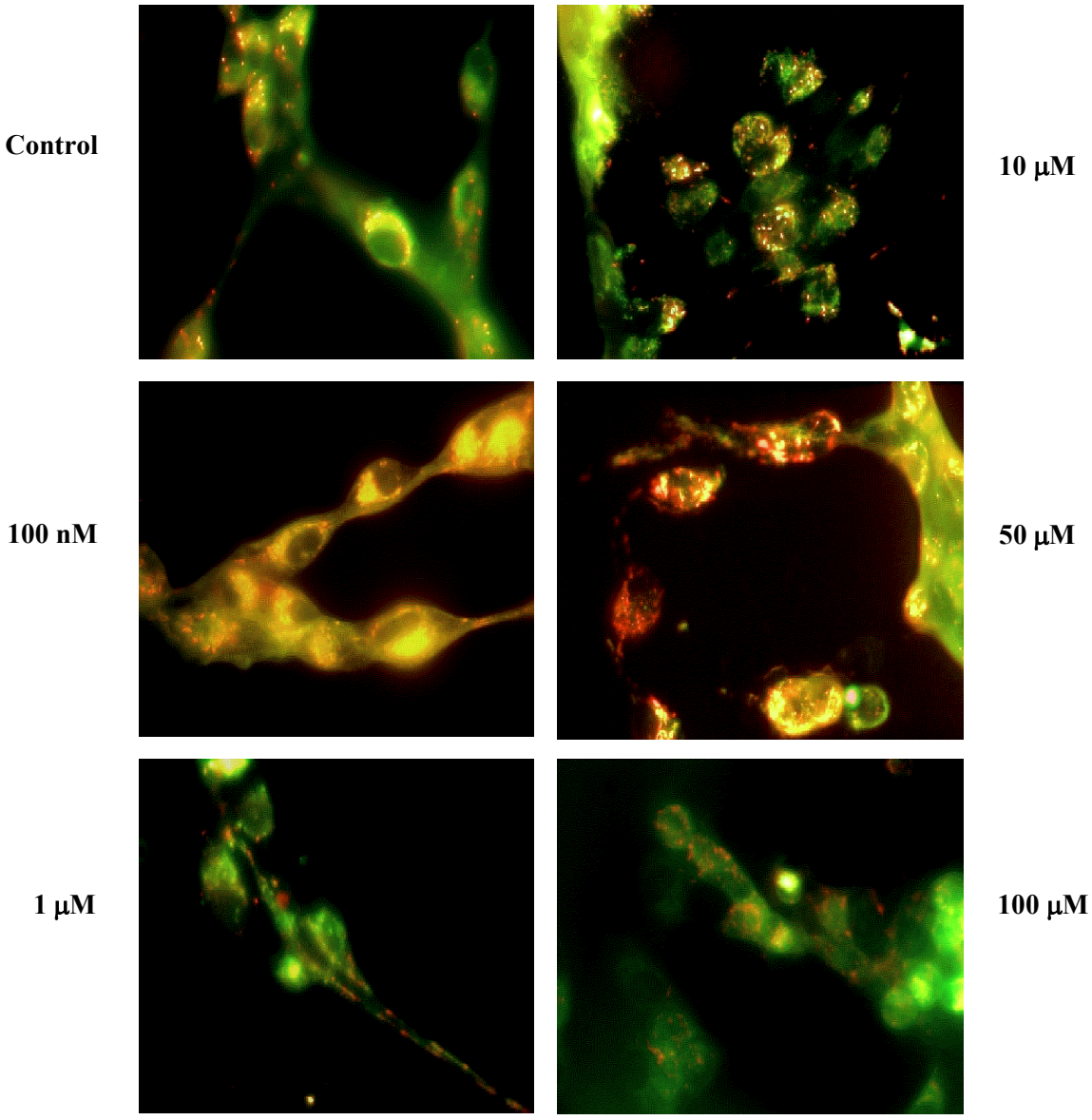

Figure 5.8 Double labeling of α-synuclein and JC-1 fluorescence observed with a high magnification (100 X) of digital fluorescence imaging microscopic analysis of dopaminergic neurons (SK-N-SH cells). Concentration-dependent increases in mitochondria and α-synuclein aggregation in response to $FeSO_4$ are shown. Fluorescence images were captured employing SpotLite digital camera and analyzed by ImagePro computer software. Target accentuation and background inhibition computer software was employed to enhance image quality (Sangchot et al., 2002).

Effect of high concentration of DFO on cell function

Investigation of DFO effects on cell function during the absence of $FeSO_4$ in SK-N-SH cells. It was found that a relatively high concentration of DFO (100 μM) induced lipid peroxidation (Fig. 5.9a), and reduced cellular ATP levels (Fig. 5.9b). These results suggest that DFO could chelate the available pool of iron, required for the normal mitochondrial oxidative phosphorylation and other physiological activities of the neuron. These observations suggest that adequate levels of iron are required to execute the neuroprotective effect of DFO, as it exerts its own neurotoxicity by reducing the concentrations of iron.

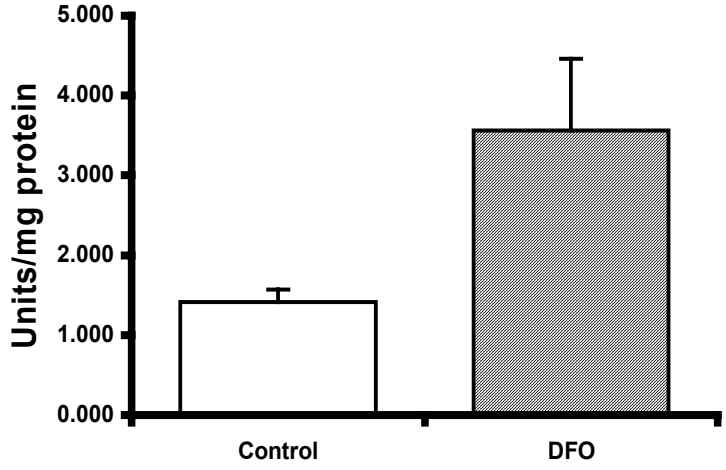

Figure 5.9a Lipid peroxidation in SK-N-SH cells treated with DFO. Cells were treated with 10 μM DFO for 24 h. The hydroperoxide levels were measured and normalized with protein concentration. Results are expressed as means ± S.E.M. (Sangchot et al., 2002).

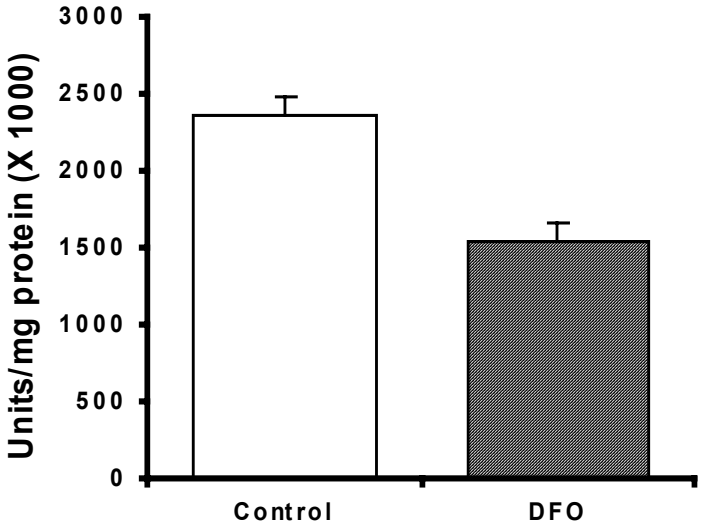

Figure 5.9b Cellular ATP levels in SK-N-SH cells treated with DFO. Cells were treated with 100 μM DFO for 24 h. Cellular ATP levels were measured and normalized with protein concentration. Results are expressed as means ± S.E.M. (Sangchot et al., 2002).

Effect of $FeSO_4$ on cellular defense mechanism

In the studies of cellular defense mechanism alteration during iron-induced toxicity, it was found that $FeSO_4$ significantly increased glutathione (Fig. 5.11) and metallothionein levels (Fig. 5.10) when SK-N-SH cells were treated with 0-1000 μM $FeSO_4$ for 24 h.

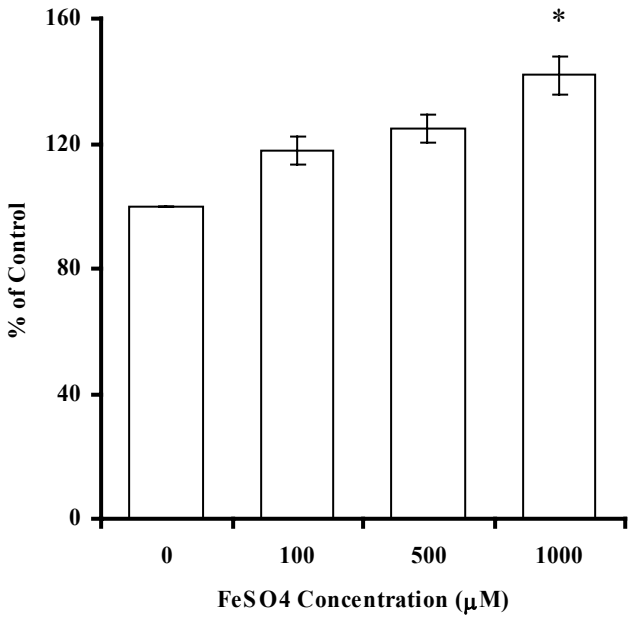

Figure 5.10 Metallothionein levels in SK-N-SH cells treated with $FeSO_4$. Cells were treated with 0-1000 μM $FeSO_4$ for 24 h, and then metallothionein levels were determined. Results are expressed as means ± S.E.M. of 4 separated experiments. *p < 0.05 compared to control

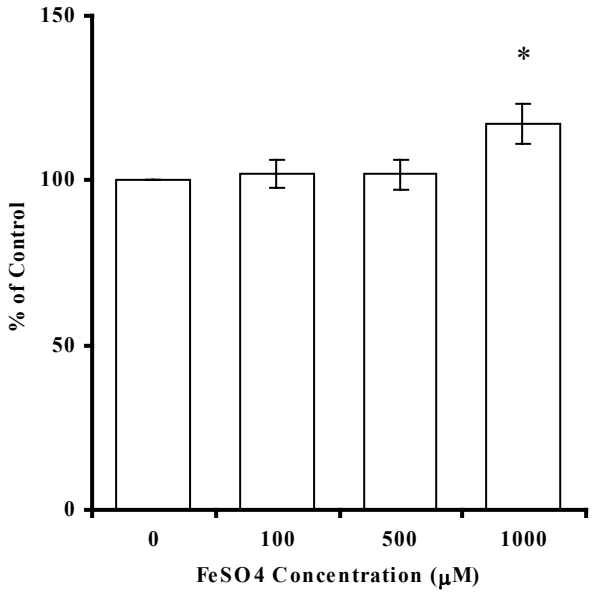

Figure 5.11 Glutathione levels in SK-N-SH cells treated with $FeSO_4$. Cells were treated with 0-1000 μM $FeSO_4$ for 24 h, and then glutathione levels were determined. Results are expressed as means ± S.E.M. of 6 separated experiments. $p< 0.05$ compared to control

Effect of $FeSO_4$ on caspase-3 activation

One hundred micromolar of $FeSO_4$ significantly increased caspase-3 activity in SK-N-SH cells (Fig. 5.12).

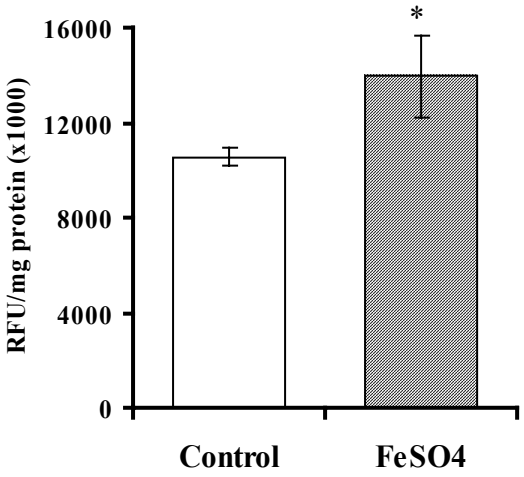

Figure 5.12 Caspase-3 activity in SK-N-SH cells treated with $FeSO_4$. Cells were treated with 100 μM $FeSO_4$ for 24 h, and then caspase-3 activity was determined. Results are expressed as means ± S.E.M. of 3 separated experiments. * $p < 0.05$ compared to control

Effect of $FeSO_4$ on NF-κB, Bcl_2 and Bax

$FeSO_4$ (100 μM) significantly increased NF-κB protein levels within 30 min and decreased to base line level after 60 min (Fig. 5.13). The upper panel shows immunoblots of NF-κB obtained from 3 separated experiments. Intensity of immunoreactivity was quantified and expressed as percentage of the control (100%). Each value represent means ± S.E.M. of NF-κB immunoreactivity which is shown in the lower panel.

After treatment of 100 μM $FeSO_4$ for 24 h, it was found that $FeSO_4$ significantly decreased Bcl_2 protein levels (Fig. 5.14). The upper panel shows the immunoblots of Bcl_2 obtained from 3 separated experiments. Intensity of immunoreactivity was quantified and expressed as percentage of the control (100%). Each value represent means ± S.E.M. of Bcl_2 immunoreactivity which is shown in the lower panel.

For studying Bax protein levels after treatment of 100 μM $FeSO_4$ for 24 h, it was found that $FeSO_4$ did not affect Bax protein levels (Fig. 5.15). The upper panel shows the immunoblots of Bax obtained from 3 separated experiments. Intensity of immunoreactivity was quantified and expressed as percentage of the control (100%). Each value represent means ± S.E.M. of Bax immunoreactivity which is shown in the lower panel.

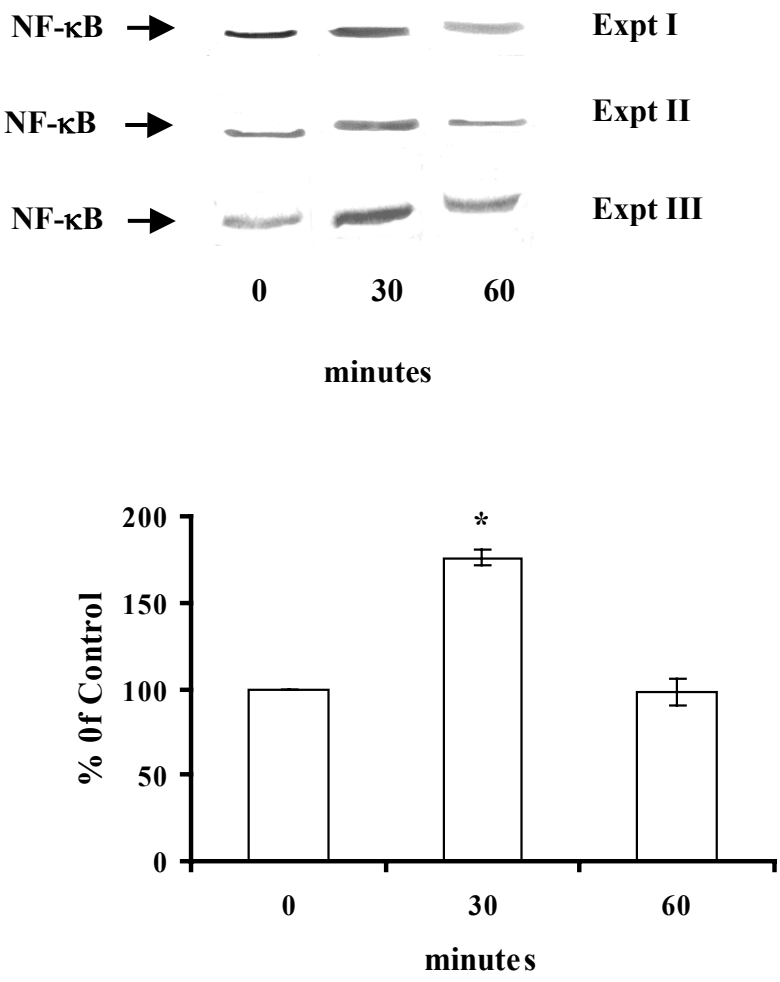

Figure 5.13 NF-κB protein levels in SK-N-SH cells treated with $FeSO_4$. Cells were treated with 100 μM $FeSO_4$ during 0, 30, 60 min, and then NF-κB protein levels were determined. Results are expressed as means ± S.E.M. of 3 separated experiments. * $p < 0.05$ compared to control

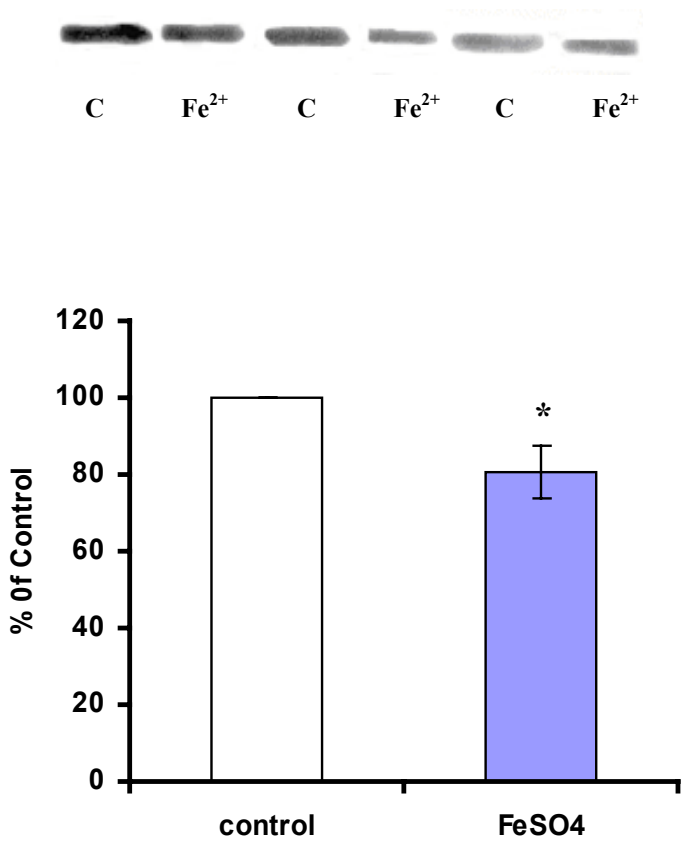

Figure 5.14 Effects of 100 μM $FeSO_4$ on Bcl_2 protein in SK-N-SH cells. Cells were treated with 100 μM $FeSO_4$ for 24 h, and then Bcl_2 protein levels were determined. Results are expressed as means ± S.E.M. of 3 separated experiments. * $p < 0.05$ compared to control

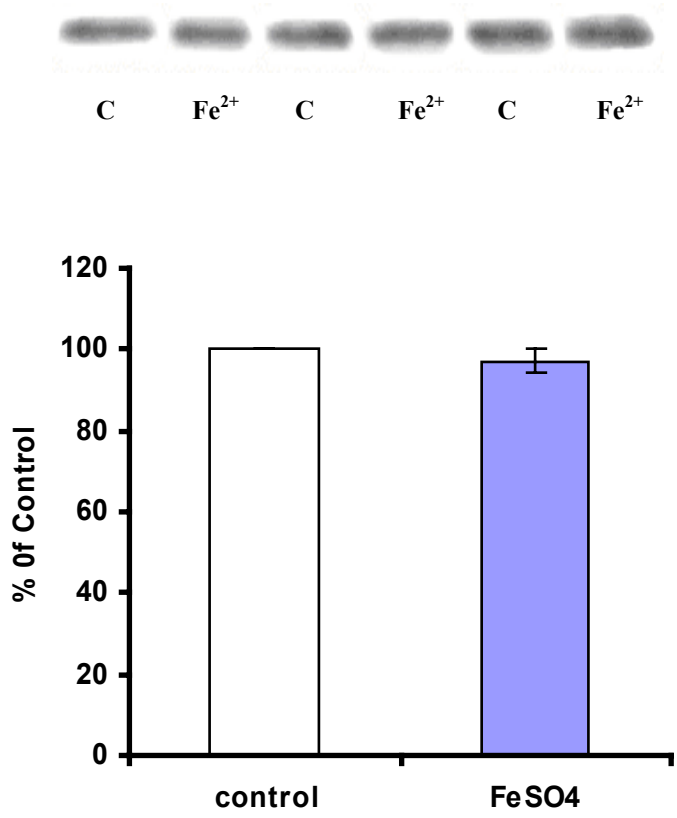

Figure 5.15 Effects of 100 μM $FeSO_4$ on Bax protein in SK-N-SH cells. Cells were treated with 100 μM $FeSO_4$ for 24 h, and then Bax protein levels were determined. Results are expressed as means ± S.E.M. of 3 separated experiments. * $p < 0.05$ compared to control

CHAPTER 6
DISCUSSION

An increase in total iron content appears to be a response to neurodegeneration in affected basal ganglia regions found in a number of movement disorders. However, only in PD were there an increase total iron level, decrease in ferritin content, decrease in copper content, and an increase in zinc concentration within SN. These findings suggest an alteration of iron handling in the SN of PD. Depending on the form in which the excess iron load exists in SN of PD; and it may contribute to the neurodegenerative process.

6.1 Iron as a Biological Pro-Oxidant

From this study it was found that an increase in the production of ROS (Fig. 5.4a) during cell exposed to iron within one hour. However, ROS remained at the same level after 24 h. This result implies toxicity of iron and cellular defense mechanism against ROS. In the cellular mechanism study, it was shown that iron toxicity caused lipid (Fig. 5.2a), proteins (Fig. 5.3a), and DNA (Fig. 5.6) damages, leading to cell death (Fig 5.1a, 5.6).

Iron is able to accept and donate electrons readily. Such ability makes it physiologically essential, as a useful component of cytochromes and oxygen-binding molecules. However, iron is also biochemically dangerous; it can damage tissues by catalyzing the conversion of hydrogen peroxide to free-radical ions that attack cellular membranes, protein and DNA. This threat is minimal in a healthy state, because iron metabolism is well regulated; therefore, there are never appreciable concentrations of free iron.

Under pathological conditions, iron metabolism and superoxide metabolism are clearly interactive. Each can exacerbate the toxicity of the other. Iron overload may amplify the damaging effects of superoxide overproduction in an inflammatory, both

acute and chronic, processes. Furthermore, chronic oxidative stress may modulate iron uptake and storage, leading to a self-sustained and ever-increasing spiral of cytotoxic and mutagenic events (Emerit, et al., 2001).

"Free iron or labile iron" is able to participate in the **Haber-Weiss** chemistry, catalyzing the formation of the $^{\bullet}OH$ capable to abstract a hydrogen atom from polyunsaturated fatty acids (LH) and initiate lipid peroxidation. Once lipid hydroperoxides (LOOH) accumulate, free iron may directly initiate additional lipid peroxidation.

The resulting accumulations of lipid hydroperoxides destroy membrane structure and functions. The radical $^{\bullet}OH$ is highly reactive and its estimated half-life in cells is only 10^{-9} seconds. It can damage lipids, proteins, DNA, sugars, and generally all organic molecules (Nelson and McCord, 1998).

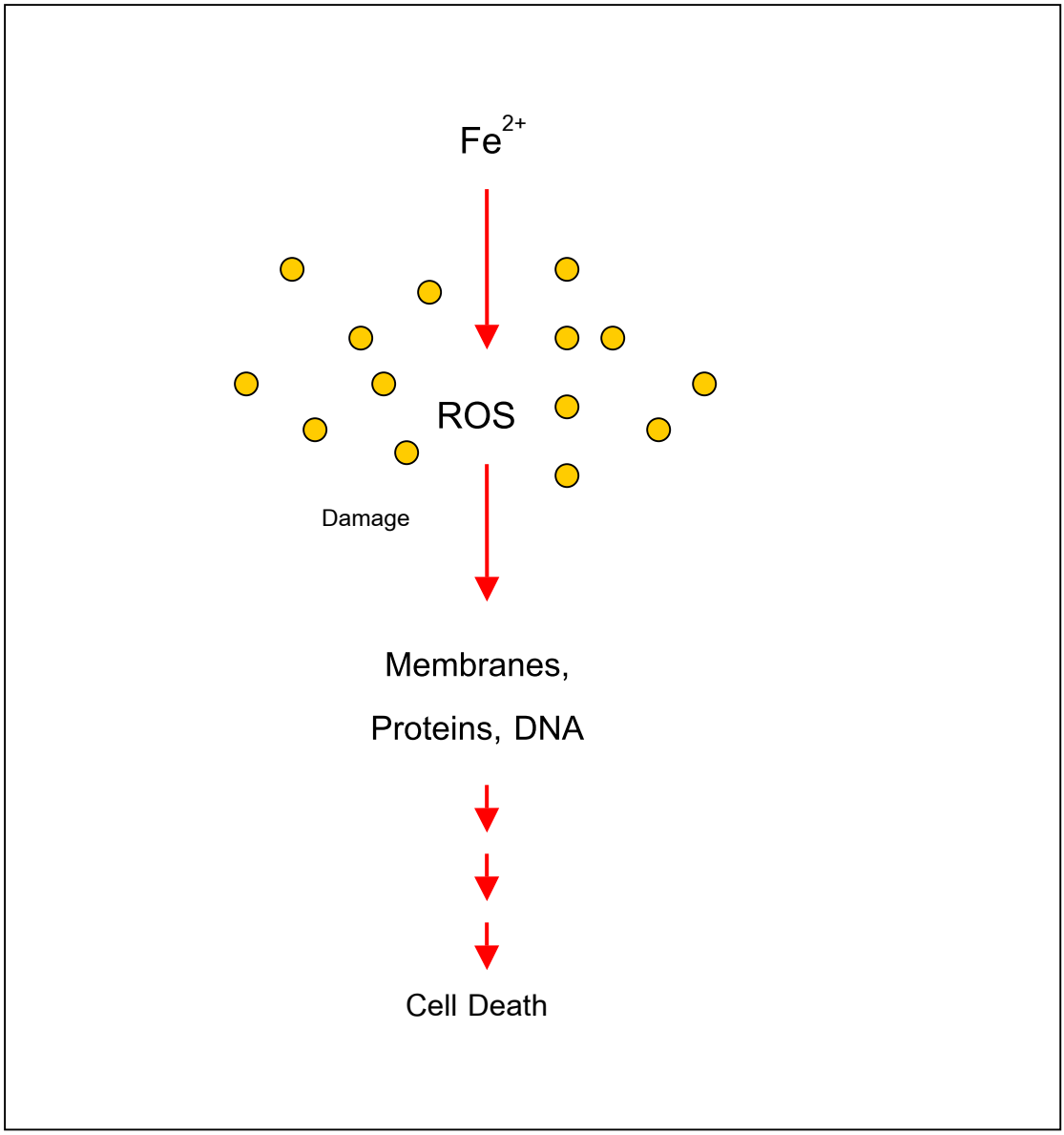

Figure 6.1 A diagram represents the toxic effects of iron, leading to cell death.

6.2 The Effects of Iron-induced Toxicity on Cellular Defense Mechanism

Glutathione (GSH) exhibits several functions in the brain chiefly acting as an antioxidant and a redox regulator. GSH depletion (Gu, et al., 1998) has been shown to affect mitochondrial function probably via selective inhibition of mitochondria complex I activity. Oxidative damage via GSH depletion may also accelerate the built-up of defective proteins, and the importance of ubiquitin-proteosome pathway of protein degradation in PD. These events eventually lead to cell death (Bharath, et al., 2002).

Metallothionein (MT) is a strong antioxidant, due to a large number of thiol groups. Oxidative stress induces MT synthesis and it may play a role in the cell similar to GSH (Min, et al., 1999). *In vitro* study showed that MT is 38.5-fold more effective on DNA protection from $^{\bullet}OH$ attacks than GSH (Able and Ruiter, 1989).

Iron has been found and measured in the nucleus by analytical methods. Moreover, ferritin is also detected in rat hepatocyte nuclei. DNA repair enzymes and transcription factors containing iron-sulfur cluster have been reported and the role of hemin as a gene activator has also been described. Although, iron is present in the nucleus, it is still unclear whether it directly binds to DNA or not.

Low molecular weight species, including metal ions, have been considered to be freely diffusible across nuclear pores. Moreover, iron transport is not inhibited by calcium ATPase pump inhibitors, suggesting that it may be transported into nucleus by a specific nuclear iron transport P-ATPase. This pump may play a role in controlling the passage of excess iron into the nucleus, leading to DNA damage (Meneghini, 1997).

The result are consistent with previous studies in rat striatum and substantia nigra, showing massive transient release of GSH after stop perfusion with MPP^{+} or Fe^{2+} (Han, et al., 1999). The typical antioxidant enzymes, catalase, glutathione peroxidase and superoxide dismutase, are cytosolic proteins. Whereas, a non-enzymatic protein, metallothionein may play a role in protecting DNA from free radical attacks. This may be due to numerous of cysteine residues. In addition, metallothionein accumulates in the nucleus during certain phases of cell cycles.

The increases in ROS production (Fig. 5.4a) together with the increases of glutathione (Fig. 5.11) and metallothionein levels (Fig. 5.10) indicate changes of antioxidants in cellular defense mechanism. The increases of both antioxidants in a dose-dependent manner indicate oxidative stress that occurred within the cells.

To counteract numerous ROS occurring during iron toxicity, both antioxidants (glutathione and metallothione) were increased. It was shown that the significant increase in antioxidants were found when using high dose of iron (1 mM) but could not detected the differences in other doses (100-500 μM). This may be due to the cellular defense mechanisms trying to counteract and remove ROS production.

The significant increases in glutathione and metallothione levels were found only in high doses. However, the levels of both antioxidants did not increase in a lower dose of iron (100-500 μM). This suggests that the small increase of both antioxidants may be used up to remove $^{\bullet}OH$ that occurs via the Haber-Weiss reaction. Alternatively, cells may use other processes to detoxify ROS production during iron-induced toxicity in a lower dose; such as SOD or any other small molecules. Hence, it needs not to increase a lot of glutathione and metallothione. In contrast, to counteract high doses of iron, cells may need more antioxidants to remove high amount of ROS. Therefore, cells produce more glutathione and metallothione levels (Fig. 6.2).

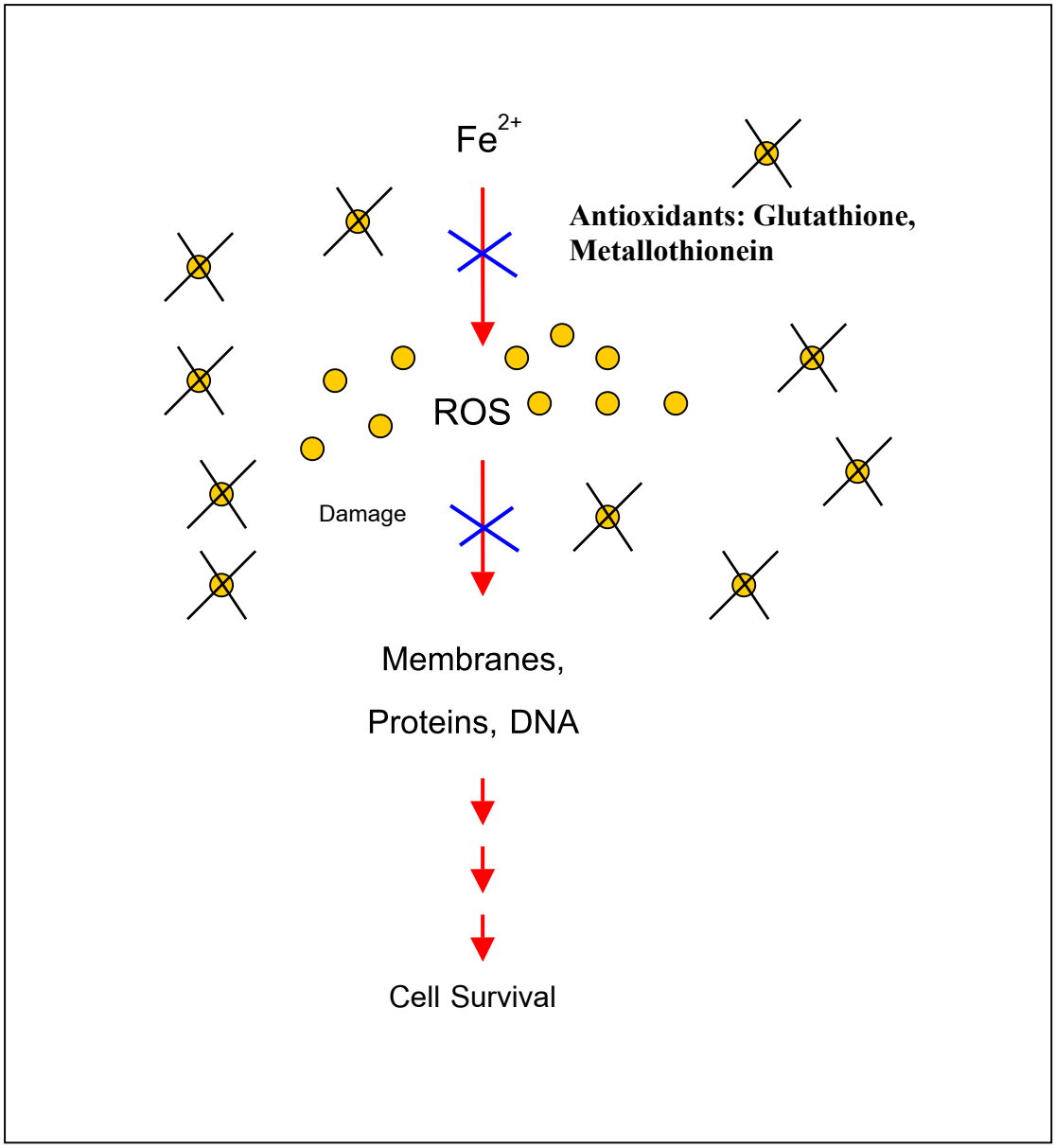

Figure 6.2 A diagram represents cellular defense mechanism during iron-induced toxicity.

6.3 The Beneficial and Deleterious Effects of Deferoxamine

"Free iron or labile iron" is able to participate in the Fenton reaction, catalyzing the formation of the $^{\bullet}OH$ and ferric ions (Fe^{3+}).

$$Fe^{2+} + H_2O_2 \longrightarrow Fe^{3+} + {}^{\bullet}OH + OH^-$$

DFO protects cells from iron-induced toxicity by chelating Fe^{3+} during the Fenton reaction. As a result, the amounts of free iron harmful to the cells are decreased. The interesting point is that ROS is also produced during the chelating period, which may become higher (Fig. 5.4b.) than that produced by iron toxicity. In this study, iron or DFO alone did not produce ROS within the cells (Fig. 5.4c), but when combined DFO with iron (Fig. 5.4b), ROS was produced. These suggest that during the chelating process, DFO may cause oxidative stress environment by mechanism involved in chelating process.

DFO is able to chelate free iron when it exists in excess, and hence reduce iron toxicity (Fig. 5.1-5.5, 5.11). On the other hand, in the absence of excess iron, by reducing the free pool of iron, it may become toxic itself. For example, DFO has been used *in vivo* and *in vitro* as a probe to study the role of iron in oxygen radical reactions (Willis, 1969; Gutteridge, et al., 1979), inflammatory joint disease (Blake, et. al., 1983), ethanol metabolism (Sinaceur, et al., 1983), complement-mediated lung injury (Ward, et al., 1983), alloxan toxicity (Grankvist and Markland, 1983), eradication of malarial parasites (Clark and Hunt, 1983), early treatment of myocardial ischemic/reperfusion injury (Reddy, et al., 1989), hemin-induced hemolysis (Baysal, et al., 1990), and retinal lipid peroxidation in experimental uveitis (Wu, et al., 1993).

In the present study, excess amounts of DFO or in the absence of free iron (Fig. 5.8a-b) DFO is harmful to the cells. This is supported by the finding that DFO is associated with neurotoxicity (Freedman, et al., 1988). The ability to prevent iron toxicity of the iron chelator, DFO, may come from its ability to replace free iron from iron storage molecules (ferritin, neuromelanin, other proteins, or smaller molecules).

The adverse effects of DFO found in this study may be due to the interference of DFO with the process in essential systems requiring iron for their metabolism, e.g. DNA/RNA synthesis, ribonuclease, dopamine synthesis in rat (Ward, et at., 1995), and human myeloid leukemic cells (Leardi, et al., 1998). Moreover, DFO alone can inhibit G1 or S-phase during cell proliferation in human myeloid leukemic cells (Fukuchi, et al., 1997; Dezza, et al., 1989), and activated caspase pathways in Hela cells (Greene, et al., 2002). This study suggests that 10 μM DFO can prevent iron toxicity, but higher doses (100 and 1000 μM) caused damage to cells, even when cells were loaded with excessive iron (Fig. 5.9a-b).

Disadvantage of DFO was found during the absence and/or low iron levels. In the absence of free iron, even low dose of DFO was harmful to cells, because it may remove essential iron needed for physiological functions. However, when used in the presence of excessive iron, DFO protects the cells. This suggests that low dose of DFO can be beneficial and be used as a drug of choice to combine with L-dopa for effective treatment in PD.

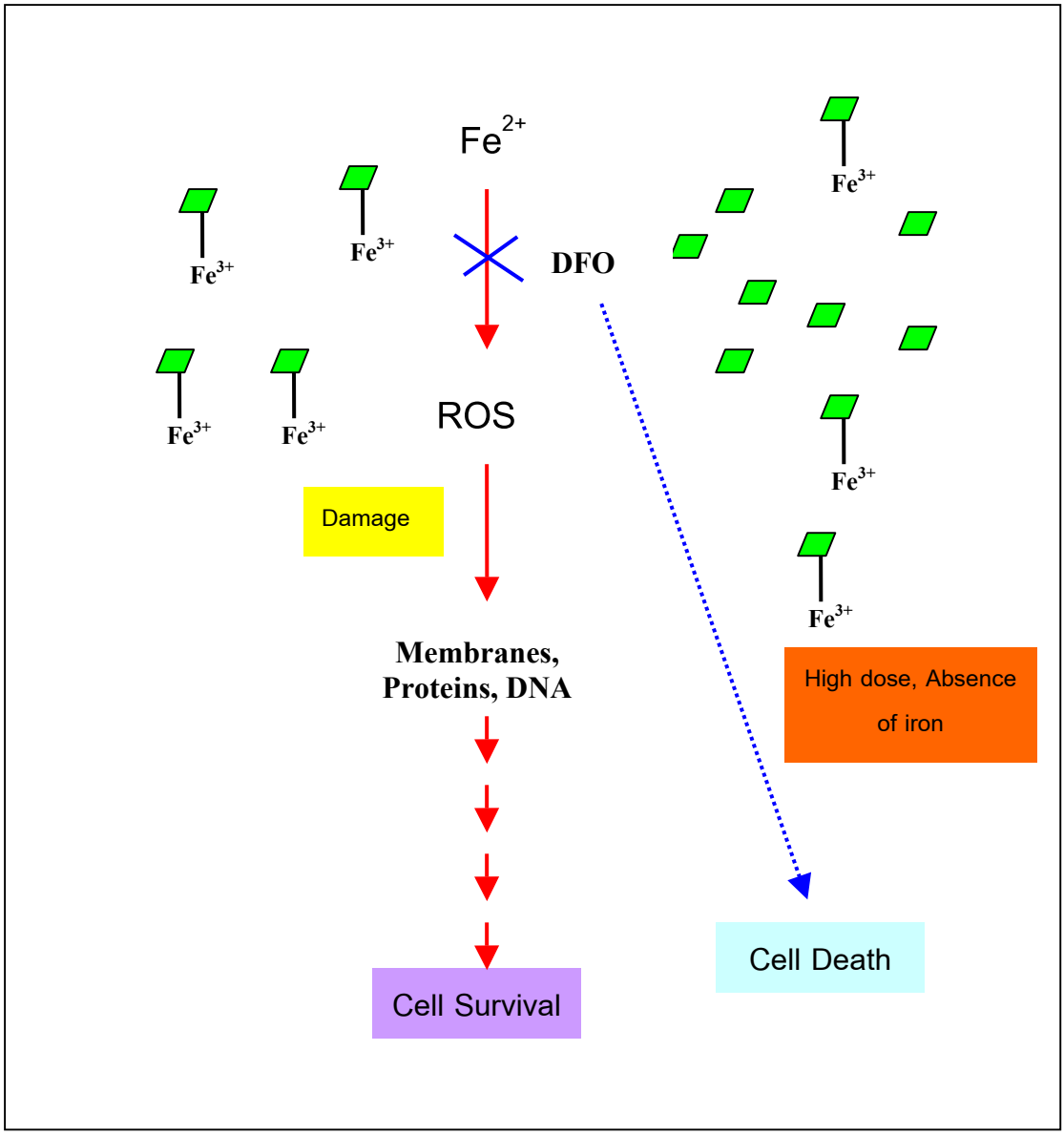

Figure 6.3 A diagram represents protective/toxic effects of DFO during iron-induced toxicity.

6.4 Iron Toxicity and Apoptosis

Apoptosis is a natural programmed cell death process, important for normal development and homeostasis of many cellular organisms. It is also important for removing damaged, infected cells. However, apoptosis can lead to adverse biological consequences. Apoptosis differs from necrosis occurring at the single cell level, whereas necrosis occurs in a group of cells. During apoptosis, an individual cell undergoes active process of cell death, set by genetic program in DNA fragmentation and the formation of apoptotic bodies (Kannan and Jain, 2000).

In the present study, iron increased nuclear factor kappa B (NF-κB) within 30 min and return to baseline level after 60 min (Fig. 5.13). This implies that NF-κB may mediate cell response to iron by activation of Tumor Necrotic Factor-α (TNF-α; She, et al., 2002) or ROS (Xiong, et al., 2003).

Upon activation, there is a phosphorylation of NF-κB and its inhibitory protein (I-κB). NF-κB is released from I-κB, translocates into nucleus, binds to specific κB-binding sites in DNA, and promotes transcription of other genes involved in inflammation, immune responses, apoptosis, and anti-apoptotic mechanism (Ghosh and Karin, 2002). This study is consistent with previous report showing that iron can activate NF-κB in Kupffer cells (She, et al., 2002), hepatic macrophages (Xiong, et al., 2003), and alcoholic liver cells injury (Tsukamoto, et al., 1999).

The regulations of NF-κB appear to exist at least in two levels: one occurs in the nucleus and the other in the cytoplasm. The former involves direct redox modifications of specific cysteine residues in DNA-binding domain of NF-κB. The oxidation of cysteine at the position 62 in p50 inhibits DNA-binding activity (Toledano and Leonard, 1991). Conversely, reduction of NF-κB by thioredoxin and Ref-1 appears to increase its activity (Mitomo, et al., 1994; Hirota, et al., 1999).

For the cytosolic regulation of NF-κB, upstream signaling is still to be determined, leading to activation of IKK, resulting in phosphorylation of two serine residues (Ser-32 and Ser-36) on I-κB, its polyubiquitination, and degradation by 26 S proteasome. TNF-α induced activation of NF-κB is abrogated by inhibition of ROS production through electron transport chain suggests that oxidative stress from

mitochondria act as a signal for this activation (Schulze-Osthoff, et al, 1993). It is also important to note that intracellular ROS generation may not be necessary for NF-κB activation in all cell types (Bonizzi, et al., 1999; Kurose, et al., 1997).

Oxidative stress-induced neuronal cell death appears to be involved in certain neurodegenerative disorders such as Alzheimer's and Parkinson's disease. Among NF-κB-inducing agents, reactive oxygen species (ROS) are widely used, and recent evidence strongly suggests that NF-κB may afford neuroprotection against oxidative insults in particular with respect to Alzheimer's disease. The situation is, however, much less clear in PD (Blum et al, 2001). Nuclear translocation of NF-κB is increased in dopaminergic neurons in PD post-mortem brains suggested that oxidative stress might be related to apoptotic death in PD through NF-κB-related signal transduction (Hunot et al, 1997). At nontoxic concentrations, iron is known to promote macrophage functions, including antimicrobial effects and tumor necrotic factor (TNF)-mediated cytotoxicity. More specifically, recent evidence suggests the role of iron in promoting cytokine expression and NF-κB activation by hepatic macrophage (She et al, 2002).

After the cells were treated with iron for 24 h, there was a significant increase of caspase-3 activity (Fig. 5.12). At the same time, levels of anti-apoptotic Bcl_2 protein were significantly reduced (Fig. 5.14), whereas pro-apoptotic Bax protein did not change (Fig.5.15). A decrease of anti-apoptotic Bcl_2 protein may result from the suppression of NF-κB activity on anti-apoptotic Bcl_2 gene transcription, but NF-κB may not have any effects on pro-apoptotic Bax proteins. In this study, unchanged pro-apoptotic Bax protein level suggested that cell death caused by iron-induced toxicity does not pass pro-apoptotic Bax protein pathway, but via other pro-apoptotic proteins.

Bcl_2 is localized on the cytoplasmic face of mitochondrial outer membrane, endoplasmic reticulum and nuclear envelope. It is believed that Bcl-2 can counterbalance oxidative damage on these compartments; maintain mitochondria membrane integrity by directly or indirectly preventing the release of cytochrome *c*. The decrease in anti-apoptotic Bcl_2 protein may disrupt normal mitochondrial functions, leading to permeability transition of mitochondrial pores. As a

consequence, defective permeability of mitochondrial pores open to larger molecules, passing pores and cause uncoupling of the respiratory chain, resulting in over generation of ROS, cessation of ATP synthesis, matrix Ca^{2+} outflow, and depletion of reduced glutathione and other reductants (Kannan and Jain, 2000). Moreover, this leads to leakage of cytochrome *c* and other pro-apoptotic proteins from the mitochondria. Cytochrome *c* is able to induce the cleavage of zymogens and then activation of caspase-9, caspase-3 and downstream cascades.

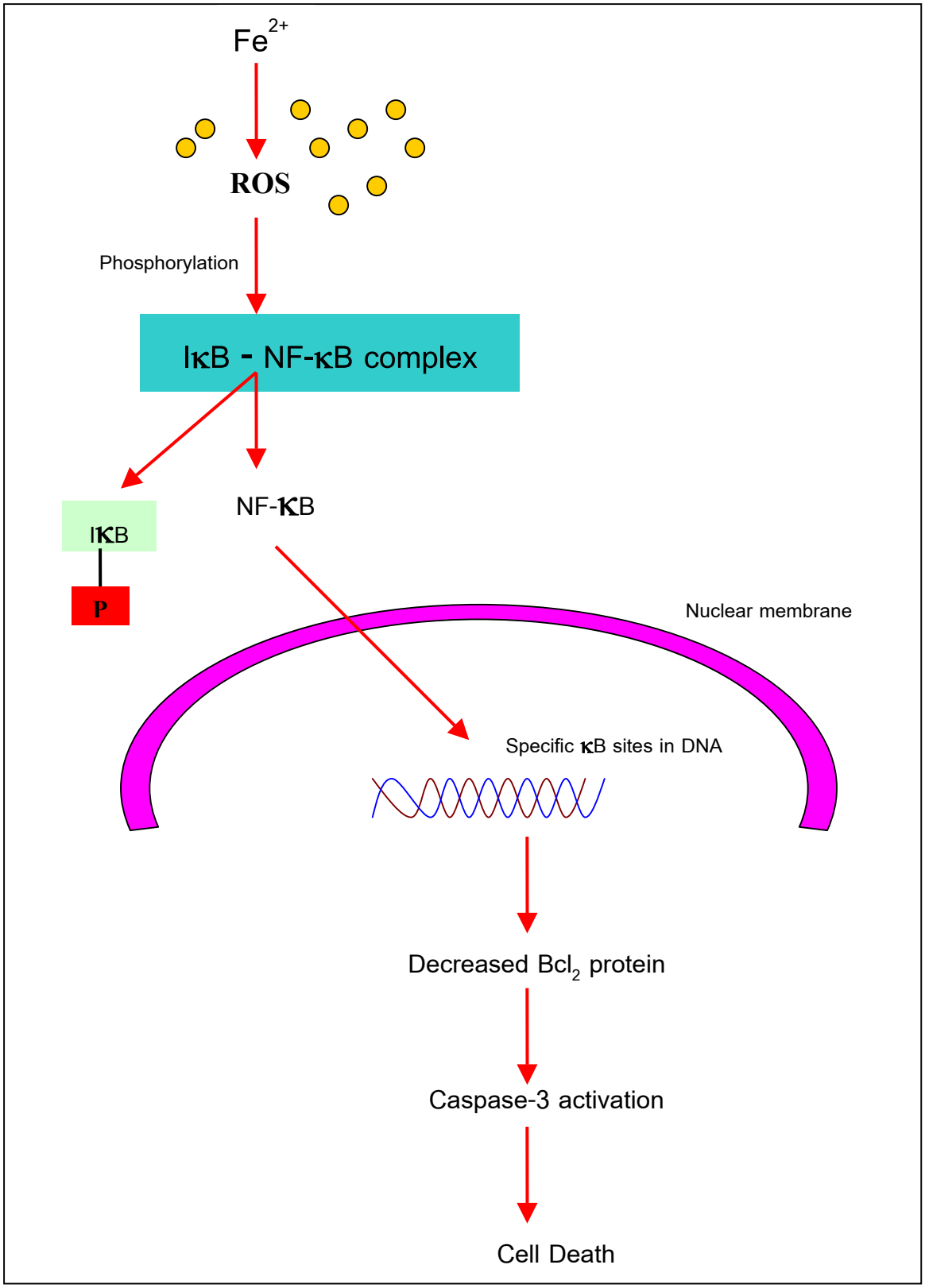

Figure 6.4 A diagram represents the possible effects of iron on cellular events.

6.5 Iron Alters Biochemical Integrity of α-Synuclein and Mitochondria

In the past two years, mutations in three different genes have been associated with familial PD. Two-point mutations have been found in the α-synuclein gene: alanine to threonine at amino acid position 53 and alanine to proline at position 30. These mutations are dominantly inherited with an early-onset, but otherwise typical PD with L-dopa responsiveness and pathology that includes the presence of Lewy bodies and severe loss of neurons in the SN pars compacta.

The family of synuclein genes encode three proteins; α , β, and γ. These proteins have several conserved residues and contain five similar-sized coding exons. Only the α-synuclein gene, however, has been linked to familial PD. α-Synuc1ein is a synaptic vesicle-associated protein expressed by many neurons in rodent brains. A fragment of α-synuclein is a nonamyloid component of senile plaques in Alzheimer's disease and an avian homolog of α-synuclein (synelfin) is elevated during the critical period for bird song development. Once the mutations in familial PD cases were identified, α-synuclein was shown to be a major component of Lewy bodies, the pathological hallmark of typical PD and diffuse Lewy body disease.

In this dissertation, SK-N-SK dopaminegic cells treated with excessive iron exhibited disruptions of nuclear membrane and translocation of α-synuclein and mitochondria in perinuclear regions (Fig. 5.7-5.8). This may be caused by ROS which is able to induce membrane disruption. This high concentration of iron could be one reason for the loss of nucleocytoplasmic signal transduction that requiring in normal neuronal functions (Fig. 6.5).

Results from double labeling of α-synuclein and JC-1 fluorescence demonstrating (Fig. 5.7) suggested that $FeSO_4$-induced apoptosis is associated with mitochondrial aggregation of α-synuclein in the perinuclear region, which may be responsible for the induction of Lewy body synthesis in PD. Perinuclear aggregation of α-synuclein may have several pathophysiological consequences including impaired nucleocytoplasmic signal transduction and hence apoptosis, observed during neurodegeneration in PD.

α-Synuclein is abundant in the brain, expressed in high levels in presynaptic nerve terminals, but its physiological functions are poorly understood. Recent studies show that the production of α-synuclein in the transgenic mice (Masliah, et al., 2000) or transgenic files (Feany and Bender, 2000) causes motor deficits and neuronal inclusions reminiscent of PD. Recent study shows that iron can cause α-synuclein aggregation both *in vivo* and *in vitro* (Uversky, et al., 2001). Several possible mechanisms for metal-stimulated fibrillation of α-synuclein can be envisaged. The simplest one involves direct interactions between α-synuclein and metal, leading to α-synuclein conformational changes.

Until now, little is known about the effect of elevated concentrations of metal ions on the structural properties and aggregation behavior of α-synuclein, although many studies believed in oxidative damage theory (Uversky, et al., 2001). The deleterious interaction among iron, α-synuclein and dopaminergic neurons (Fig. 5.6-5.7) and the possible effects of DFO in neutralizing iron toxicity on α-synuclein needs to be further investigated.

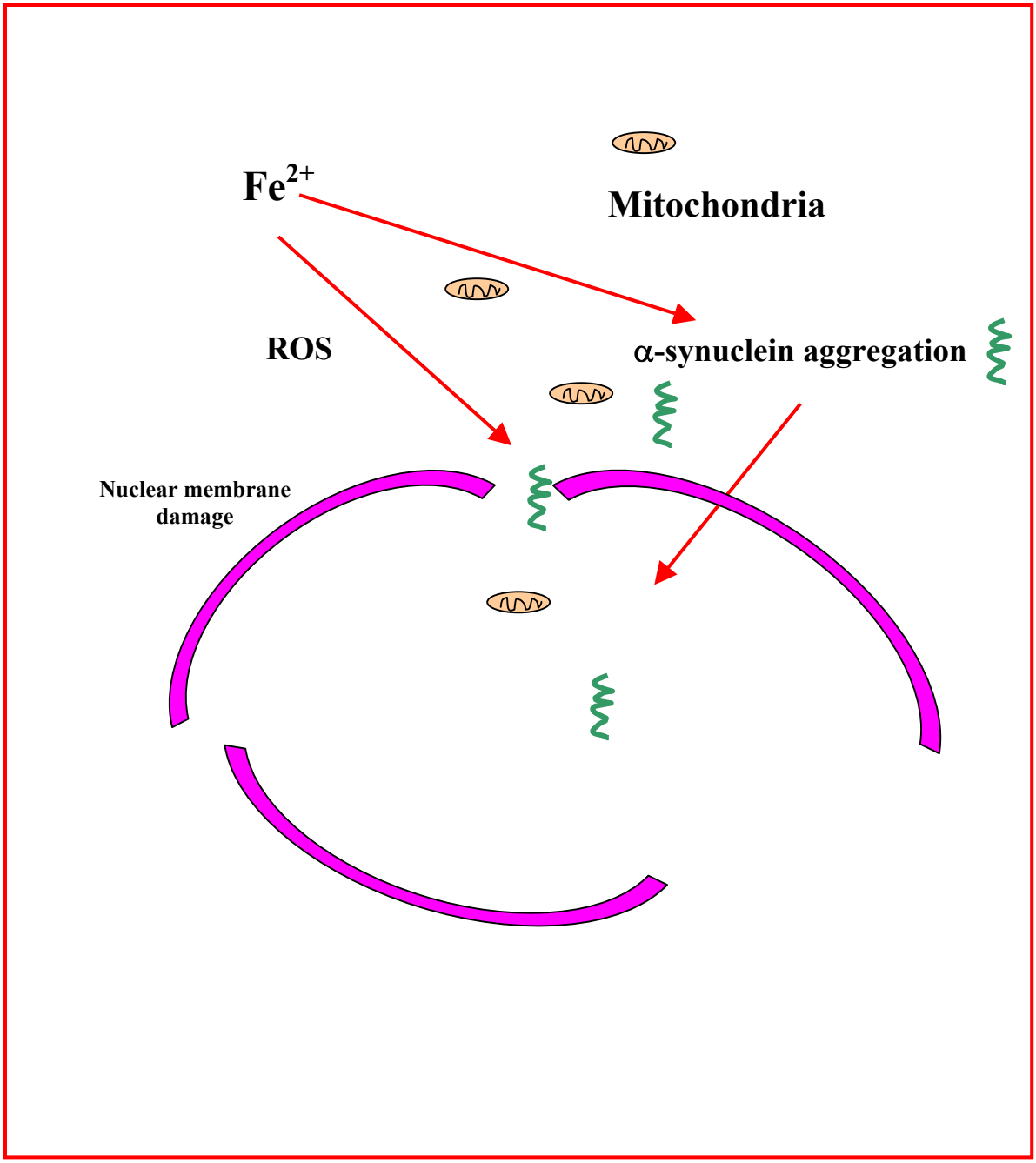

Figure 6.5 A diagram represents possible effects of iron on the alteration of biochemical integrity of α-synuclein and mitochondria.

6.6 SK-N-SH dopaminergic neuroblastoma cells: a model for PD studies

There are many models used to study the cellular events occurring in PD both *in vivo* and *in vitro*. A cell culture is one of those with a lot of benefits; such as easy-to-control environment, homogeneity of cells, economy, scale, mechanization, and *in vivo* modeling. To study PD, investigators can use both cell lines and primary cell cultures. Compared to primary cell cultures, cell lines are easier to get from the commercials, produce more passages, easy for culture and subcultures. In this study, I choose human type, matching our concerns. Other characteristics that we need should come from brain cells or neurons, which show dopaminergic characteristics. One marker that shows dopaminergic characteristics is tyrosine hydroxylase, a rate-limiting enzyme for dopamine synthesis.

Previous studies showed that dopaminergic neurons can produce free radicals through DA auto-oxidation and enzymatic catabolism (Olanow, 1993). DA can spontaneously undergo auto-oxidation due to its quinone structure *in vitro* or through an enzymatic-catalyzed reaction *in vivo*, and both pathways were shown to generate free radicals (Hasting, 1995). From the above reasons, SK-N-SH cell lines were chosen because of the dopaminergic characteristics. Moreover, SK-N-SH cell lines are human cells, not animal cells. These make SK-N-SH cells appropriate for the study of cellular changes in PD. Finally, according to the interaction of Fe^{2+} and dopamine, we expected that this SK-N-SH cell type could show effects of iron toxicity and oxidative stress. From these three reasons made it strong enough to choose SK-N-SH cells as a model to study Parkinson's disease.

CHAPTER 7
CONCLUSION

The conclusions of the present study are as follows:

1. High levels of free iron are harmful to the cells. Because it produced oxidative stress by promoting ROS; damaged lipid and protein, decreased cellular ATP levels; enhanced NF-κB translocation; activated caspase-3; and increased glutathione and metallothionein levels within the SK-N-SH dopaminergic cells. DFO can prevent these effects.
2. In the absence of excess iron, DFO could cause damage to SK-N-SH dopaminergic cells.
3. Free iron induced augment of antioxidants; glutathione and metallothionein, indicating cellular defense mechanisms that occurring within SK-N-SH dopaminergic cells.
4. Excessive iron induced the activation of transcription factors, NF-κB, in SK-N-SH dopaminergic cells. Anti-apoptotic Bcl_2 protein levels were decreased, whereas pro-apoptotic Bax levels remain unchanged in treated cells.

The possible mechanism in which iron damaged and caused cell death may be due to the excess levels of free iron (Fe^{2+}) caused an increase in hydroxyl radical level, a potent reactive oxygen species (ROS), via Fenton reaction. High level of ROS caused oxidative stress environment within the cell, which in turn, damaged lipid, protein and DNA and lead to cell death as a consequence (Fig. 7.1).

Moreover, an auto-oxidation of DA produces hydrogen peroxide. In the present of free iron, hydrogen peroxide is decomposed via the Fenton reaction and produce hydroxyl radicals. This may lead to more oxidative damage of the cells. The oxidative damaged caused an alteration of mitochondria function lead to energy depletion and cause cell death.

DFO, an iron chelator, help decrease free iron within the cell and prevent hydroxyl radical-induced cell damage from Fenton reaction. An increase in antioxidant levels, glutathione and metallothionein, may indicate the cellular defense mechanism against ROS. However, the persistence of ROS level by iron indicated that this response of cellular defense mechanism by glutathione and metallothionein was not high enough to clear up ROS (Fig. 5.11 and Fig. 5.10).

Free iron caused an aggregation of α-synuclein and accumulation mitochondria near to peri-nuclear region. Especially, in high doses, iron lead to nuclear membrane damage and caused the translocation of α-synuclein and mitochondria from peri-nuclear region into nucleus. These results indicated cell membrane alteration and damaged from iron toxicity (Fig. 7.1).

Moreover, free iron might activate tumor necrotic factor (TNF) which could stimulate the phosphorylation of inhibitory-κB (I-κB) by IKK and consequently enhanced the translocation of nuclear factor kappa B (NF-κB) into nucleus (She et al, 2002, Schulze-Osthoff, et al, 1993). After translocation NF-κB bind to its DNA-binding site and might suppress Bcl_2, an anti apoptotic protein, gene expression. In general, Bcl_2 is located inside mitochondria membrane and control membrane permeability. A decrease in Bcl_2 proteins cause alters mitochondrial membrane permeability and lead to leakage of cytochrome *c* from mitochondria to cytosol.

In cytoplasm, cytochrome *c* binds to apaf-1 and activates procasepase-9 and form apoptosome. This apoptosome, in turn, active caspase-3 activity and cause activation of down stream caspase cascade and, finally, lead to apoptotic cell death (Fig. 7.2). Altogether, these finding may be one of the possible mechanism which can explain toxicity of iron-induced oxidative damaged and finally lead to apoptotic cell death in Parkinson's disease.

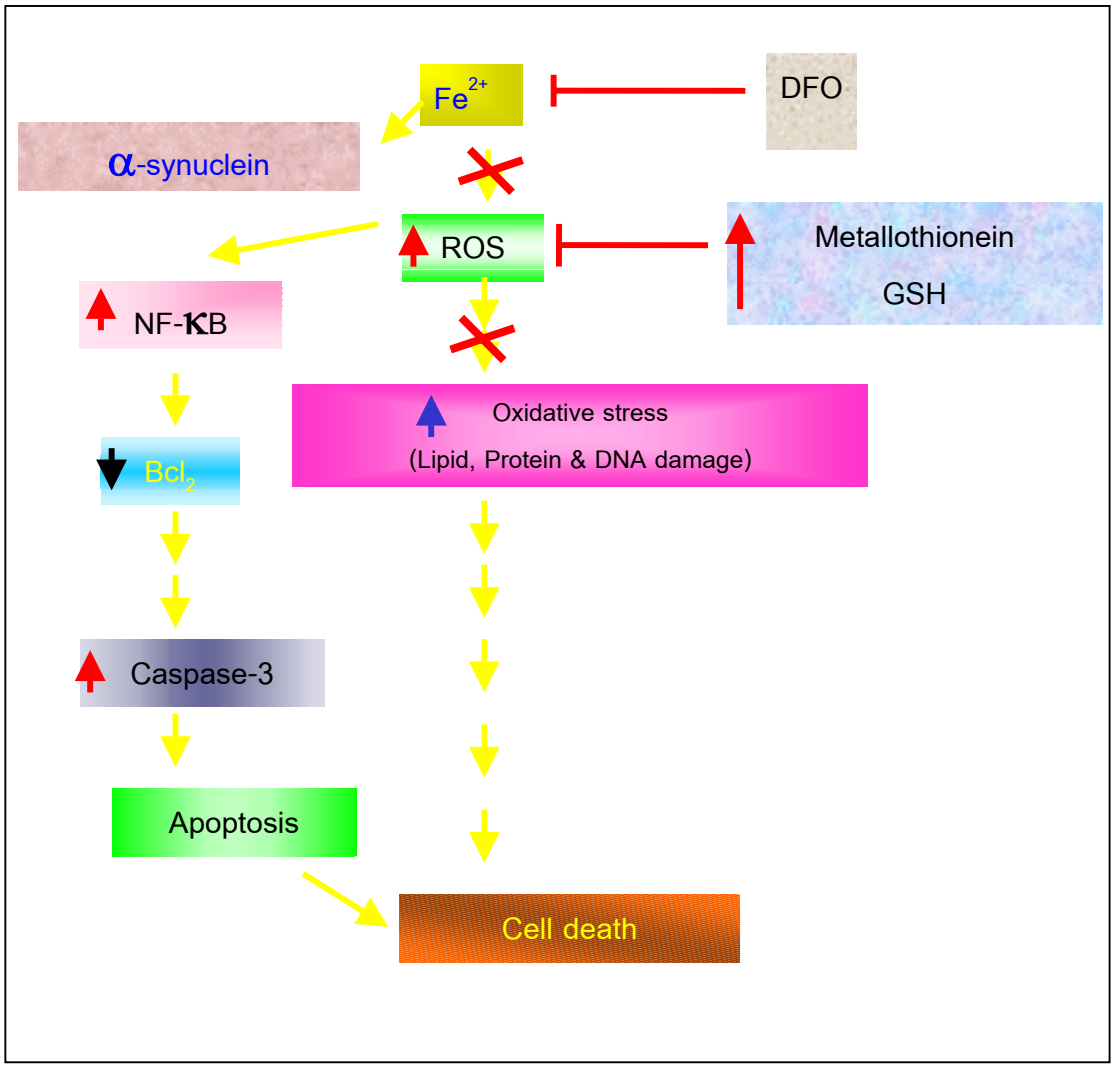

Figure 7.1 Schematic diagram represents the effects of iron on the alteration of cell biochemical and physiological from the study.

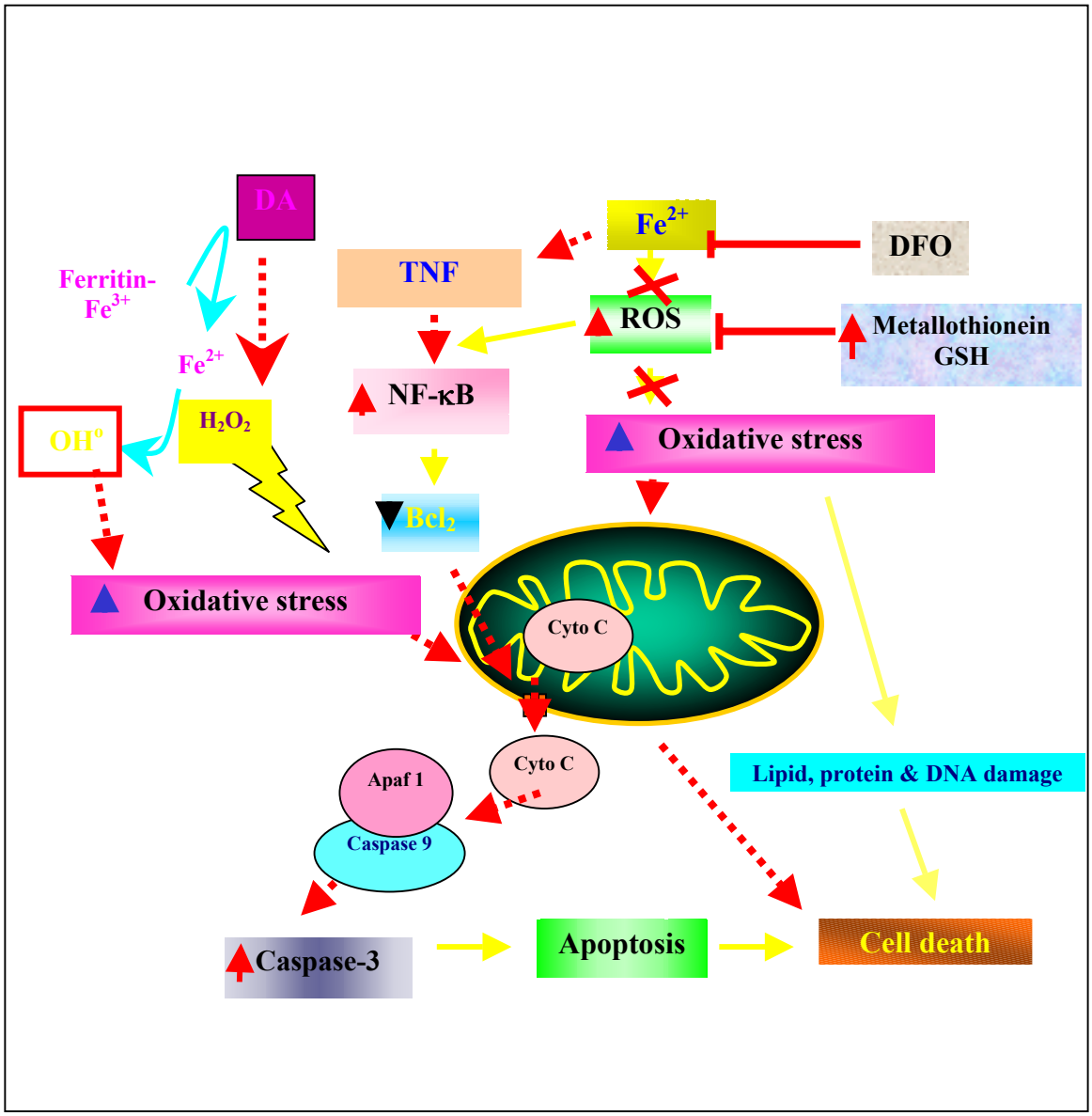

Figure 7.2 Schematic represents the possible effects of iron on the alteration of cell biochemical and physiological and lead to cell death via apoptosis.

BIBLIOGRAPHY

Able J, Ruiter N (1989) Inhibition of hydroxyl-radical-generated DNA degradation by metallothionein. Toxicol Lett 47: 191-196.

Aoki S, Okada Y, Nishimura K (1989) Normal deposition of brain iron in childhood and adolescence: MR imaging at 1.5 T. Radiology 172:381–385.

Attieh ZK, Mukhopadhyay CK, Seshadri V, Tripoulas NA, Fox PL (1999) Ceruloplasmin ferroxidase activity stimulates cellular iron uptake by a trivalent cation-specific transport mechanism. J Biol Chem 274: 1116-1123.

Bartzokis G, Beckson M, Hance D, Marx P, Foster J, Marder S (1997) MR evaluation of age-related increase of brain iron in young adult and older normal males. Magn Reson Imaging 15: 29-35.

Bartzokis G, Cummings J, Markham C, Marmarelis P, Treciokas L, Tishler T, Marder S, Mintz J (1999) MRI evaluation of brain iron in earlier and later-onset Parkinson's disease and normal subjects. Magn Reson Imaging 17: 213-222.

Bartzokis G, Cummings J, Perlman S, Hance D, Mintz J (1999) Increased basal ganglia iron levels in Huntington disease. Arch Neurol 56: 569-574.

Bastin J, Jones M, O'Callaghan C, Schimanski L, Mason D, Townsend A (1998) Kupffer cell staining by an HFE-specific monoclonal antibody: Implications for hereditary haemochromatosis. Br J Haematol 103: 931-941.

Baysal E, Monteiro HP, Sullivan SG, Stern, A (1990) Desferrioxamine protects human red blood cells from hemin-induced hemolysis. Free Radical Biology & Medicine, 9: 5–10.

Beal MF (1998) Mitochondrial dysfunction in neurodegenerative diseases. Biochim Biophys Acta 1366: 211-223.

Beard JL, Connor JR, Jones BC (1993) Iron in the brain. Nutrition Reviews 51: 157-170.

Ben-Shachar D, Eshel G, Finberg JPM, Youdim MBH (1991) The iron chelator desferrioxamine (desferal) retards 6-hydroxydopamine-induced degeneration of nigrostriatal dopamine neurons. J Neurochem 56: 1141-1444.

Bharath S, Hsu M, Kaur D, Rajagopalan S, Anderson JK (2002) Glutathione, iron and Parkinson's disease. Biochem Pharmacol 64: 1037-1048.

Blake DR, Hall ND, Baron A, Dieppe PA, Halliwell B, Gutteridge JMC (1983) Effect of specific iron chelating agents on animal models of inflammation. Ann Rheum Dis 42: 89-93.

Bonizzi G, Piette J, Schoonbroodt S, Greimers R, Havard L, Merville MP, Bours V (1999) Reactive oxygen intermediate-dependent NF-kappa B activation by interleukin-1beta requires 5-lipoxygenase or NADPH oxidase activity. Mol Cell Biol 19: 1950-1960.

Bowman BH, Jansen L, Yang F, Adrian GS, Zhao M, Atherton SS, Buchanan JM, Greene R, Walter C, Herbert DC (1995) Discovery of a brain promoter from the human transferrin gene and its utilization for development of transgenic mice that express human apolipoprotein E alleles. Proc Natl Acad Sci USA 92: 12115-12119.

Bradbury MW, (1997) Transport of iron in the blood-brain-cerebrospinal fluid system. J Neurochem 69: 443-454.

Buege JA and Aust SD (1998) Microsomal lipid peroxidation. Methods Mol Bio 108: 302-310.

Burdo JR, Martin J, Menzies SL, Dolan KG, Romano MA, Fletcher RJ, Garrick MD, Garrick LM, Cannor JR (1999) Cellular distribution of iron in the brain of the Belgrade rat. Neuroscience 93: 1189-1196.

Calabrese V, Scapagnini G, Ravagna A, Fariello RG, Giuffrida Stella AM, Abraham Ng (2002) Regional distribution of heme oxygenase, HSP70, and glutathione in the brain: Relevance for endogenous oxidant/antioxidant balance and stress tolerance. J Neurosci Res 68: 65-75.

Campbell A, Smith MA, Sayre LM, Bondy SC, Perry G (2001) Mechanisms by which metals promote events connected to neurodegenerative diseases. Brain Res Bull 55: 125-132.

Campuzano V, Montermini L, Lutz Y, Cova L, Hindelang C, Jiralerspong S, Trottier Y, Kish S, Faucheux B, Trouillas P, Authier F, Durr A, Mandel J, Vescovi A, Pandolfo M, Koenig M (1999) Frataxin is reduced in Friedreich ataxia patients and is associated with mitochondrial membranes. Hum Mol Genet 6: 1771-1780.

Carpenter MB (1978) The mesencephalon. In: Core text of neuroanatomy (2nd eds) Williams & Wilkins company, Baltimore, pp157-159.

Castellani RJ, Siedlak SL, Perry G, Smith MA (2000) Sequestration of iron by Lewy bodies in Parkinson's disease. Acta Neuropathol (Berl) 100: 111-114.

Cazzola M, Bergamaschi G, Dezza L, Arosino P (1990) Manipulations of cellular iron metabolism for modulating normal and malignant cell proliferation: achievement and prospects. Blood 75: 1903-1919.

Clark IA, Hunt NH (1983) Evidence for reactive oxygen intermediates causing hemolysis and parasite death in malaria. Infect. Immun 39: 1–6.

Connor JR, Menzies SL (1996) Relation of iron to oligodendrocytes and myelination. Glia 17: 83-93.

Connor JR, Menzies SL, Burdo JR, Boyer PJ (2001) Iron and iron management proteins in neurobiology. Pediatr Neurol 25: 118-129.

Connor JR, Pavlick G, Karli D, Menzies SL, Palmer C (1995) A histochemical study of iron-positive cells in the developing rat brain. J Comp Neurol 355: 111-123.

Connor JR, Snyder BS, Beard JL, Fine RE, Mufson EJ (1992) Regional distribution of iron and iron-regulatory proteins in the brain in aging and Alzheimer's disease. J Neurosci Res 31: 327-335.

Crowe A, Morgan EH (1992) Iron and transferrin uptake by brain and cerebrospinal fluid in the rat. Brain Res 592: 8-16.

D'Sa CM, Arthur RE Jr, States JC, Kuhn DM (1996) Tryptophan hydroxylase: Cloning and expression of the rat brain enzyme in mammalian cells. J Neurochem 67: 900-906.

Dexter DT, Carayon A, Javoy-Agid F, Agid Y, Wells FR, Daniel SE, Lees AJ, Jenner P, Marsden, CD (1991) Alterations in the levels of iron, ferritin, and other trace metals in Parkinson's disease and other neurodegenerative diseases affecting the basal ganglia. Brain 114: 1953–1975.

Dezza L, Cazzola M, Danova M, Carlo-Stella C, Bergamaschi G, Brugnatelli S, Invernizzi R, Mazzini G, Riccardi A, Ascari E (1989) Effects of deferoxamine on normal and leukemic human hematopoietic cell growth: in vitro and in vivo studies. Leukemia 3: 104-107.

Donovan A, Brownlie A, Zhou Y, Shepard J, Pratt S, Moynihan J, Paw B, Drejer A, Barut B, Zapata A, Law T, Brugnara C, Lux S, Pinkus G, Pinkus J, Kingsley P, Palis J, Fleming M, Andrews N, Zon L (2000) Positoinal cloning of zebrafish ferroportin1 identifies a conserved vertebrate iron exporter. Nature 403: 776-781.

Double KL, Zecca L, Costi P, Mauer M, Griesinger C, Ito S, Ben-Shachar D, Bringmann G, Fariello RG, Riederer P, Gerlach M (2000) Structural characteristics of human substatia nigra neuromelanin and synthetic neuromelanins. J Neurochem 75: 2583-2589.

Dringen R (2000) Metabolism and functions of glutathione in brain. Prog Neurobiol 62: 649-671.

Dugan LL, Choi DW (1999) Hypoxic-ischemic brain injury and Oxidative stress. In: Basic neurochemistry: Molecular, cellular and medical aspects. Siegel GJ (6th eds) Lippincott-Raven, Philadelphia, pp927-929.

Dwork AJ, Lawler G, Ztbert PA, Durkin M, Osman M, Willson N, Barkai AI (1990) An autoradiographic study of the uptake and distribution of iron of the young rat. Brain Res 518: 31-39.

Ebadi M, Govitrapong P, Sharma S, Muralikrishnan D, Shavali S, Pellett L, Schafer R, Albano C, Eken, J (2001) Ubiquinone (CoenzymeQ10) and mitochondria in oxidative stress of Parkinson's disease. Biol Signals Recept 10: 224–253.

Ebadi M, Hiramatsu M (2000) Glutathione and metallothionein in oxidative stress of Parkinson's disease; in Poli G, Cadenas E, (eds): Free Radicals in Brain Pathophysiology. Marcel Dekker, Inc, New York, pp 427–465.

Ebadi M, Srinivasan S, Baxi M (1996) Oxidative stress and antioxidant therapy in Parkinson's disease. Prog. Neurobiol 48: 1–19.

Eberwine J (1999) Transcription factors in the central nervous system. In: Basic neurochemistry: Molecular, cellular and medical aspects. Siegel GJ (6th eds) Lippincott-Raven, Philadelphia, pp 525-526.

Eisenstein R (2000) Iron regulatory proteins and the molecular control of mammalian iron metabolism. Ann Rev Nutr 20: 627-662.

Emerit J, Beaumont C, Trivin F (2001) Iron metabolism, free radicals, and oxidative injury. Biomed Pharmacother 55: 333–339.

Faucheux BA, Nillesse N, Damier P, Spik G, Mouatt-Prigent A, Pierce A, Leveugle B, Kubis N, Hauw JJ, Agid Y (1995) Expressions of lactoferrin is increased in the mesencephalon of patients with Parkinson's disease. Proc Natl Acad Sci USA 92: 9603-9607.

Feany MB, Bender WW (2000) Drosophilia model of Parkinson's disease. Nature 404: 394-398.

Fernandez-Gonzalez A, Perez-Otano I, Morgan JI (2000) MPTP selectively induces haem oxygenase-1 expression in strial astrocytes. Eur J Neurosci 12: 1573-1583.

Ferris CD, Jaffrey SR, Sawa A, Takahashi M, Brady SD, Barrow RK, Tysoe SA, Wolosker H, Baranano DE, Dore S, Poss KD, Synder SH (1999) Haem oxygenase-1 prevents cell death by regulating cellular iron. Nat Cell Biol 1: 152-157.

Freedman MH, Boyden M, Taylor M, Skarf B (1988) Neurotoxicity associated with deferoxamine therapy. Toxiology 49: 283–290.

Freshney RI (2000) Introduction. In: Culture of animal cells: a manual of basic technique. (4^{th} eds) Wiley-Liss, Toronto, pp 1-8.

Fukuchi K, Tomoyasu S, Tsuroka N, Gomi K (1994) Iron deprivation-induced apoptosis in HL-60 cells. FEBS Lett 350: 139-142.

Fukuchi K, Tomoyasu S, Watanabe H, Kaetsu S, Tsuroka N, Gomi K (1995) Iron deprivation results in an increase in p53 expression. Biol Chem Hoppe-Seyler 376: 627-630.

Fukuchi K, Tomoyasu S, Watanabe H, Tsuruoka N, Gomi (1997) G1 accumulation caused by iron deprivation with deferoxamine does not accompany change pRB status in ML-1 cells. Biochim Biophy Acta 1357: 297-305.

Good PF, Olanow CW, Perl DP (1992) Neuromelanin-containing neurons of the substantia nigra accumulation iron and aluminum in Parkinson's disease: A LAMMA study. Brain Res 593: 343-346.

Ghosh S, Karin M (2002) Missing pieces in the NF-kappaB puzzle. Cell 109 (suppl.) S81-S96.

Grankvist K, Marklund SL (1983) Opposite effects of two metalchelators on alloxan-induced diabetes in mice. Life Sci 33: 2535–2540.

Greene BT, Thorburn J, Willingham MC, Thorburn A, Planalp RP, Brechbiel MW, Jennings-Gee J, Wilkinson IV J, Torti FM, Torti SV (2002) Activation of caspase pathways during iron chelator-mediated apoptosis. J Bio Chem 277: 25568-25575.

Gu M, Owen AD, Toffa SEK, Cooper JM, Dexter DT, Jenner P, Marsden CD, Schapira AHV (1998) Mitochondrial function, GSH and iron in neurodegenration and Lewy body diseases. J Neurol Sci 158: 24-29.

Gutteridge JMC, Richmond R, Halliwell B (1979) Inhibition of iron-catalysed formation of hydroxyl radicals from super-oxide and lipid peroxidation by desferrioxamine. Biochem J 184: 469–472.

Guttmacher AE and Collins FS (2003) Alzheimer's disease and Parkinson's disease. N Engl J Med 348: 1356-64.

Hallgren B, Sourander P (1958) The effect of age on the nonhaemin iron in the human brain. J Neurochem 3: 41–51.

Hasting TG (1995) Enzymatic oxidation of dopamine: the role of postagladin H synthesis. J Neurochem 64: 919-924.

Hashimoto M, Hsu LJ, Xia Y, Takeda A, Sisk A, Sundsmo M, Masliah E (1999) Oxidative stress induces amyloid-like aggregation formation of NACP/alpha-synuclein in vitro. Neuroreport 10: 717-721.

Henry C, Rakba N, Imbert D, Thomas F, Baret P, Serratrice G, Gaude D, Pierre JL, Ward RJ, Crichton RR, Lescoat G (2001) New 8-hydroxyquinoline and catecholate iron chelators: Influence of their partition coefficient on their biological activity. Biochem Pharmacol 62: 1355-1362.

Hirota K, Murata M, Sachi Y, Nakamura H, Takeuchi J, Mori K, Yodoi J (1999) Distinct roles of thioredoxin in the cytoplasm and in the nucleuss. A two-step mechanism of redox regulation of transcription factor NF-kappa B. J Biol Chem 27891-27897.

Hirsch E, Faucheux B (1998) Iron metabolism and Parkinson's disease. Mov Disord 13 (suppl 1): 39-45.

Hoffbrand AV, Ganeshaguru K, Hooton JWL, Tattersall MHN (1976) Effect of iron deficiency and desferrioxamine of DNA synthesis in human cells. Br J Haematol 33: 517-526.

Hulet SW, Powers S, Connor JR (1999) Distribution of transferring and ferritin binding in normal and multiple sclerotic human brains. J Neurol Sci 165: 48-55.

Ihara Y, Chuda M, Kuroda S, Hayabara T (1999) Hydroxyl radical and superoxide dismutase in blood of patients with Parkinson's disease: Relationship to clinical data. J Neurosci Res 170: 90-95.

Jellinger KA (1999) The role of iron in neurodegeneration: Prospects for pharmacotherapy of Parkinson's disease. Drugs & Aging 14: 115–140.

Kannan K, Jain SK (2000) Oxidative stress and apoptosis. Pathophysiol 27: 153-163.

Kawamata T, Tooyama I, Yamada T, Walker DG, McGeer PL (1993) Lactotransferrin immunocytochemistry in Alzheimer and normal human brain. Am J Pathol 142: 1574-1585.

Kitada T, Asakawa S, Hattori N (1998) Mutations in the Parkin gene cause autosomal recessive juvenile parkinsonism. Nature 392: 605-608.

Klomp L, Gitlin J (1996) Expression of the ceruloplasmin gene in the human retina and brain: Implications for a pathogenic model in aceruloplaminia. Hum Mol Genet 5: 1989-1996.

Kosaka K, Iseki E (1996) Dementia with Lewy bodies. Curr Opin Neurol 9: 271-275.

Krause GS, Kumar K, White BC, Aust SD, Weigenstein JC (1986) Ischemia, resuscitation and reperfusion: mechanism of tissue injury and prospects for protection. Am Heart J 3: 768-780.

Kruger R, Kuhn W, Muller T (1998) Ala30Pro mutation in the gene encoding alpha-synuclein in Parkinson's disease. Nat Genet 18: 106-108.

Kurose I, Saito H, Miura S, Ebinuma H, Higuchi H, Watanabe N, Zeki S, Nakamura T, Takaishi M, Ishii H (1997) CD18/ICAM-1-dependent oxidative NF-kappa B activation leading to nitric oxide production in rat kupffer cells cocultured with syngenetic hepatoma cells. J Clin Invest 99: 867-878.

La Vaute T, Smith S, Cooperman S, Iwai K, Land W, Meyron-Holtz E, Drake S, Miller G, Abu-Asab M, Tsokos M, Switzer R III, Grinberg A, Love P, Tresser N, Rouault T (2001) Targeted deletion of the gene encoding iron regulatory protein-2 causes misregulation of iron metabolism and neurodegenerative disease in mice. Nat Genet 27: 209-214.

Leardi A, Caraglia M, Selleri C, Pepe S, Pizzi C, Notaro R, Fabbrocini A, De Lorenzo S, Musico M, Abbruzzese A, Bianco AR, Tagliaferri P (1998) Desferioxamine increases iron depletion and apoptosis induced by arc-C of human myeloid leukemic cells. British J Haematol 102: 746-752.

Leroy E, Boyer R, Auburger G (1998) The ubiquitin pathway in Parkinson's disease. Nature 395: 451-452.

Leveugle B, Spik G, Perl DP, Bouras C, Fillit HM, Hof PR (1994) The iron-binding protein lactotransferrin is present in pathologic lesions in a variety of neurodegenerative disorders: A comparative immunohistochemical analysis. Brain Res 650: 20-31.

LeVine RL, Garland D., Oliver CN, Amici A., Climent I, Lenz AG, Ahn S, Shaltiel S., Stadtman ER (1990) Determination of carbonyl content in oxidatively modified proteins. Methods Enzymol 186: 464-478.

Lieu P, Heiskala M, Peterson P, Yang Y (2001) The roles of iron in health and disease. Mol Aspects Med 22: 1-87.

Louis ED, Fahn S (1996) Pathologically diagnosed diffuse Lewy body disease and Parkinson's disease: do the Parkinsonian features differ? Adv Neurol 69: 311-314.

Lovell MA, Robertson JD, Teesdale WJ, Campbell JL, Markesbery WR (1998) Copper, iron and zinc in Alzheimer's disease senile plaques. J Neurochem 158: 47-52.

Maines M (2000) The heme oxygenase system and its functions in the brain. Cell Mol Biol (Noisy-le-grand) 46: 573-585.

Masliah E, Rockenstein E, Veinbergs I, Mallory M, Hashimoto M, Takeda A, Sagara Y, Sisk A, Mucke L (2000) Dopaminergic loss and inclusion body formation in α-synuclein mice: implications for neurodegenerative disorders. Science 287: 1265-1269.

Matsumine H, Saito M, Shimoda-Matsubayashi S (1997) Localization of a gene for an autosomal recessive form of juvenile Parkinsonism to chromosome 6q25.2-27. Am J Hum Genet 60: 588-596.

McNaught KS, Olanow CW, Halliwell B, Isacson O, Jenner P (2001) Failure of the ubiquitin-proteosome system in Parkinson's disease. Nat Rev Neurosci 2: 589-594.

Meneghini R (1997) Iron, homeostasis, oxidative stress, and DNA damage. Free Rad Biol & Med 23: 783-792.

Min K-S, Nishida K, Onosaka S (1999) Protective effect of metallothionein to ras DNA damage induced by hydrogen peroxide and ferric ion-nitrilotriacetic acid. Chemico-Bio Int 122: 137-152.

Mitomo K, Nakayama K, Fujimoto K, Sun X, Seki S, Yamamoto K (1994) Two different cellular redox systems regulate the DNS-binding activity of the p50 subunit of NF-kappa B in vitro. Gene (Amst) 145: 197-203.

Miyajima H, Fujimoto M, Kohno S, Kaneko E, Gitlin JD (1998) CSF abnormalities in patients with aceruloplasminemia. Neurology 51: 1188-1190.

Moos T, (1996) Immunohistochemical localization of intraneuronal transferrin receptor immunoreactivity in the adult mouse central nervous system. J Comp Neurol 375: 675-692.

Moos T, Morgan E (2000) Transferrin and transferrin receptor function in brain barrier system. Cell Mol Neurobiol 20: 77-95.

Moos T, Trinder D, Morgan EH (2000) Cellular distribution of ferric iron, ferritin, transferrin and divalent metal transporter 1 (DMT 1) in substantia nigra and basal ganglia of normal and beta2 microglobulin deficient mouse brain. Cell Mol Biol (Noisy-le-grand) 46: 549-561.

Morris CM, Candy JM, Keith AB, Oakley AE, Taylor GA, Pullen RG, Bloxham CA, Gocht A, Edwardson JA (1992) Brain iron homeostasis. J Inorg Biochem 47: 257-265.

Nelson SK, McCord JM (1998) Iron, oxygen radicals, and disease (1998): Adv Mol Cell Biol 25: 157–183.

Nose K (2000) Role of reactive oxygen species in the regulation of physiological functions. Biol Pharm Bull 23: 897-903.

Patel B, Dunn R, David S (2000) Alternative RNA splicing generates a glycosylphosphatidylinositol-anchored form of ceruloplasmin in mammalian brain. J Biol Chem 275: 4305-4310.

Polymeropoulos MH, Lavedan C, Leroy E (1997) Mutation in the alpha-synuclein gene identified in families with Parkinson's disease. Science 276: 2045-2047.

Qian ZM, Liao QK, To Y, Ke Y, Tsooi YK, Wang GF, Ho KP (2000) Transferrin-bound and transferrin free iron uptake by cultured rat astrocytes. Cell Mol Biol 46: 541-548.

Olanow CW (1993) A radical hypothesis for neurodegeneration. Trends Neurosci 16: 439-444.

Reddy BR, Kloner RA, Przyklenk K (1989) Early treatment with deferoxamine limits myocardial ischemic/reperfusion injury. Free Radical Biology & Medicine 7: 45–52.

Rouault T (2001) Systemic iron metabolism: A review and implications for brain iron, metabolism. Pediat Neurol 25: 130-137.

Roy C, Andrews N (2001) Recent advances in disorder of iron metabolism: mutations, mechanisms and modifiers. Hum Mol Genet 10: 2181-2186.

Sayre LM, Perry G, Harris PLR, Liu Y, Schubert KA, Smith MA (2000) In situ oxidative catalysis by neurofibrillary tangles and senile plaques in Alzheimer's disease: A central role for bound transition metals. J Neurochem 74: 270-279.

Schipper HM (2000) Heme Oxygenase-1: Role in brain aging and neurodegeneration. Exp Gerontol 35: 821-830.

Schipper HM, Bernier L, Mehindate K, Frankel D (1999) Mitochondrial iron sequestration in dopamine-challenged astroglia: Role of heme oxygenase-1 and the permeability transition pore. J Neurochem 72: 1802-1811.

Schulze-Osthoff K, Beyaert R, Vandevoorde V, Haegeman G, Herzenberg LA (1993) Depletion of the mitochondrial electron transport abrogates the cytotoxic and gene-inductive effects of TNF. EMBO J 12: 3095-3104.

She H, Xiong S, Lin M, Zandi E, Giulivi C, Tsukamoto H (2002) Iron activates NF-κB in Kupffer cells. Am J Physiol (Gastrointest Liver Physiol) 283: G719-G726.

Shimura H, Schlossmacher MG, Hattori N (2001) Ubiquitination of a new form of alpha-synuclein by parkin from human brain: implication for Parkinson's disease. Science 293: 263-269.

Sinaceur R, Ribiere C, Abu-Murad C, Nordmann J, Nordmann R (1983) Reduction in the rate of ethanol elimination in vivo by desferrioxamine and diethylenetrimine penta acetic acid: suggestion for involvement of hydroxyl radicals in ethanol oxidation. Biochem Pharm 32: 2371–2373.

Spillantini MG, Schmidt ML, Lee VM, Trojanowski JQ, Jakes R, Goedert M (1997) α-Synuclein in Lewy bodies. Nature 388: 839-840.

Toledano MB, Leonard WJ (1991) Modulation of transcription factor NF-kappaB binding activity by oxidation-reduction in vitro. Proc Natl Acad Sci USA 88: 4328-4332.

Torti SV, Torti FM, Whitman SP, Brechbiel MW, Park G, Planalp RP (1998) Tumor cell cytotoxicity of novel metal chelator. Blood 92: 1384-1389.

Tsukamoto H, Lin M, Ohata M, Giulivi C, French SW, Brittenham G (1999) Iron primes hepatic macrophages for NF-κB activation in alcoholic liver injury. Am J Physiol (Gastrointest Liver Physiol 40) 277: G1240-1250.

Uversky VN, Li J, Fink AL (2001) Metal-triggered structural transformations, aggregation, and fibrillation of human α-synuclein: A possible molecular link between Parkinson's disease and heavy metal exposure. J Biol Chem 276: 44284–44296.

Van Eden ME, Aust SD (2000) Intact human ceruloplasmin is required for the incorporation of iron into human ferritin. Arch Biochem Biophys 381: 119-126.

Ward PA, Till GO, Kundel R, Beauchamp C (1983) Evidence for role of hydroxyl radical in complement and neutrophil-dependent tissue injury. J Clin Invest 72: 789-801.

Ward RJ, Dexter D, Florence A, Aouad F, Hider R, Jenner P, Crichton RR. (1995) Brain iron in the ferrocene-loaded rat: its chelation and influence on dopamine metabolism. Biochem Pharmacol 12: 1821-1826.

Willis ED, (1969) Lipid peroxide formation in microsomes. The role of non-haem iron. Biochem J 113: 325–332.

Wolfe L, Olivier N, Sallan D (1985) Prevention of cardiac disease by subcutaneous desferroxamine in patients with thalassemia major. N Engl J Med 312: 1600-1603.

Wu GS, Walker J, Rao NA (1993) Effect of deferoxamine on retinal lipid peroxidation in experimental uveitis. Invest Ophthalmol Vis Sci 34: 3084–3089.

Xiong S, She H, Takeuchi H, Han B, Engelhardt JF, Barton CH, Zandi E, Giulivi C, Tsukamoto H (2003) Signaling role of intracellular iron in NF-κB activation. J Bio Chem 278: 17646-17654.

Yoshida K, Kaneko E, Miyajima H, Tokuda T, Nakamura A, Kato M, Ikeda S (2000) Increased lipid peroxidation in the brains of aceruloplasminemia patients. J Neurol Sci 175: 91-95.

Zecca L, Tampellini D, Gerlach M, Riederer P, Fariello RG, Sulzer D (2001) Substantia nigra neuromelanin: Structure, synthesis, and molecular behaviour. Mol Pathol 54: 414-418.

BIOGRAPHY

NAME	Mrs.Patcharee Kooncumchoo
DATE OF BIRTH	16 November 1970
PLACE OF BIRTH	Khon Kaen, Thailand
INSTITUTIONS ATTENDED	Khon Kaen University, 1992: Bachelor of Science (Physical Therapy) Mahidol University, 1997: Master of Science (Neuroscience)
POSITION&OFFICE	Faculty of Allied Health Science, Thammasat University, Rangsit campus, Prathum thani, Thailand Position: Lecturer Tel: 02-926-9441-2 E-mail: s_patree@hotmail.com
HOME ADDRESS	65/15 Soi Arthorn-U-Prathum, Pracharat 1 rd., Bang sue, Bangkok, Thailand Tel: 02-587-1803